

R. & M. No. 3186

ROYAL AIRCRAFT ESTABLISHMENT
BEDFORD.

R. & M. No. 3186
(20,727)
A.R.C. Technical Report



MINISTRY OF AVIATION

AERONAUTICAL RESEARCH COUNCIL
REPORTS AND MEMORANDA

Low-Speed Wind-Tunnel Tests on a Series of
Uncambered Slender Pointed Wings
with Sharp Edges

By D. H. PECKHAM, B.Sc., A.F.R.Ae.S.

Maskell Ref.

LONDON: HER MAJESTY'S STATIONERY OFFICE

1961

PRICE £2 7s. 6d. NET

Low-Speed Wind-Tunnel Tests on a Series of Uncambered Slender Pointed Wings with Sharp Edges

By D. H. PECKHAM, B.Sc., A.F.R.Ae.S.

COMMUNICATED BY THE DEPUTY CONTROLLER AIRCRAFT (RESEARCH AND DEVELOPMENT),
MINISTRY OF SUPPLY

*Reports and Memoranda No. 3186**
December, 1958

Summary. A series of three thick uncambered slender wings and twelve flat-plate slender wings, all with sharp edges, have been tested in the 13 ft \times 9 ft Low-Speed Wind Tunnel at the Royal Aircraft Establishment, Bedford.

Pressure plotting, balance measurements and flow-visualisation tests were made to investigate the effects of plan-form shape, thickness, and aspect ratio on their aerodynamic characteristics at low speeds.

1. Introduction. Slender pointed wings whose leading edges are subsonic and swept at an angle of 60 deg or more are of interest for supersonic flight. To obtain a high lift/drag ratio at the cruise condition, such wings can be cambered to give attached flow at a small incidence, but then flow separations are certain to occur at conditions other than the cruise, particularly at the high incidences associated with take-off and landing. On slender pointed wings, these flow separations usually take the form of two free vortex layers joined to the leading edges of the wing, which roll up to form spiral-shaped vortex sheets above the upper surface^{1, 2}; in some cases, with highly cambered wings, for instance, more complicated forms are possible.

It has been argued that though these separations are inevitable, they are not necessarily undesirable provided their primary lines of separation are fixed. The flow should then be steady and of one type throughout the range of flight conditions at which flow separations from the leading edges occur. This argument leads naturally to the slender pointed wing with sharp leading edges as one type of wing on which such properties can be realised.

Slender wings are not limited to the delta plan-form shape, so that the effects of varying the plan-form shape, cross-section shape and area distribution need to be considered. Various cross-section shapes have been suggested, a simple family of wings being obtained, for example, by defining the cross-section of the wing as a diamond. One such wing is the delta proposed by Newby³, which has a biconvex parabolic-arc streamwise section of linearly decreasing thickness/chord ratio across the span; its geometry is discussed in Ref. 4. These plan-form and cross-section shapes can

* R.A.E. Report Aero. 2613, received 27th January, 1959.

be profitably combined with a favourable area distribution^{5, 6, 7, 8}. For instance, a curved parabolic and convex leading-edge plan shape can be combined with a biconvex parabolic-arc shape at the centre-line and diamond cross-sections, to give a suitable area distribution.

The object of the present tests was to investigate the effects at low speeds of leading-edge shape, trailing-edge sweep, thickness and aspect ratio on the aerodynamics of sharp-edged slender pointed wings with zero or small camber.

The tests were made in the 13 ft × 9 ft Low-Speed Wind Tunnel at the Royal Aircraft Establishment, Bedford.

2. Description of Models and Tests. Fifteen models of slender pointed wings were tested, all of which had sharp edges and were uncambered, or nearly so.

The three wings, A, B and C illustrated in Fig. 1, all have a symmetrical 12 per cent biconvex parabolic-arc section at the centre-line, straight unswept trailing edges and an aspect ratio of 1. Wing A is a gothic, in which the leading-edge plan-form shape is a parabola with its vertex at the wing tip. The wing surface is generated by straight lines which are parallel to the trailing edge (in plan-form projection) and so produce section shapes and thickness/chord ratios which vary across the span. Wing B is a delta with its surface generated by radial straight lines from the tips, giving a constant section shape and thickness/chord ratio across the span. Wing C is a delta with its surface generated by two sets of straight lines which, in plan-form projection, are parallel to the trailing edge and the leading edge respectively, so as to give a constant section shape across the span and a thickness/chord ratio which decreases linearly across the span. The geometry of these wings is discussed in detail in Ref. 4.

Wings A, B and C were used for six-component balance measurements, pressure plotting and flow-visualisation tests. One set of pressure holes was located along the centre-line, the others being arranged in spanwise rows on both upper and lower surfaces at a spacing of 1/10th of the local span (Fig. 2), with additional holes at a spacing of 1/20th of the local span in the region $0.5 > y/s(x) > 0.9$ on wings A and B. These extra holes allowed more accurate location of the suction peaks at low incidence. Pressure measurements were made over an incidence range of 0 deg to 30 deg at zero yaw, and also at 5 deg yaw in the case of wing C.

Six-component balance measurements were made on wings A and C at speeds ranging from 80 ft/sec to 300 ft/sec, corresponding to a Reynolds-number range of 2.3×10^6 to 8.6×10^6 based on mean chord; the ranges of incidence covered at the higher speeds were restricted by the strength limitations of the wire supporting rig. No significant Reynolds-number effects were apparent and, for this reason, tests over a range of tunnel speeds were not made with wing B, the last model of the series to be tested. Force and moment coefficients are quoted relative to stability axes (see Fig. 3) with the mean quarter-chord point as the origin of the axes system. Corrections to the measured forces and moments for tunnel wall effects have been made by the method described in Ref. 9.

Two flow-visualisation techniques were used, the oil-flow method, and the smoke technique described in Ref. 10.

The twelve wings shown in Fig. 4 were flat-plate models with sharp edges and a thickness/chord ratio of 0.01. To simplify investigations on the effects of the coiled vortex sheets, the upper surfaces of these models were kept completely flat, only the lower surfaces of the wings being bevelled (at 14 deg) to give the sharp edges. However, since this bevel on only one surface introduced a camber effect, two extra models (models 2A and 8A) with equal amounts of bevel on each surface were also tested. This series of fourteen flat-plate wings was made up from four basic models, sets

of leading and trailing edges being quickly interchangeable to give a fresh plan-form shape with the model still rigged in the tunnel working-section. In this way, a wide range of plan-form shapes was tested without using tunnel time in rigging separate models.

These flat-plate models were designed to provide basic information as follows:

- (i) Wings 1, 2, 3, 8, 9 and 10: the effect of changing aspect ratio (and the ratio of span to root chord) on the behaviour of gothic and delta wings.
- (ii) Wings 4, 2, 5, 6 and 7: the effect of varying the trailing-edge sweep on a wing with a gothic leading-edge shape.
- (iii) Wings 11 and 12: the effect of modifying the gothic shape by increasing the leading-edge sweep at the nose to produce a combination of gothic and delta plan-forms.
- (iv) Wings 2A and 8A: the effect of wing thickness (when compared with wings A, B and C).

Three-component balance measurements were made on all the models, with six-component measurements on wings 2A and 8A where a comparison with the thick wings A, B and C was required. The tests were limited to a maximum incidence of about 20 deg and a tunnel speed of 100 ft/sec because of the flexibility of the models. Flow-visualisation tests were also made, and the position of the cores of the vortex sheets measured using smoke.

3. *Flow Observations.* 3.1. *General.* The nature of the flow with free leading-edge vortex sheets that occurs on slender delta wings is well known and has been described, for instance, by Weber and Maskell in Refs. 1 and 2 respectively, and a description of flow-visualisation experiments on a gothic wing (wing A of this report) is given in Ref. 9. In general, the description of the flow given in these references applies also to the wings described in this report.

However, on the thick delta wing of constant thickness/chord ratio (wing B), flow visualisation indicated that although the flow separated at the sharp leading edges, the coiled vortex sheets did not develop as rapidly at low angles of incidence as on the comparable flat-plate wing. It would appear that the effects of the separations were so localised, in this range, that the flow external to the boundary layer was not significantly different from the so-called 'attached flow' which would have been expected with rounded leading edges; this is discussed more fully in the next Section.

3.2. *Flow at Very Low Angles of Incidence.* On an uncambered wing with sharp leading edges at a non-zero angle of incidence, the stagnation line must be on the lower surface, with the flow consequently separating to form a free shear layer joined to each leading edge. These layers then curl above the upper surface of the wing and concentrate a region of vorticity above and inside each leading edge. Evidence of the existence of coiled vortex layers of this kind was well marked in the oil flow pattern on wing A at an incidence of only 1 deg* (Figs. 6 and 7), this gothic wing having a shallow diamond cross-sectional shape. The behaviour of the flow over wing C, a delta wing of diamond cross-sectional shape, was similar. For wing B, however, a delta similar to wing C but with a more convex cross-sectional shape, the appropriate part of the oil-flow pattern was only just evident at an incidence of 2 deg (Fig. 5), suggesting that the initial rate of growth of the vortex sheets was significantly less in this case.

This phenomenon is not yet well understood and requires further investigation, particularly on cambered wings, which may have complicated edge shapes. The growth of the coiled vortex sheets

* The angles of incidence quoted in the text are given to the nearest degree for simplicity; the exact values are given in the Tables and Figures.

from the leading edges of wing B seems to occur in two distinct phases, though not necessarily with a discontinuous change from the one to the other. It appears likely that this is due to the larger edge-angle of wing B (88 deg in the cross-flow plane) as compared with the other two wings on which the angle is 88 deg at the front decreasing to zero at the tip.

3.3. *Flow with Well-developed Coiled Leading-Edge Vortex Sheets.* 3.3.1. *Unyawed wing.* With reservations regarding the behaviour of wing B at very low angles of incidence, it can be said that for the slender wings described in this report the flow separates at the sharp leading edges when the wing is at incidence to form coiled vortex sheets with a 'core' of high vorticity above and inside the leading edges of the wing. The size and strength of the coiled vortex sheets increase with increasing incidence and they become a dominating feature of the flow, which remains steady throughout the range of practical flight attitudes of the wing.

The effects of the coiled vortex sheets on the flow direction at the wing upper surface were investigated by the oil-flow technique. A photograph of a typical surface oil-flow pattern is given in Fig. 8 with the main features identified, and a set of photographs of patterns on wing C covering an incidence range of 5 deg to 40 deg (at 5 deg intervals) is given in Fig. 9. From such photographs, and pressure-plotting results when available, the mean spanwise positions of the attachment line, peak-suction line and secondary-separation line have been estimated. The least certain of these is the estimated position of the attachment line. However, any errors involved should be consistent between the various models, and the results show the qualitative effects of plan-form shape and aspect ratio on the location of the attachment line. Within the approximate limit $0 < x/c_0 < 0.5$ the values obtained are reasonably independent of chordwise position and are the ones plotted in Figs. 10 to 17; aft of $x/c_0 = 0.5$ the effect of the trailing edge becomes noticeable. Results of measurements on both thick wings and flat-plate wings of aspect ratio 1 are plotted in Figs. 10 to 13, and on flat-plate gothic and delta wings covering a range of aspect ratios in Figs. 14 to 17.

From these results, the following conclusions can be drawn regarding the non-dimensional spanwise positions $y/s(x)$ of the attachment line, peak-suction line and secondary-separation line:

- (a) For the same incidence, they lie farther inboard on the delta wing than on the gothic wing of the same aspect ratio (or the same slenderness ratio, semi-span/root chord);
- (b) The effect of increasing the aspect ratio is to move the attachment line and the peak-suction line farther outboard;
- (c) The effect of increasing the wing thickness is to move them farther outboard.

The position of the cores of the coiled vortex sheets was measured at a number of chordwise stations on the delta and gothic wings by using the smoke technique. Results for angles of incidence of approximately 15 deg and 30 deg are plotted in Figs. 18 to 22. In side elevation, the paths of the cores of the vortex sheets on the gothic wings are approximately straight from the wing apex back as far as the vicinity of the trailing edge, where they curve to a streamwise direction. If straight paths are assumed, the angle between the cores and the wing chordal plane can be calculated at each measured point as $\theta = \tan^{-1} z/x$. Values of θ/α are plotted in Fig. 19, and it can be seen that this ratio is reasonably constant for each aspect ratio, values of about 0.31, 0.34 and 0.38 being obtained for wings of aspect ratio 0.75, 1.0 and 1.25 respectively. With the delta wings (Fig. 20), the paths of the vortex cores are also approximately straight from the wing apex to the trailing edge, but remain closer to the wing than with the gothics, giving a mean θ/α of about 0.25. Comparing the results for thick wings B and C in Fig. 18, it can be seen that, for the same incidence, the fatter

cross-section shape of wing B causes the cores of the vortex sheets to be slightly farther away from the wing chordal plane over the central region of the wing; if the comparison is made at the same lift coefficient, this effect is more marked.

Plan views of the paths of the vortex sheet cores on wings A, B and C are shown in Fig. 22, and it is found that the cores lie farther outboard on the gothic wing than on the delta wings. The position of the cores is related to the position of the peak suctions on a wing. For a flat-plate wing the vortex cores lie on normals from the wing surface at the peak-suction line. This appears to be approximately true also for the wings with diamond cross-sections (A and C), the cores being farther outboard than the peak-suction lines. However, this is not the case with wing B where it is found that the cores are actually inboard of the peak-suction line.

3.3.2. Yawed wing. Photographs are given in Figs. 23 and 24 showing the effect of yaw on the surface-flow pattern, and the smoke pattern, for wing C at an incidence of 20 deg; a corresponding surface-flow pattern for wing A is given in Ref. 9. Unfortunately the flow pattern in Fig. 24 is less distinct because the tunnel speed had to be reduced with the larger angle of yaw.

Both with 5 deg and with 10 deg yaw the surface-flow patterns show no basic differences from the unyawed case except for the presence of a separation and its associated coiled vortex sheet springing from the centre-line ridge, although the secondary separations are yawed with respect to the symmetry of the model. Smoke tests show that the paths of the vortex cores change with angle of yaw both in plan and height although, with 5 deg yaw, the spanwise position of the suction peaks (Fig. 25) and the estimated positions of the points of inflexion on the surface-flow patterns (Fig. 23) remain symmetrically disposed about the centre-line. This suggests that the vortex cores have moved along normals to the sloping surface of the wing in the cross-flow plane.

Fig. 20 of Ref. 9 showed a breakdown of flow in the vortex core of wing A on the leading side when yawed. Fig. 26 in the present report shows the change in position of the breakdown with yaw at an incidence of 23 deg and illustrates its great sensitivity to small angles of yaw. With model C, the breakdown occurs near to the trailing edge for the conditions represented in Fig. 24 and its position is indicated by the sudden change of slope in the secondary separation line.

4. Balance Measurements. *4.1. Wings with Straight Unswept Trailing Edges.* Results of balance measurements on wings B and C are given in Tables 2 to 7; the results for wing A have already been published in Ref. 9. Tables 8 to 10 give the results for the flat-plate wings.

Lift and pitching-moment characteristics of the thick wings of aspect ratio 1 (A, B and C) are compared in Fig. 27. It is seen that more lift is obtained from the gothic wing at a given incidence than with the delta wings, and that the delta of the greater mean thickness (wing B) gives the least lift. Results for these thick wings compared with those for their flat-plate counterparts (Figs. 28 and 29), show that thickness causes a reduction in lift and a more negative pitching moment, which indicates that a greater proportion of the loss of lift occurs over the forward parts of the wings, where their cross-section shapes are most steep-sided. This is consistent with the flow-visualisation experiments, where it was found that cross-section shape affected the rate of growth of the coiled vortex sheets and presumably the lift obtained from their effect on the upper surface of the wing. In addition, pressure plotting tests on the deltas (B and C) showed somewhat lower local cross-load coefficients over the forward parts of the wings than over their central region, particularly at higher incidences (Figs. 67 and 68).

The Jones value of $\pi A/2$ for the linear-lift slope ($dC_L/d\alpha$ at $\alpha = 0$) is included in both Figs. 27 and 28, and is found to be high relative to all the experimental results. However, the value for the linear-lift slope for delta wings given by Weber¹ appears to be in reasonable agreement with the results for the flat-plate delta wings (Fig. 28); admittedly the slope at zero lift is difficult to estimate from the experimental curves.

Although theory gives nearly the same linear-lift contribution for delta and gothic wings of the same aspect ratio, the overall lift coefficients are not the same. Instead, it is found that they are the same for gothic and delta wings of the same slenderness ratio (semi-span/root chord) (Fig. 30). Furthermore, this can also be said of slender wings with mixed curved and straight leading-edge plan-form shapes (Fig. 31).

To investigate further the significance of slenderness ratio, the results for the flat-plate wings 1, 2, 3, 8, 9 and 10 are plotted in Fig. 32, the C_L values having been corrected to give zero lift at zero incidence in order to eliminate the effect of the cambered edges. These values are plotted in Fig. 33 in terms of (slenderness ratio)^{1/2} and they collapse satisfactorily onto a single curve. This result does not have any known theoretical basis, but nevertheless it should be useful for estimation purposes within the range of aspect ratios tested.

The positions of the centres of pressure calculated from balance measurements on the gothic and delta wings of aspect ratio 1 are plotted in Fig. 34 as percentages of the aerodynamic mean chord. They remain fairly constant at lift coefficients greater than about 0·4, being about 32 per cent \bar{c} and 40 per cent \bar{c} on the flat-plate gothic and delta wings respectively; the centroid of the plan-form shape is at 50 per cent \bar{c} by definition. On the delta wings, the effect of thickness is to cause a 5 per cent \bar{c} rearward shift of the centre-of-pressure position; on the gothic wing the rearward shift is only 3 per cent \bar{c} .

The drag due to lift of a thin flat wing is $L \tan \alpha$, giving an L/D ratio of $\cot \alpha$ (in the absence of skin friction), which is independent of aspect ratio. Profile drag actually reduces the L/D ratio below this value, but with a thick wing an opposite effect can occur due to the suctions induced by the coiled vortex sheets acting on forward-sloping parts of the wing upper surface to give a thrust force. At the larger incidences, this can be sufficient to raise the L/D ratio above $\cot \alpha$. At any given incidence, the L/D ratios of the thick gothic and delta wings ($A = 1$) are about the same (Fig. 35a) and for incidences greater than 10 deg give values above $\cot \alpha$. But, since the gothic has the higher lift at a given incidence, its maximum L/D occurs at a slightly higher C_L and, at high lift coefficients, it has larger L/D ratios than the delta. A further analysis of the drag characteristics of these wings is given in Fig. 36.

The effects of the coiled vortex sheets on the drag-due-to-lift factor, are illustrated in Fig. 37 for wing C. Curve (a) shows the theoretical values which would be obtained from a thin flat wing giving linear-lift only. The effect of the vortex sheets is to produce a non-linear lift increment which reduces the incidence at which a given lift is obtained, and therefore the drag contribution $\tan \alpha$, leading to curve (b). With a thick wing, the axial force which results from the suctions due to the vortex sheets acting on forward-sloping surfaces reduces the drag still further below the values of curve (b). The axial force is plotted in Fig. 38.

When the wings are yawed there is no significant change in their longitudinal force and moment characteristics, which agrees with the indication from flow-visualisation tests that yaw did not upset the basic flow pattern. Fig. 25 shows that higher peak suctions are obtained on the leading half of the wing, and lower ones on the trailing half, but their spanwise position is almost unaffected.

This pressure distribution gives a negative rolling moment with a positive sideslip, so that $dC_l/d\beta$ is negative, which is equivalent to the effect of dihedral. As the suctions caused by the vortex sheets act on sideways-sloping surfaces, a positive sideslip gives a positive side force and a positive $dC_y/d\beta$. The resulting yawing moment obtained from this side force depends on the relative positions of the centre of pressure of the side force and the yawing-moment axis; about a likely centre-of-gravity position for these wings, this side force would give a small stable yawing-moment contribution. On a cambered wing, part of the mean surface will probably have a sideways slope and these effects may then be more pronounced. Lateral force and moment measurements on wing C at angles of yaw up to 15 deg are plotted in Figs. 39 and 40, and are typical of the behaviour of the three thick wings, the forces and moments varying linearly over a yaw range of ± 5 deg up to very high incidences. The static sideslip derivatives for the three thick wings are compared in Fig. 41; it should be noted that all the wings have the same side area but that the side force and yawing-moment coefficients are referred to wing area and to wing area and span, respectively. This has the effect of exaggerating the difference between the gothic and delta wings, the side force and yawing moment being more dependent on side area and cross-section shape. The effect of wing thickness on the rolling and yawing static sideslip derivatives is shown in Fig. 42, no significant side force arising from the flat-plate wings. The rolling-moment derivatives are slightly less for the flat-plate wings, which is consistent with the vortex sheets being farther inboard and the suctions induced by them acting at a smaller moment arm.

The effect of aspect ratio and slenderness ratio on the lift and pitching-moment characteristics of gothic and delta wings is shown in Figs. 43 and 44. As shown earlier, the lift characteristics of gothic and delta wings of the same slenderness ratio are the same. Increasing aspect ratio causes a slight forward shift of the aerodynamic centre, amounting to about 3 per cent of the aerodynamic mean chord for the range of aspect ratio covered.

A possible method of increasing the low-speed lifting ability of slender wings for take-off and landing is to have leading-edge flaps which can be extended in a spanwise direction over part, or all, of the length of the leading edge. The lift-coefficient increments this could produce, for a full-length leading-edge flap, are shown in Figs. 45 and 46 where the results from Figs. 43 and 44 are shown based on the most slender gothic and delta wing, respectively. Lift-coefficient increments of approximately 0.3 and 0.6 are obtained at an incidence of 15 deg for increases in span of $33\frac{1}{3}$ and $66\frac{2}{3}$ per cent respectively, for both the gothic and delta wings (allowing for the zero-lift angle of these flat-plate wings).

4.2. Wings with Swept Trailing Edges. The effect of trailing-edge sweep on the lift and pitching-moment characteristics of slender wings was investigated on a flat-plate with a parabolic leading-edge plan-form shape which, in the case of zero trailing-edge sweep, gave a gothic wing of aspect ratio 1. The range of sweep angles covered was -15 deg to 56.3 deg, corresponding to an aspect ratio range of 0.94 to 1.6. Fig. 47 shows that, with increasing sweepback of the trailing edge, the lift curves become straighter with a greater slope at zero lift which more than compensates for any loss of the non-linear lift contribution. Pitching moments, taken about the mean quarter-chord point of each wing, are plotted in Fig. 48. A slight pitch-up is first manifest with 30 deg trailing-edge sweep, and occurs at an incidence of about 20 deg. On the wing of 56.3 deg trailing-edge sweep this develops into a strong pitch-up commencing at an incidence of about 6 deg.

5. Pressure Measurements. **5.1. General.** Results of surface-pressure measurements on wings A, B and C are given in Tables 11 to 14, and the values derived for the local cross-load coefficient

$C_N(x)$ in Tables 15 to 17. The incidence range covered was 0 to 30 deg, measurements being made at 5 deg yaw as well as zero yaw in the case of wing C. Selected measurements are plotted in Figs. 49 to 65 to illustrate the nature of the pressure distribution, and in Figs. 66 to 72 to show the local load distributions.

5.2. Pressure Distribution at Zero Incidence. The supersonic velocity distributions at zero incidence on the centre-lines of wings A, B and C are compared in Fig. 49, the theoretical estimate by Newby⁸ for wing C being shown by a broken line. It is seen that the experimental supersonic velocities are lower than the theoretical values, though the shape of the distribution agrees quite well with theory. This is because Ref. 3 assumes that the wing thickness is small compared with the span, which clearly does not hold here.

Isobar patterns at zero incidence for the three wings are given in Figs. 50 to 52. The main differences between the patterns on delta and gothic wings, are that on the delta wing:

- (a) The isobars are more highly swept over the rear third of the wing;
- (b) The isobars are more closely spaced in the region close to the trailing edge, indicating a steeper adverse pressure gradient there.

On gothic and delta wings of diamond cross-section shape (A and C), the supersonic velocity distributions at the maximum thickness line are very similar (Fig. 53a).

The main effect of thickness distribution on the isobar patterns for delta wings, is that on the constant thickness/chord ratio wing the supersonic velocities are higher outboard of the centre-line, while on the wing with a decreasing thickness/chord ratio spanwise, the supersonic velocities are lower than these at the centre-line. The supersonic velocities at the maximum thickness lines on delta wings B and C are compared in Fig. 53b.

5.3. Pressure Distribution at Incidence. In Figs. 54 to 59, the results for wings A, B and C at incidences of about 15 deg have been chosen to illustrate the effects of the coiled vortex sheets on the pressure distribution on gothic and delta wings. Pressure coefficients on lines of constant $y/s(x)$ are plotted in Figs. 54, 56 and 58 while in Figs. 55, 57 and 59 pressure coefficients are shown plotted at constant values of x/c_0 for various chordwise locations on the wing. From these plots, isobar patterns of the upper-surface pressure distribution on the wings have been produced, and are given in Figs. 60, 61 and 62.

The suction over the central region of the wings, between the attachment lines, are seen to be slightly higher than the values obtained at zero incidence, as predicted by slender-wing theory. The positions of the attachment lines are clearly defined over the forward part of the wing and the pressure distributions of Figs. 63 to 65 show a dip at this line.

The main differences between the pressure distributions for the two plan-form shapes occur in the region beneath the coiled vortex sheets and are as follows:

- (a) Where, as on the delta wing, the suction on rays from the apex reach a peak at an x/c_0 between about 0.7 and 0.8 and then decrease, on the gothic wing the suction are highest near the apex of the wing and decrease steadily towards the trailing-edge, as slender-wing theory suggests.
- (b) On the gothic wing, the attachment lines and peak-suction lines are farther outboard than on the delta wing, and the peak suction obtained are much higher.

The variation of the upper-surface pressure distribution with incidence on gothic and delta wings is illustrated in Figs. 63, 64 and 65. At high incidences, the effects of the secondary separation

become apparent, a further suction peak developing close to the leading edge of the wing just outboard of the secondary separation line.

The differences ΔC_p , between the upper-surface and lower-surface pressure coefficients have been integrated with respect to $y/s(x)$ at various chordwise locations (constant x/c_0), to give a local cross-load coefficient, $C_N(x)$. The longitudinal variations of this coefficient on the three wings A, B and C are plotted in Figs. 66, 67 and 68 for a range of incidence up to about 30 deg. It is found that with the delta wings (B and C), the effect of the trailing edge is noticeable aft of $x/c_0 \approx 0.6$, and that ahead of this the load is nearly constant, the flow being approximately conical at the lower incidences. On the gothic wing, the effect of the trailing edge is not marked ahead of $x/c_0 = 0.8$; from the apex of the wing to this position the local cross-load coefficient decreases almost linearly with distance from the wing apex. A comparison of the longitudinal distribution of local cross-load coefficients on gothic wing A and delta wing C is given in Fig. 69a for an incidence of 15 deg, and in Fig. 69b for a lift coefficient of 0.5.

The product of cross-load coefficient and local semi-span, $s(x)/(b/2)$, to give the local cross-load*, $C_N(x) \cdot s(x)/(b/2)$, is plotted in Figs. 70, 71 and 72 for the three wings A, B and C.

6. Conclusions. (a) The flow with coiled leading-edge vortex sheets is perfectly steady and gives a smooth variation of overall forces and moments over the whole range of attitudes likely to be encountered in flight conditions. Nevertheless, certain combinations of leading-edge sweep and cross-section shape retard the initial growth of coiled vortex sheets, as discussed in Sections 3.1 and 3.2.

(b) Increasing aspect ratio, increasing thickness, and increasing convexity of the leading-edge plan-form shape, all have the effect of moving the attachment line, peak-suction line and secondary separation line farther outboard. They also have the effect of moving the cores of the coiled vortex sheets farther away from the wing chordal plane (these conclusions are not necessarily true for increasing thickness if it has the effect of retarding the rate of growth of the coiled vortex sheets).

(c) A gothic wing gives more lift coefficient at a given incidence than a delta wing of the same aspect ratio. However, gothic and delta wings of the same slenderness ratio (semi-span/root chord) and similar thickness distribution, have the same lift characteristics. This is also true for wings with a mixed curved/straight leading-edge plan-form shape. The effect of increase in wing thickness is to reduce lift.

(d) The theoretical linear-lift slope given by Weber for delta wings agrees reasonably well with the experimental results for flat-plate delta wings near zero incidence. To a close approximation, the overall lift of gothic, delta and mixed gothic/delta plan-form shapes is proportional to (slenderness ratio) $^{1/2}$.

(e) The centres of pressure on flat-plate gothic and delta wings of aspect ratio 1 are at 32 per cent and 40 per cent aerodynamic mean chord, respectively; a root thickness/chord ratio of 12 per cent causes a rearward shift of 3 per cent \bar{c} and 5 per cent \bar{c} , respectively. Increase of aspect ratio causes a small forward shift of the centre of pressure.

* Note that the overall normal force is given by the relation

$$C_N = \frac{bc_0}{S} \int_0^1 C_N(x) \frac{s(x)}{b/2} d\left(\frac{x}{c_0}\right),$$

where the plan-form parameter $bc_0/S = 3/2$ for the gothic wings and 2 for the delta wings.

(f) On a thick slender wing, suctions induced on the wing upper surface by the coiled vortex sheets act on forward-facing surfaces to give a thrust force, which increases the L/D ratio above $\cot \alpha$ at angles of incidence beyond about 10 deg for wings of 12 per cent thickness/chord ratio. The drag-due-to-lift factor, K , is also reduced by this effect. Similarly, when the wing is yawed, suctions acting on sideways-facing surfaces give a side force in a direction such as to give a positive $dC_y/d\beta$. These effects may be more marked on a cambered wing.

(g) Positive sideslip gives a large negative rolling moment. That is, $dC_l/d\beta$ is negative, which is equivalent to the effect of dihedral.

(h) Lower supersonic velocities are obtained on thick delta wings at zero incidence than predicted by thin-wing theory³, though the shape of the distribution agrees well with the theory.

(i) The cross-load distributions on gothic and delta wings differ mainly in that on a gothic wing the local cross-load coefficient is at its maximum at the wing apex and decreases steadily towards the trailing edge, while on a delta the local cross-load coefficient is approximately constant over the front two-thirds of the wing before falling to zero at the trailing edge.

LIST OF SYMBOLS

x, y, z	Rectangular body co-ordinates, x chordwise from apex, y spanwise
b	Wing span
c	Wing chord
c_0	Centre-line chord of wings without trailing-edge sweep (for wings with trailing-edge sweep the value for the basic wing is used)
\bar{c}	Aerodynamic mean chord = $\frac{\int_{-b/2}^{b/2} c^2 dy}{\int_{-b/2}^{b/2} c dy}$
l_{14}	Distance of mean quarter-chord point from wing apex
s	Wing semi-span
$s(x)$	Wing local semi-span
t_0	Maximum thickness of centre-line aerofoil section
$v_x(x)$	Chordwise supersonic velocity component
A	Aspect ratio
K	$= \frac{C_D - C_{D0}}{C_L^2/\pi A}$, drag-due-to-lift factor
R	Reynolds number, based on aerodynamic mean chord
S	Wing area
α	Angle of incidence
β	Angle of sideslip
ψ	Angle of yaw ($= -\beta$)
θ	Angle between vortex core path and wing chordal plane (in side elevation)
ϕ	Edge sweep
C_L	Overall lift coefficient
ΔC_L	Lift coefficient increment
C_D	Overall drag coefficient
C_A	Overall axial-force coefficient
C_N	Overall normal-force coefficient
C_Y	Overall side-force coefficient, positive to starboard
C_c	Overall cross-wind-force coefficient
C_l	Rolling moment coefficient = $\frac{l}{\frac{1}{2}\rho V^2 S \bar{c}}$
C_m	Pitching-moment coefficient = $\frac{m}{\frac{1}{2}\rho V^2 S \bar{c}}$ taken about mean quarter-chord

LIST OF SYMBOLS—*continued*

C_n	Yawing-moment coefficient = $\frac{n}{\frac{1}{2}\rho V^2 S b}$ taken about mean quarter-chord.
$\frac{dC_l}{d\beta}$	Per radian
$\frac{dC_n}{d\beta}$	Per radian
$\frac{dC_y}{d\beta}$	Per radian
C_p	Pressure coefficient
ΔC_p	$= C_{p \text{ U.S.}} - C_{p \text{ L.S.}}$
$C_N(x)$	Local cross-load coefficient = $\int_0^1 \Delta C_p d \left[\frac{y}{s(x)} \right]$

Suffixes

U.S.	Upper surface
L.S.	Lower surface
L.E.	Leading edge
T.E.	Trailing edge

REFERENCES

No.	Author		Title, etc.
1	J. Weber	Some effects of flow separation on slender delta wings. A.R.C. 18,073. November, 1955.
2	<u>E. C. Maskell</u>	Flow separation in three dimensions. A.R.C. 18,063. November, 1955.
3	K. W. Newby	The effects of taper on the supersonicities on three-dimensional wings at zero incidence. A.R.C. 18,205. June, 1955.
4	D. H. Peckham	The geometry of wing surfaces generated by straight lines and with a high rate of thickness taper at the root. A.R.C. 19,548. May, 1957.
5	W. T. Lord and B. Green	Some thickness distributions for narrow wings. A.R.C. 19,459. February, 1957.
6	W. T. Lord and G. G. Brebner	Supersonic flow past narrow wings with 'similar' cross-sections at zero lift. (Unpublished M.o.S. Report.)
7	J. Weber	Slender delta wings with sharp edges at zero lift. A.R.C. 19,549. May, 1957.
8	J. Weber	The pressure distribution over a 'gothic wing' at zero lift in supersonic flow. A.R.C. 19,457. February, 1957.
9	D. H. Peckham and S. A. Atkinson	Preliminary results of low-speed wind-tunnel tests on a gothic wing of aspect ratio 1·0. A.R.C. 19,632. April, 1957.
10	R. L. Maltby and D. H. Peckham	Low-speed flow studies of the vortex patterns above inclined slender bodies using a new smoke technique. A.R.C. 19,541. November, 1956.

TABLE 1
Details of Flat-Plate Wings

Model	<i>A</i>	$\frac{s}{c_0}$	$\frac{S}{bc_0}$	$\frac{\bar{c}}{c_0}$	$\frac{l_{1/4}}{c_0}$	$\varphi_{L.E.}$ (deg)	$\varphi_{T.E.}$ (deg)
1	0.75	0.250	0.667	0.750	0.438	63.4	0
2, 2A	1.00	0.333	0.667	0.750	0.438	56.3	0
3	1.25	0.417	0.667	0.750	0.438	49.1	0
4	0.94	0.333	0.711	0.816	0.449	56.3	-15
5	1.07	0.333	0.622	0.693	0.427	56.3	15
6	1.17	0.333	0.571	0.628	0.416	56.3	30
7	1.60	0.333	0.417	0.440	0.390	56.3	56.3
8, 8A	1.00	0.250	0.500	0.667	0.500	76.0	0
9	1.33	0.333	0.500	0.667	0.500	71.6	0
10	1.67	0.417	0.500	0.667	0.500	67.4	0
11	1.13	0.333	0.592	0.693	0.480	67.4	0
12	0.76	0.250	0.657	0.739	0.446	67.4	0

Note.—For gothic wings, $\varphi_{L.E.}$ is the sweep of the leading edge at the wing apex.

TABLE 2
Wing B
Coefficients of Overall Lift, Drag and Pitching Moment at Zero Yaw

$V = 152 \text{ ft/sec}$		$R = 3.8 \times 10^6$	
α	C_L	C_D	C_m
- 2.02	-0.031	0.0077	+0.0015
- 1.01	-0.013	0.0074	-0.0008
0	+0.002	0.0068	-0.0016
+ 1.01	0.020	0.0075	-0.0046
2.02	0.033	0.0083	-0.0044
3.04	0.054	0.0091	-0.0076
4.05	0.077	0.0106	-0.0120
5.07	0.102	0.0131	-0.0176
6.09	0.130	0.0168	-0.0244
7.11	0.158	0.0213	-0.0303
8.13	0.187	0.0270	-0.0368
10.17	0.250	0.0420	-0.0506
12.22	0.316	0.0623	-0.0633
14.26	0.385	0.0877	-0.0764
16.31	0.458	0.1198	-0.0900
18.36	0.531	0.1573	-0.1033
20.42	0.611	0.2036	-0.1181
22.47	0.694	0.2588	-0.1342
24.53	0.782	0.3232	-0.1512
26.59	0.864	0.3935	-0.1663
28.64	0.943	0.4700	-0.1808
+ 30.70	+1.022	0.5587	-0.1972

$V = 102 \text{ ft/sec}$		$R = 2.6 \times 10^6$	
α	C_L	C_D	C_m
32.75	1.101	0.6475	-0.2105
34.80	1.168	0.7484	-0.2225
36.84	1.233	0.8557	-0.2340

TABLE 3
Wing B
Coefficients of Overall Side Force, Rolling Moment and Yawing Moment

$\alpha = 0 \text{ deg}$		$V = 152 \text{ ft/sec}$			$R = 3.8 \times 10^6$		
β	C_L	C_D	C_m	C_Y	C_l	C_n	
+ 5.0	0	0.0075	-0.0007	-0.0019	+0.0002	-0.0032	
+ 2.5	+0.001	0.0070	-0.0008	-0.0007	+0.0001	-0.0019	
0	+0.003	0.0061	-0.0013	+0.0004	0	0	
- 2.5	0	0.0066	0	0.0011	0	+0.0022	
- 5.0	0	0.0066	-0.0003	0.0023	0	0.0044	
-10.0	0	0.0063	-0.0004	0.0062	-0.0002	0.0097	
-15.0	-0.001	0.0064	-0.0001	+0.0136	-0.0003	+0.0154	

$\alpha = 4.05 \text{ deg}$		$V = 152 \text{ ft/sec}$			$R = 3.8 \times 10^6$		
β	C_L	C_D	C_m	C_Y	C_l	C_n	
+ 5.0	0.082	0.0113	-0.0142	-0.0027	-0.0031	-0.0027	
+ 2.5	0.080	0.0105	-0.0132	-0.0005	-0.0016	-0.0014	
0	0.076	0.0095	-0.0115	+0.0004	0	+0.0007	
- 2.5	0.079	0.0099	-0.0129	0.0012	+0.0015	0.0028	
- 5.0	0.080	0.0100	-0.0134	0.0021	0.0032	0.0051	
-10.0	0.079	0.0102	-0.0138	0.0059	0.0062	0.0102	
-15.0	0.078	0.0104	-0.0145	+0.0131	+0.0092	+0.0159	

$\alpha = 8.13 \text{ deg}$		$V = 152 \text{ ft/sec}$			$R = 3.8 \times 10^6$		
β	C_L	C_D	C_m	C_Y	C_l	C_n	
+ 5.0	0.192	0.0274	-0.0391	+0.0001	-0.0072	-0.0032	
+ 2.5	0.192	0.0268	-0.0384	+0.0009	-0.0024	-0.0016	
0	0.188	0.0261	-0.0365	0	+0.0008	+0.0008	
- 2.5	0.190	0.0262	-0.0378	-0.0006	0.0038	0.0033	
- 5.0	0.191	0.0260	-0.0385	-0.0006	0.0075	0.0056	
-10.0	0.183	0.0250	-0.0355	+0.0011	0.0148	0.0117	
-15.0	0.174	0.0242	-0.0336	+0.0024	+0.0204	+0.0178	

TABLE 3—*continued*

Wing B

$\alpha = 12 \cdot 22 \text{ deg}$		$V = 152 \text{ ft/sec}$			$R = 3 \cdot 8 \times 10^6$	
β	C_L	C_D	C_m	C_Y	C_l	C_n
+ 5·0	0·322	0·0631	-0·0659	+0·0040	-0·0139	-0·0017
+ 2·5	0·321	0·0624	-0·0651	+0·0027	-0·0072	-0·0005
0	0·317	0·0613	-0·0630	-0·0004	+0·0004	+0·0012
- 2·5	0·320	0·0620	-0·0653	-0·0035	0·0079	0·0028
- 5·0	0·322	0·0621	-0·0653	-0·0057	0·0150	0·0046
-10·0	0·313	0·0598	-0·0636	-0·0082	0·0269	0·0094
-15·0	0·293	0·0555	-0·0569	-0·0059	+0·0351	+0·0152

$\alpha = 16 \cdot 31 \text{ deg}$		$V = 152 \text{ ft/sec}$			$R = 3 \cdot 8 \times 10^6$	
β	C_L	C_D	C_m	C_Y	C_l	C_n
+ 5·0	0·467	0·1217	-0·0940	+0·0113	-0·0221	0·0005
+ 2·5	0·461	0·1200	-0·0917	+0·0059	-0·0116	0·0005
0	0·458	0·1185	-0·0898	-0·0017	+0·0002	0·0012
- 2·5	0·460	0·1195	-0·0917	-0·0093	0·0124	0·0021
- 5·0	0·462	0·1204	-0·0940	-0·0157	0·0246	0·0030
-10·0	0·460	0·1189	-0·0951	-0·0248	+0·0424	0·0052

$\alpha = 20 \cdot 42 \text{ deg}$		$V = 152 \text{ ft/sec}$			$R = 3 \cdot 8 \times 10^6$	
β	C_L	C_D	C_m	C_Y	C_l	C_n
+ 5·0	0·623	0·2085	-0·1233	+0·0220	-0·0302	+0·0042
+ 2·5	0·620	0·2069	-0·1219	+0·0092	-0·0148	0·0030
0	0·613	0·2035	-0·1181	-0·0050	+0·0014	0·0019
- 2·5	0·618	0·2055	-0·1215	-0·0184	0·0175	0·0009
- 5·0	0·620	0·2060	-0·1231	-0·0310	0·0326	+0·0003
-10·0	0·608	0·2011	-0·1191	-0·0494	+0·0556	-0·0005

TABLE 3—*continued**Wing B*

$\alpha = 24 \cdot 53 \text{ deg}$		$V = 102 \text{ ft/sec}$		$R = 2 \cdot 6 \times 10^6$		
β	C_L	C_D	C_m	C_Y	C_l	C_n
+ 5·0	0·780	0·3201	-0·1501	+0·0378	-0·0378	+0·0087
+ 2·5	0·778	0·3172	-0·1487	+0·0176	-0·0187	0·0043
0	0·780	0·3161	-0·1489	-0·0074	+0·0025	+0·0010
- 2·5	0·774	0·3142	-0·1478	-0·0317	0·0231	-0·0020
- 5·0	0·779	0·3152	-0·1490	-0·0541	+0·0428	-0·0049

$\alpha = 28 \cdot 64 \text{ deg}$		$V = 102 \text{ ft/sec}$		$R = 2 \cdot 6 \times 10^6$		
β	C_L	C_D	C_m	C_Y	C_l	C_n
+ 5·0	0·944	0·4646	-0·1911	+0·0557	-0·0444	+0·0155
+ 2·5	0·943	0·4631	-0·1923	+0·0233	-0·0218	0·0077
0	0·944	0·4634	-0·1924	-0·0148	+0·0047	+0·0007
- 2·5	0·938	0·4617	-0·1913	-0·0704	0·0287	-0·0054
- 5·0	0·932	0·4584	-0·1892	-0·1220	+0·0518	-0·0115

$\alpha = 32 \cdot 75 \text{ deg}$		$V = 102 \text{ ft/sec}$		$R = 2 \cdot 6 \times 10^6$		
β	C_L	C_D	C_m	C_Y	C_l	C_n
+ 2·5	1·111	0·653	-0·2141	+0·0306	-0·0249	+0·0148
0	1·106	0·649	-0·2116	-0·0260	+0·0084	+0·0025
- 2·5	1·100	0·647	-0·2121	-0·0764	+0·0382	-0·0082

TABLE 4

*Wing B**Lateral Derivatives*

α	C_L	$\frac{dC_Y}{d\beta}$	$\frac{dC_l}{d\beta}$	$\frac{dC_n}{d\beta}$
0	0.003	-0.021	0	-0.047
4.05	0.076	-0.020	-0.036	-0.048
8.13	0.188	+0.017	-0.071	-0.056
12.22	0.317	0.071	-0.173	-0.038
16.31	0.458	0.174	-0.275	-0.018
20.42	0.613	0.316	-0.370	+0.024
24.53	0.780	0.565	-0.479	0.072
28.64	0.944	1.075	-0.579	0.150
32.75	1.106	+1.227	-0.724	+0.264

TABLE 5
Wing C
Coefficients of Overall Lift, Drag and Pitching Moment at Zero Yaw

$V = 102 \text{ ft/sec}$		$R = 2.6 \times 10^6$		$V = 152 \text{ ft/sec}$		$R = 3.8 \times 10^6$	
α	C_L	C_D	C_m	α	C_L	C_D	C_m
- 1.82	-0.037	0.0089	+0.0048	- 1.83	-0.040	0.0095	+0.0071
- 0.81	-0.009	0.0078	-0.0004	- 0.81	-0.016	0.0085	0.0021
+ 0.20	+0.006	0.0065	-0.0033	+ 0.20	+0.004	0.0075	+0.0016
1.22	0.024	0.0085	-0.0049	1.22	0.024	0.0089	-0.0049
2.23	0.046	0.0099	-0.0094	2.23	0.047	0.0100	-0.0099
3.25	0.071	0.0115	-0.0148	3.25	0.073	0.0121	-0.0159
4.27	0.100	0.0142	-0.0211	4.27	0.101	0.0146	-0.0218
5.29	0.128	0.0180	-0.0269	5.29	0.129	0.0182	-0.0275
6.31	0.160	0.0228	-0.0336	6.31	0.161	0.0229	-0.0341
7.33	0.189	0.0277	-0.0396	7.33	0.191	0.0284	-0.0403
8.35	0.225	0.0350	-0.0472	8.35	0.225	0.0356	-0.0473
10.40	0.292	0.0532	-0.0607	10.40	0.295	0.0540	-0.0609
12.45	0.365	0.0773	-0.0750	12.45	0.368	0.0780	-0.0751
14.50	0.446	0.1090	-0.0909	14.51	0.448	0.1103	-0.0906
16.56	0.524	0.1467	-0.1055	16.56	0.530	0.1485	-0.1060
18.62	0.608	0.1917	-0.1215	18.62	0.615	0.1944	-0.1222
20.68	0.697	0.2478	-0.1377	20.68	0.701	0.2489	-0.1383
22.74	0.784	0.3060	-0.1545	22.74	0.790	0.3109	-0.1558
24.80	0.874	0.3767	-0.1710	24.80	0.878	0.3818	-0.1731
26.86	0.959	0.4532	-0.1881	26.86	0.967	0.4612	-0.1905
28.92	1.047	0.5423	-0.2080	+28.92	+1.053	0.5494	-0.2071
30.97	1.128	0.6334	-0.2230				
33.03	1.208	0.7326	-0.2390				
35.09	1.268	0.8305	-0.2517				
37.11	1.334	0.9360	-0.2665				
+39.14	+1.381	1.0488	-0.2779				

$V = 303 \text{ ft/sec}$		$R = 7.6 \times 10^6$		$V = 202 \text{ ft/sec}$		$R = 5.1 \times 10^6$	
α	C_L	C_D	C_m	α	C_L	C_D	C_m
- 1.93	-0.044	0.0078	+0.0096	- 1.83	-0.043	0.0069	+0.0079
- 0.91	-0.020	0.0068	0.0047	- 0.81	-0.018	0.0060	+0.0023
+ 0.15	+0.003	0.0065	+0.0003	+ 0.20	+0.004	0.0054	-0.0020
1.17	0.025	0.0070	-0.0039	1.22	0.025	0.0064	-0.0057
2.23	0.049	0.0078	-0.0088	2.23	0.049	0.0073	-0.0098
3.30	0.076	0.0097	-0.0144	3.25	0.075	0.0093	-0.0165
4.32	0.103	0.0124	-0.0199	4.27	0.102	0.0119	-0.0222
5.29	0.132	0.0162	-0.0258	5.29	0.132	0.0157	-0.0282
6.41	0.162	0.0211	-0.0320	6.31	0.162	0.0204	-0.0346
7.43	0.195	0.0271	-0.0386	7.33	0.193	0.0262	-0.0409
8.56	0.229	0.0347	-0.0453	8.35	0.227	0.0336	-0.0477
+10.60	+0.299	0.0541	-0.0591	10.40	0.296	0.0524	-0.0615
				12.45	0.370	0.0767	-0.0759
				14.51	0.451	0.1094	-0.0917
				16.56	0.533	0.1482	-0.1073
				18.62	0.619	0.1950	-0.1234
				+20.68	+0.706	0.2508	-0.1400

TABLE 6
Wing C
Coefficients of Overall Side Force, Rolling Moment and Yawing Moment

$\alpha = 0 \text{ deg}$		$V = 152 \text{ ft/sec}$		$R = 3.8 \times 10^6$		
β	C_L	C_D	C_m	C_Y	C_l	C_n
+ 5.0	+0.003	0.0083	-0.0012	-0.0028	-0.0004	-0.0024
+ 2.5	0.003	0.0080	-0.0013	-0.0011	-0.0004	-0.0002
0	0.003	0.0072	-0.0018	-0.0004	-0.0004	+0.0019
- 2.5	0.002	0.0077	-0.0010	+0.0007	-0.0005	0.0039
- 5.0	+0.001	0.0076	-0.0006	0.0028	-0.0006	0.0061
-10.0	0	0.0074	-0.0001	0.0102	-0.0007	0.0111
-15.0	-0.002	0.0074	+0.0005	+0.0239	-0.0008	+0.0166

$\alpha = 4.07 \text{ deg}$		$V = 152 \text{ ft/sec}$		$R = 3.8 \times 10^6$		
β	C_L	C_D	C_m	C_Y	C_l	C_n
+ 5.0	0.102	0.0141	-0.0216	-0.0034	-0.0047	-0.0019
+ 2.5	0.101	0.0139	-0.0216	-0.0014	-0.0026	+0.0001
0	0.101	0.0137	-0.0213	-0.0004	-0.0004	0.0019
- 2.5	0.101	0.0137	-0.0215	+0.0002	+0.0019	0.0040
- 5.0	0.100	0.0136	-0.0212	0.0020	0.0040	0.0059
-10.0	0.096	0.0138	-0.0203	0.0096	0.0079	0.0106
-15.0	0.091	0.0136	-0.0196	+0.0229	+0.0108	+0.0162

$\alpha = 8.15 \text{ deg}$		$V = 152 \text{ ft/sec}$		$R = 3.8 \times 10^6$		
β	C_L	C_D	C_m	C_Y	C_l	C_n
+ 5.0	0.222	0.0339	-0.0468	-0.0022	-0.0098	-0.0013
+ 2.5	0.221	0.0338	-0.0465	-0.0011	-0.0051	+0.0006
0	0.220	0.0335	-0.0458	-0.0012	0	0.0021
- 2.5	0.220	0.0337	-0.0462	-0.0010	+0.0050	0.0038
- 5.0	0.220	0.0336	-0.0463	-0.0004	0.0097	0.0056
-10.0	0.215	0.0334	-0.0456	+0.0055	0.0183	0.0101
-15.0	0.207	0.0368	-0.0452	+0.0009	+0.0250	+0.0192

TABLE 6—*continued**Wing C*

$\alpha = 12.25 \text{ deg}$		$V = 152 \text{ ft/sec}$		$R = 3.8 \times 10^6$		
β	C_L	C_D	C_m	C_Y	C_l	C_n
+ 5.0	0.364	0.0749	-0.0793	+0.0014	-0.0159	0.0004
+ 2.5	0.364	0.0748	-0.0795	0	-0.0078	0.0016
0	0.362	0.0746	-0.0796	-0.0017	+0.0004	0.0024
- 2.5	0.362	0.0744	-0.0791	-0.0039	0.0085	0.0033
- 5.0	0.361	0.0742	-0.0783	-0.0048	0.0166	0.0045
- 10.0	0.355	0.0733	-0.0768	-0.0028	0.0304	0.0077
- 15.0	0.342	0.0708	-0.0735	+0.0060	+0.0410	0.0122

$\alpha = 16.36 \text{ deg}$		$V = 152 \text{ ft/sec}$		$R = 3.8 \times 10^6$		
β	C_L	C_D	C_m	C_Y	C_l	C_n
+ 5.0	0.524	0.1427	-0.1063	+0.0071	-0.0226	0.0029
+ 2.5	0.522	0.1425	-0.1056	+0.0025	-0.0109	0.0029
0	0.521	0.1421	-0.1045	-0.0025	+0.0009	0.0025
- 2.5	0.521	0.1425	-0.1055	-0.0079	0.0128	0.0022
- 5.0	0.522	0.1421	-0.1062	-0.0120	0.0242	0.0020
- 10.0	0.512	0.1394	-0.1043	-0.0161	0.0441	0.0033
- 15.0	0.509	0.1400	-0.0880	-0.0066	+0.0433	0.0016

$\alpha = 20.47 \text{ deg}$		$V = 152 \text{ ft/sec}$		$R = 3.8 \times 10^6$		
β	C_L	C_D	C_m	C_Y	C_l	C_n
+ 5.0	0.695	0.2412	-0.1380	+0.0137	-0.0237	+0.0072
+ 2.5	0.695	0.2409	-0.1377	+0.0044	-0.0136	0.0055
0	0.693	0.2397	-0.1368	-0.0066	+0.0026	0.0032
- 2.5	0.692	0.2398	-0.1372	-0.0162	0.0183	+0.0008
- 5.0	0.694	0.2396	-0.1379	-0.0250	0.0330	-0.0010
- 10.0	0.662	0.2287	-0.1246	-0.0351	0.0544	-0.0029
- 15.0	0.599	0.2113	-0.1071	-0.0317	+0.0591	-0.0011

TABLE 6—*continued**Wing C*

$\alpha = 24 \cdot 59 \text{ deg}$		$V = 102 \text{ ft/sec}$		$R = 2 \cdot 6 \times 10^6$		
β	C_L	C_D	C_m	C_Y	C_l	C_n
+ 5·0	0·862	0·3622	-0·1684	+0·0251	-0·0351	+0·0122
+ 2·5	0·869	0·3644	-0·1704	+0·0091	-0·0167	0·0082
0	0·863	0·3612	-0·1687	-0·0102	+0·0046	+0·0040
- 2·5	0·861	0·3617	-0·1686	-0·0297	0·0243	-0·0011
- 5·0	0·861	0·3617	-0·1689	-0·0447	0·0428	-0·0052
- 10·0	0·783	0·3325	-0·1406	-0·0553	0·0556	-0·0101
- 15·0	0·708	0·3071	-0·1196	-0·0484	+0·0573	-0·0101

$\alpha = 28 \cdot 71 \text{ deg}$		$V = 102 \text{ ft/sec}$		$R = 2 \cdot 6 \times 10^6$		
β	C_L	C_D	C_m	C_Y	C_l	C_n
+ 5·0	1·033	0·5213	-0·2006	+0·0400	-0·0420	+0·0186
+ 2·5	1·043	0·5266	-0·2052	+0·0151	-0·0201	0·0116
0	1·041	0·5253	-0·2052	-0·0158	+0·0064	+0·0029
- 2·5	1·036	0·5229	-0·2028	-0·0440	0·0315	-0·0051
- 5·0	1·031	0·5198	-0·2002	-0·0691	0·0530	-0·0122
- 10·0	0·878	0·4536	-0·1507	-0·0670	+0·0500	-0·0187

$\alpha = 32 \cdot 82 \text{ deg}$		$V = 102 \text{ ft/sec}$		$R = 2 \cdot 6 \times 10^6$		
β	C_L	C_D	C_m	C_Y	C_l	C_n
+ 5·0	1·118	0·6683	-0·2084	+0·0430	-0·0334	+0·0254
+ 2·5	1·200	0·7157	-0·2366	+0·0226	-0·0231	0·0161
0	1·197	0·7131	-0·2368	-0·0223	+0·0094	+0·0016
- 2·5	1·197	0·7139	-0·2362	-0·0635	0·0404	-0·0109
- 5·0	1·075	0·6480	-0·1973	-0·0718	+0·0414	-0·0178

TABLE 7
Wing C
Lateral Derivatives

α	C_L	$\frac{dC_Y}{d\beta}$	$\frac{dC_l}{d\beta}$	$\frac{dC_n}{d\beta}$
0	0.003	-0.021	0	-0.047
4.07	0.101	-0.018	-0.052	-0.045
8.15	0.220	-0.001	-0.115	-0.037
12.25	0.362	+0.045	-0.187	-0.019
16.36	0.521	0.120	-0.271	+0.008
20.47	0.693	0.236	-0.365	0.054
24.59	0.863	0.445	-0.470	0.108
28.71	1.041	0.675	-0.590	0.192
32.82	1.197	+0.986	-0.726	+0.310

TABLE 8

Flat-Plate Wings 1 to 12. Coefficients of Overall Lift, Drag and Pitching Moment at Zero Yaw

Wing 1				Wing 2			
α	C_L	C_D	C_m	α	C_L	C_D	C_m
- 1.07	-0.071	0.0082	+0.0321	- 1.12	-0.097	0.0090	+0.0432
- 0.05	-0.051	0.0077	0.0314	- 0.09	-0.070	0.0082	0.0420
+ 0.97	-0.028	0.0075	0.0302	+ 0.95	-0.042	0.0078	0.0407
2.00	-0.002	0.0081	0.0287	1.99	-0.012	0.0083	0.0396
3.02	+0.024	0.0097	0.0275	3.03	+0.022	0.0102	0.0378
4.05	0.054	0.0125	0.0253	4.07	0.057	0.0143	0.0359
5.08	0.086	0.0167	0.0232	5.12	0.095	0.0189	0.0334
6.11	0.119	0.0219	0.0210	6.17	0.134	0.0251	0.0309
7.15	0.155	0.0286	0.0182	7.22	0.173	0.0324	0.0294
8.18	0.191	0.0366	0.0161	8.27	0.213	0.0414	0.0273
10.26	0.266	0.0578	0.0101	10.39	0.303	0.0664	0.0212
12.33	0.349	0.0863	+0.0036	12.51	0.400	0.1000	0.0144
14.42	0.438	0.1229	-0.0047	14.64	0.497	0.1409	+0.0067
16.51	0.532	0.1695	-0.0128	16.77	0.602	0.1927	-0.0014
18.61	0.630	0.2252	-0.0217	+18.91	+0.711	0.2551	-0.0100
+20.70	+0.730	0.2905	-0.0311				

Wing 3				Wing 4			
α	C_L	C_D	C_m	α	C_L	C_D	C_m
- 1.18	-0.112	0.0085	0.0377	- 1.14	-0.094	0.0089	+0.0355
- 0.13	-0.080	0.0089	0.0365	- 0.10	-0.068	0.0081	0.0346
+ 0.93	-0.045	0.0090	0.0359	+ 0.94	-0.043	0.0075	0.0340
1.99	-0.006	0.0094	0.0347	1.98	-0.015	0.0080	0.0333
3.05	+0.034	0.0124	0.0335	3.02	+0.016	0.0094	0.0325
4.12	0.076	0.0166	0.0322	4.07	0.048	0.0124	0.0310
5.19	0.119	0.0218	0.0303	5.12	0.085	0.0168	0.0297
6.26	0.164	0.0301	0.0283	6.18	0.122	0.0224	0.0278
7.33	0.207	0.0386	0.0266	7.23	0.161	0.0295	0.0261
8.40	0.252	0.0491	0.0262	8.29	0.199	0.0379	0.0247
10.56	0.348	0.0768	0.0222	10.41	0.284	0.0612	0.0197
12.72	0.450	0.1134	0.0168	12.55	0.377	0.0925	0.0139
+14.88	+0.551	0.1583	0.0111	14.69	0.475	0.1336	+0.0067

TABLE 8—*continued*

Wing 5

α	C_L	C_D	C_m
- 1.12	-0.103	0.0091	+0.0403
- 0.09	-0.074	0.0083	0.0389
+ 0.95	-0.046	0.0077	0.0378
1.98	-0.015	0.0083	0.0360
3.02	+0.019	0.0100	0.0342
4.06	0.054	0.0130	0.0320
5.11	0.093	0.0176	0.0299
6.16	0.134	0.0239	0.0271
7.21	0.176	0.0316	0.0248
8.26	0.217	0.0405	0.0231
10.36	0.305	0.0653	0.0178
12.48	0.402	0.0979	0.0121
14.60	0.503	0.1404	+0.0045
16.73	0.606	0.1918	-0.0024
18.86	0.714	0.2531	-0.0100
+20.98	+0.821	0.3186	-0.0170

Wing 6

α	C_L	C_D	C_m
- 1.11	-0.101	0.0088	+0.0411
- 0.08	-0.071	0.0081	0.0386
+ 0.95	-0.043	0.0077	0.0368
1.99	-0.009	0.0083	0.0339
3.03	+0.026	0.0102	0.0309
4.07	0.064	0.0136	0.0275
5.11	0.104	0.0186	0.0240
6.16	0.148	0.0253	0.0205
7.20	0.190	0.0330	0.0175
8.25	0.232	0.0426	0.0145
10.35	0.324	0.0682	0.0076
12.45	0.418	0.1021	+0.0005
14.56	0.520	0.1441	-0.0077
16.67	0.624	0.1961	-0.0162
18.78	0.732	0.2585	-0.0247
+20.89	+0.826	0.3261	-0.0292

Wing 7

α	C_L	C_D	C_m
- 1.06	-0.090	0.0074	0.0289
- 0.04	-0.058	0.0071	0.0272
+ 0.98	-0.025	0.0073	0.0269
2.01	+0.013	0.0086	0.0249
3.04	0.053	0.0114	0.0233
4.07	0.095	0.0160	0.0210
5.10	0.140	0.0222	0.0190
6.13	0.184	0.0298	0.0184
7.17	0.229	0.0389	0.0176
8.19	0.272	0.0495	0.0195
10.26	0.365	0.0772	0.0216
12.33	0.458	0.1126	0.0263
14.39	0.548	0.1543	0.0333
16.46	0.642	0.2047	0.0384
18.53	0.732	0.2614	0.0481
+20.60	+0.823	0.3276	0.0580

Wing 8

α	C_L	C_D	C_m
- 1.06	-0.092	0.0087	+0.0448
- 0.05	-0.071	0.0080	0.0421
+ 0.97	-0.046	0.0075	0.0381
1.99	-0.018	0.0082	0.0333
3.01	+0.012	0.0096	0.0289
4.03	0.041	0.0122	0.0243
5.05	0.073	0.0161	0.0197
6.07	0.107	0.0226	0.0147
7.10	0.141	0.0280	0.0101
8.12	0.178	0.0364	+0.0050
10.17	0.251	0.0575	-0.0044
12.23	0.334	0.0853	-0.0151
14.28	0.416	0.1188	-0.0258
16.34	0.504	0.1615	-0.0368
18.41	0.594	0.2114	-0.0483
+20.47	+0.684	0.2710	-0.0596

TABLE 8—*continued*

Wing 9

α	C_L	C_D	C_m
- 1.10	-0.102	0.0083	+0.0496
- 0.07	-0.075	0.0079	0.0457
+ 0.96	-0.047	0.0077	0.0421
1.99	-0.014	0.0087	0.0375
3.02	+0.022	0.0106	0.0326
4.05	0.056	0.0143	0.0283
5.09	0.094	0.0191	0.0236
6.13	0.134	0.0254	0.0184
7.17	0.175	0.0336	0.0136
8.21	0.214	0.0429	+0.0093
10.29	0.303	0.0680	-0.0010
12.31	0.395	0.0997	-0.0107
14.47	0.490	0.1408	-0.0203
16.56	0.586	0.1902	-0.0299
18.66	0.690	0.2492	-0.0401
+20.76	+0.791	0.3198	-0.0499

Wing 10

α	C_L	C_D	C_m
- 1.15	-0.129	0.0091	+0.0556
- 0.11	-0.095	0.0086	0.0515
+ 0.93	-0.060	0.0083	0.0472
1.97	-0.022	0.0089	0.0422
3.02	+0.019	0.0111	0.0376
4.07	0.060	0.0149	0.0326
5.13	0.105	0.0203	0.0279
6.18	0.151	0.0278	0.0229
7.24	0.196	0.0368	0.0183
8.29	0.242	0.0473	0.0135
10.41	0.339	0.0748	+0.0041
12.53	0.441	0.1110	-0.0057
14.66	0.547	0.1568	-0.0150
16.79	0.655	0.2125	-0.0238
18.92	0.760	0.2700	-0.0310
+21.04	+0.863	0.3434	-0.0378

Wing 11

α	C_L	C_D	C_m
- 1.12	-0.106	0.0086	+0.0434
- 0.09	-0.078	0.0084	0.0407
+ 0.95	-0.048	0.0078	0.0388
1.98	-0.016	0.0085	0.0360
3.02	+0.014	0.0098	0.0336
4.06	0.056	0.0136	0.0303
5.11	0.095	0.0183	0.0271
6.15	0.136	0.0246	0.0238
7.20	0.178	0.0325	0.0200
8.25	0.220	0.0423	0.0170
10.35	0.309	0.0668	0.0094
12.46	0.404	0.0998	+0.0009
14.58	0.507	0.1429	-0.0077
16.70	0.612	0.1955	-0.0167
18.82	0.716	0.2568	-0.0253
+20.93	+0.816	0.3236	-0.0344

Wing 12

α	C_L	C_D	C_m
- 1.08	-0.080	0.0080	+0.0339
- 0.06	-0.061	0.0075	0.0330
+ 0.96	-0.039	0.0070	0.0320
1.99	-0.014	0.0074	0.0308
3.01	+0.011	0.0087	0.0295
4.04	0.041	0.0111	0.0268
5.07	0.071	0.0147	0.0254
6.10	0.105	0.0200	0.0230
7.13	0.139	0.0262	0.0204
8.17	0.175	0.0342	0.0174
10.24	0.250	0.0547	0.0111
12.31	0.331	0.0817	+0.0041
14.40	0.420	0.1177	-0.0039
16.48	0.512	0.1624	-0.0125
18.58	0.609	0.2160	-0.0215
+20.66	+0.701	0.2742	-0.0311

TABLE 9

Flat-Plate Wings 2A, 8A. Coefficients of Overall Lift, Drag and Pitching Moment at Zero Yaw

Wing 2A				Wing 8A			
α	C_L	C_D	C_m	α	C_L	C_D	C_m
- 1.04	-0.035	0.0059	+0.0043	- 1.02	-0.028	0.0065	+0.0052
- 0.01	-0.005	0.0042	+0.0005	0	0	0.0051	-0.0005
+ 1.03	+0.027	0.0057	-0.0018	+ 1.02	+0.025	0.0065	-0.0048
2.06	0.050	0.0068	-0.0032	2.03	0.042	0.0073	-0.0060
3.10	0.077	0.0088	-0.0038	3.05	0.068	0.0096	-0.0103
4.14	0.111	0.0122	-0.0058	4.07	0.100	0.0128	-0.0162
5.19	0.149	0.0173	-0.0084	5.09	0.129	0.0171	-0.0206
6.24	0.187	0.0236	-0.0112	6.11	0.163	0.0228	-0.0262
7.29	0.226	0.0316	-0.0136	7.13	0.197	0.0295	-0.0314
8.34	0.267	0.0414	-0.0168	8.16	0.233	0.0383	-0.0366
10.46	0.355	0.0661	-0.0232	10.21	0.308	0.0596	-0.0468
12.57	0.447	0.0989	-0.0303	12.26	0.383	0.0868	-0.0564
14.70	0.546	0.1403	-0.0380	14.32	0.467	0.1216	-0.0674
16.83	0.649	0.1919	-0.0465	16.38	0.553	0.1639	-0.0779
+18.97	+0.753	0.2514	-0.0531	18.44	0.639	0.2149	-0.0888
				+20.50	+0.731	0.2753	-0.1001

TABLE 10

Flat-Plate Wings 2A, 8A. Lateral Derivatives

Wing 2A				Wing 8A			
α	$\frac{dC_Y}{d\beta}$	$\frac{dC_l}{d\beta}$	$\frac{dC_n}{d\beta}$	α	$\frac{dC_Y}{d\beta}$	$\frac{dC_l}{d\beta}$	$\frac{dC_n}{d\beta}$
0	0	-0.010	0.005	0	0	0.009	0.011
6.24	-0.006	-0.105	0.013	6.11	-0.002	-0.096	0.024
12.57	-0.009	-0.194	0.044	12.26	-0.003	-0.200	0.062
18.97	-0.018	-0.287	0.100	18.44	+0.016	-0.277	0.116

WING A

TABLE 11
Pressure Coefficients at Zero Yaw

 $\alpha = 0 \text{ deg}$ C_p

$\frac{x}{c_0}$	$\frac{y}{s(x)}$	0		0.1		0.2		0.3		0.4		0.5		0.55	
		U.S.	L.S.	U.S.	L.S.										
0.2	-0.003	-0.004	-0.003	-0.002	-0.003	-0.003	-0.002	+0.002	+0.006	+0.005	+0.012	+0.012	+0.016	+0.016	
0.4	-0.102	-0.127	-0.126	-0.114	-0.116	-0.124	-0.111	-0.118	-0.110	-0.103	-0.101	-0.101	-0.096	-0.099	
0.6	-0.148	-0.144	-0.154	-0.154	-0.149	-0.150	-0.148	-0.147	-0.145	-0.148	-0.132	-0.135	-0.126	-0.135	
0.8	-0.098	-0.091	-0.099	-0.085	-0.098	-0.094	-0.098	-0.098	-0.101	-0.096	-0.096	-0.092	-0.091	-0.092	
0.9	—	—	+0.002	-0.001	-0.001	-0.005	-0.012	-0.011	-0.023	-0.021	-0.019	-0.020	-0.024	-0.026	

29

$\frac{x}{c_0}$	$\frac{y}{s(x)}$	0.6		0.65		0.7		0.75		0.8		0.85		0.9	
		U.S.	L.S.	U.S.	L.S.										
0.2	+0.023	+0.019	+0.028	+0.023	+0.033	+0.024	+0.042	+0.033	+0.049	+0.037	+0.063	+0.050	+0.075	+0.071	
0.4	-0.091	-0.092	-0.084	-0.092	-0.081	-0.083	-0.070	-0.076	-0.064	-0.067	-0.052	-0.057	-0.038	-0.042	
0.6	-0.122	-0.130	-0.126	-0.124	-0.117	-0.114	-0.103	-0.115	-0.097	-0.108	-0.092	-0.097	-0.079	-0.087	
0.8	-0.092	-0.092	-0.092	-0.090	-0.085	-0.085	-0.080	-0.079	-0.077	-0.081	-0.071	-0.065	-0.062	-0.063	
0.9	-0.031	-0.029	-0.029	-0.037	-0.030	-0.038	-0.030	-0.036	-0.030	-0.037	-0.026	-0.034	-0.036	-0.019	

TABLE 11—*continued*

WING A

 $\alpha = 2.06 \text{ deg}$ C_p

$\frac{x}{c_0}$	$\frac{y}{s(x)}$	0		0.1		0.2		0.3		0.4		0.5		0.55	
		U.S.	L.S.	U.S.	L.S.										
0.2	-0.035	+0.035	-0.039	+0.039	-0.039	+0.038	-0.038	+0.046	-0.035	+0.048	-0.027	+0.056	-0.020	+0.062	
0.4	-0.128	-0.100	-0.147	-0.081	-0.143	-0.092	-0.138	-0.079	-0.135	-0.070	-0.134	-0.069	-0.127	-0.061	
0.6	-0.163	-0.129	-0.163	-0.135	-0.162	-0.132	-0.164	-0.125	-0.159	-0.122	-0.154	-0.113	-0.146	-0.108	
0.8	-0.098	-0.091	-0.095	-0.079	-0.101	-0.088	-0.100	-0.087	-0.104	-0.082	-0.105	-0.080	-0.099	-0.078	
0.9	—	—	+0.010	-0.001	+0.002	-0.007	-0.008	-0.008	-0.020	-0.014	-0.024	-0.016	-0.028	-0.016	

30

$\frac{x}{c_0}$	$\frac{y}{s(x)}$	0.6		0.65		0.7		0.75		0.8		0.85		0.9	
		U.S.	L.S.	U.S.	L.S.										
0.2	-0.018	+0.068	-0.012	+0.073	-0.011	+0.073	-0.009	+0.083	-0.011	+0.090	+0.012	+0.014	+0.016	+0.178	
0.4	-0.124	-0.054	-0.121	-0.049	-0.115	-0.036	-0.099	-0.027	-0.094	-0.021	-0.084	-0.008	-0.064	+0.012	
0.6	-0.146	-0.105	-0.149	-0.098	-0.142	-0.088	-0.132	-0.080	-0.124	-0.068	-0.125	-0.056	-0.093	-0.043	
0.8	-0.104	-0.074	-0.104	-0.071	-0.100	-0.068	-0.097	-0.061	-0.094	-0.058	-0.086	-0.044	-0.069	-0.039	
0.9	-0.036	-0.018	-0.035	-0.025	-0.038	-0.026	-0.041	-0.023	-0.040	-0.021	-0.035	-0.017	-0.041	-0.007	

TABLE 11—*continued*

WING A

 $\alpha = 4.14 \text{ deg}$ C_p

$\frac{x}{c_0}$	$\frac{y}{s(x)}$	0		0.1		0.2		0.3		0.4		0.5		0.55	
		U.S.	L.S.	U.S.	L.S.										
0.2	-0.080	+0.084	-0.079	+0.085	-0.078	0.083	-0.081	0.089	-0.074	+0.096	-0.071	+0.101	-0.063	+0.108	
0.4	-0.151	-0.061	-0.173	-0.048	-0.169	-0.057	-0.168	-0.047	-0.164	-0.034	-0.168	-0.034	-0.159	-0.024	
0.6	-0.176	-0.101	-0.181	-0.113	-0.179	-0.107	-0.182	-0.103	-0.180	-0.099	-0.178	-0.086	-0.167	-0.081	
0.8	-0.102	-0.074	-0.100	-0.069	-0.109	-0.075	-0.108	-0.075	-0.116	-0.070	-0.118	-0.065	-0.112	-0.061	
0.9	—	—	+0.011	0.003	+0.002	-0.001	-0.011	-0.005	-0.025	-0.008	-0.031	-0.006	-0.036	-0.005	

31

$\frac{x}{c_0}$	$\frac{y}{s(x)}$	0.6		0.65		0.7		0.75		0.8		0.85		0.9	
		U.S.	L.S.	U.S.	L.S.										
0.2	-0.061	+0.111	-0.051	+0.121	-0.047	+0.119	-0.024	+0.130	-0.009	+0.138	-0.217	+0.153	-0.334	+0.180	
0.4	-0.155	-0.018	-0.150	-0.009	-0.146	+0.004	-0.113	+0.013	-0.082	+0.018	-0.195	+0.038	-0.429	+0.054	
0.6	-0.167	-0.076	-0.170	-0.068	-0.163	-0.058	-0.138	-0.051	-0.099	-0.040	-0.231	-0.025	-0.421	-0.006	
0.8	-0.118	-0.058	-0.116	-0.052	-0.112	-0.048	-0.099	-0.038	-0.074	-0.040	-0.150	-0.021	-0.356	-0.017	
0.9	-0.048	-0.008	-0.043	-0.011	-0.047	-0.012	-0.044	-0.008	-0.026	-0.006	-0.065	-0.001	-0.269	+0.008	

TABLE 11—*continued*

WING A

 $\alpha = 6.23 \text{ deg}$ C_p

$\frac{x}{c_0}$	$\frac{y}{s(x)}$	0		0.1		0.2		0.3		0.4		0.5		0.55	
		U.S.	L.S.	U.S.	L.S.										
0.2	-0.120	+0.125	-0.116	+0.128	-0.117	+0.130	-0.121	+0.136	-0.117	+0.140	-0.108	+0.148	-0.099	+0.154	
0.4	-0.179	-0.032	-0.202	-0.014	-0.199	-0.021	-0.197	-0.010	-0.197	+0.003	-0.197	+0.007	-0.187	+0.016	
0.6	-0.194	-0.082	-0.199	-0.088	-0.196	-0.082	-0.202	-0.074	-0.200	-0.071	-0.196	-0.056	-0.187	-0.052	
0.8	-0.110	-0.068	-0.108	-0.057	-0.115	-0.063	-0.118	-0.060	-0.128	-0.051	-0.130	-0.046	-0.123	-0.041	
0.9	—	—	+0.009	+0.007	+0.003	+0.003	-0.015	+0.003	-0.033	0.003	-0.038	-0.005	+0.045	+0.006	

$\frac{x}{c_0}$	$\frac{y}{s(x)}$	0.6		0.65		0.7		0.75		0.8		0.85		0.9	
		U.S.	L.S.	U.S.	L.S.	U.S.	L.S.								
0.2	-0.089	+0.159	-0.064	+0.167	-0.027	+0.164	-0.021	+0.175	-0.441	+0.184	-0.623	0.195	-0.530	0.216	
0.4	-0.179	+0.022	-0.161	+0.030	-0.130	+0.041	-0.088	+0.052	-0.351	+0.058	-0.639	0.075	-0.593	0.090	
0.6	-0.183	-0.046	-0.180	-0.037	-0.155	-0.028	-0.115	-0.018	-0.249	-0.005	-0.618	0.005	-0.589	0.018	
0.8	-0.128	-0.039	-0.124	-0.031	-0.112	-0.028	-0.095	-0.017	-0.153	-0.013	-0.438	0	-0.504	0.003	
0.9	-0.055	+0.006	-0.048	+0.003	-0.049	+0.002	-0.044	+0.007	-0.076	+0.009	-0.263	0.012	-0.404	0.021	

TABLE 11—*continued*WING A $\alpha = 8.32 \text{ deg}$ C_p

$\frac{x}{c_0}$	$\frac{y}{s(x)}$	0		0.1		0.2		0.3		0.4		0.5		0.55	
		U.S.	L.S.	U.S.	L.S.										
0.2	-0.158	0.173	-0.158	+0.177	-0.158	+0.176	-0.163	+0.181	-0.153	+0.188	-0.141	+0.193	-0.123	+0.200	
0.4	-0.205	0.010	-0.230	+0.026	-0.226	+0.021	-0.226	+0.024	-0.223	+0.041	-0.222	+0.047	-0.206	+0.056	
0.6	-0.209	-0.053	-0.216	-0.059	-0.214	-0.052	-0.222	-0.046	-0.218	-0.040	-0.213	-0.025	-0.200	-0.020	
0.8	-0.116	-0.052	-0.117	-0.042	-0.123	-0.047	-0.130	-0.044	-0.136	-0.032	-0.142	-0.026	-0.132	-0.020	
0.9	—	—	+0.007	+0.015	-0.001	+0.012	-0.020	+0.011	-0.036	0.014	-0.045	0.018	-0.051	+0.020	

33

$\frac{x}{c_0}$	$\frac{y}{s(x)}$	0.6		0.65		0.7		0.75		0.8		0.85		0.9	
		U.S.	L.S.	U.S.	L.S.	U.S.	L.S.	U.S.	L.S.	U.S.	L.S.	U.S.	L.S.	U.S.	L.S.
0.2	-0.099	+0.204	-0.055	+0.210	-0.034	+0.209	-0.326	0.217	-0.907	0.227	-0.980	0.234	-0.693	0.248	
0.4	-0.188	+0.062	-0.155	+0.069	-0.118	0.080	-0.251	0.090	-0.744	0.099	-0.977	0.108	-0.708	0.119	
0.6	-0.190	-0.014	-0.179	-0.005	-0.152	+0.005	-0.213	0.012	-0.571	0.029	-0.914	0.033	-0.645	0.045	
0.8	-0.134	-0.017	-0.128	-0.009	-0.119	-0.004	-0.160	0.006	-0.367	0.012	-0.666	0.021	-0.530	0.023	
0.9	-0.060	+0.018	-0.052	+0.017	-0.060	+0.017	-0.090	0.020	-0.218	0.029	-0.441	0.027	-0.441	0.035	

TABLE 11—*continued*WING A $\alpha = 10.43 \text{ deg}$ C_p

$\frac{x}{c_0}$	$\frac{y}{s(x)}$	0		0.1		0.2		0.3		0.4		0.5		0.55	
		U.S.	L.S.	U.S.	L.S.										
0.2	-0.203	+0.221	-0.199	+0.224	-0.201	+0.225	-0.205	+0.227	-0.196	+0.232	-0.171	+0.237	-0.141	0.243	
0.4	-0.233	+0.048	-0.259	+0.063	-0.254	+0.061	-0.254	+0.063	-0.254	+0.075	-0.245	0.084	-0.220	0.092	
0.6	-0.230	-0.024	-0.235	-0.032	-0.233	-0.019	-0.242	-0.012	-0.239	-0.008	-0.231	+0.008	-0.213	0.012	
0.8	-0.129	-0.037	-0.127	-0.026	-0.135	-0.025	-0.143	-0.020	-0.154	-0.010	-0.157	-0.006	-0.146	0.001	
0.9	—	—	0	+0.022	-0.007	+0.022	-0.028	+0.025	-0.048	+0.026	-0.055	-0.029	-0.061	0.034	

$\frac{x}{c_0}$	$\frac{y}{s(x)}$	0.6		0.65		0.7		0.75		0.8		0.85		0.9	
		U.S.	L.S.	U.S.	L.S.										
0.2	-0.105	0.249	-0.064	0.255	-0.222	0.252	-0.783	0.259	-1.400	0.264	-1.248	0.268	-0.853	0.270	
0.4	-0.194	0.103	-0.159	0.109	-0.216	0.118	-0.618	0.125	-1.177	0.128	-1.221	0.137	-0.800	0.144	
0.6	-0.198	0.019	-0.190	0.027	-0.224	0.036	-0.479	0.044	-0.938	0.054	-1.120	0.060	-0.669	0.068	
0.8	-0.148	0.007	-0.148	0.015	-0.179	0.018	-0.324	0.028	-0.615	0.029	-0.916	0.040	-0.510	0.041	
0.9	-0.072	0.034	-0.071	0.031	-0.107	0.032	-0.201	0.035	-0.390	0.037	-0.563	0.041	-0.434	0.046	

WING A

TABLE 11—*continued* $\alpha = 15.73 \text{ deg}$ C_p

$\frac{x}{c_0}$	$\frac{y}{s(x)}$	0		0.1		0.2		0.3		0.4		0.5		0.55	
		U.S.	L.S.	U.S.	L.S.										
0.2	-0.319	0.339	-0.320	0.342	-0.319	0.338	-0.315	0.340	-0.283	0.347	-0.239	0.344	-0.209	0.346	
0.4	-0.319	0.152	-0.345	0.169	-0.344	0.162	-0.338	0.166	-0.318	0.180	-0.299	0.184	-0.284	0.189	
0.6	-0.295	0.057	-0.302	0.055	-0.306	0.060	-0.306	0.068	-0.289	0.082	-0.284	0.087	-0.279	0.095	
0.8	-0.182	0.014	-0.180	0.025	-0.191	0.023	-0.195	0.034	-0.199	0.053	-0.214	0.057	-0.220	0.065	
0.9	—	—	-0.031	0.050	-0.043	0.049	-0.064	0.052	-0.078	0.063	-0.102	0.068	-0.123	0.071	

35

$\frac{x}{c_0}$	$\frac{y}{s(x)}$	0.6		0.65		0.7		0.75		0.8		0.85		0.9	
		U.S.	L.S.	U.S.	L.S.										
0.2	-0.239	0.346	-0.492	0.349	-1.276	0.348	-2.197	0.347	-2.506	0.345	-1.566	0.336	-1.379	0.290	
0.4	-0.312	0.193	-0.501	0.197	-1.034	0.202	-1.783	0.206	-1.983	0.206	-1.277	0.198	-1.171	0.181	
0.6	-0.319	0.101	-0.478	0.107	-0.840	0.114	-1.363	0.119	-1.557	0.125	-1.100	0.119	-0.888	0.109	
0.8	-0.269	0.068	-0.375	0.078	-0.569	0.081	-0.845	0.090	-1.011	0.093	-0.854	0.090	-0.549	0.084	
0.9	-0.167	0.069	-0.230	0.070	-0.365	0.071	-0.539	0.074	-0.666	0.003	-0.627	0.076	-0.379	0.076	

TABLE 11—*continued*

WING A

 $\alpha = 21.06$ deg C_p

$\frac{x}{c_0}$	$\frac{y}{s(x)}$	0		0.1		0.2		0.3		0.4		0.5		0.55	
		U.S.	L.S.	U.S.	L.S.										
0.2	-0.461	0.469	-0.460	0.469	-0.453	0.461	-0.442	0.459	-0.405	0.451	-0.408	0.447	-0.513	0.443	
0.4	-0.424	0.272	-0.455	0.281	-0.448	0.276	-0.443	0.270	-0.436	0.202	-0.461	0.287	-0.559	0.288	
0.6	-0.388	0.157	-0.401	0.151	-0.397	0.158	-0.405	0.167	-0.407	0.170	-0.459	0.183	-0.553	0.186	
0.8	-0.258	0.082	-0.262	0.088	-0.271	0.094	-0.281	0.105	-0.308	0.113	-0.374	0.128	-0.447	0.134	
0.9	—	—	-0.088	0.091	-0.101	0.094	-0.123	0.102	-0.161	0.102	-0.215	0.114	-0.279	0.117	

$\frac{x}{c_0}$	$\frac{y}{s(x)}$	0.6		0.65		0.7		0.75		0.8		0.85		0.9	
		U.S.	L.S.	U.S.	L.S.										
0.2	-0.893	0.436	-1.696	0.423	-2.951	0.430	-3.587	0.420	-3.043	0.405	-2.019	0.382	-1.934	0.271	
0.4	-0.829	0.288	-1.377	0.284	-2.185	0.286	-2.697	0.278	-2.172	0.265	-1.588	0.244	-1.583	0.199	
0.6	-0.773	0.190	-1.169	0.190	-1.677	0.195	-2.001	0.193	-1.685	0.187	-1.177	0.175	-1.134	0.142	
0.8	-0.592	0.136	-0.795	0.138	-1.024	0.148	-1.204	0.150	-1.117	0.151	-0.786	0.143	-0.646	0.121	
0.9	-0.376	0.118	-0.497	0.114	-0.647	0.119	-0.770	0.104	-0.761	0.119	-0.604	0.116	-0.405	0.102	

TABLE 11—*continued*

WING A

 $\alpha = 26.46$ deg C_p

$\frac{x}{c_0}$	$\frac{y}{s(x)}$	0		0.1		0.2		0.3		0.4		0.5		0.55	
		U.S.	L.S.	U.S.	L.S.										
0.2	-0.632	0.577	-0.618	0.586	-0.604	0.573	-0.595	0.570	-0.603	0.536	-0.858	0.531	-1.291	0.520	
0.4	-0.556	0.376	-0.558	0.396	-0.551	0.396	-0.559	0.391	-0.585	0.365	-0.743	0.380	-1.077	0.377	
0.6	-0.509	0.243	-0.508	0.256	-0.505	0.268	-0.530	0.266	-0.585	0.247	-0.754	0.272	-0.966	0.273	
0.8	-0.362	0.142	-0.347	0.160	-0.367	0.176	-0.387	0.180	-0.461	0.173	-0.606	0.196	-0.713	0.202	
0.9	—	—	-0.128	0.139	-0.158	0.158	-0.195	0.155	-0.269	0.141	-0.358	0.160	-0.452	0.159	

37

$\frac{x}{c_0}$	$\frac{y}{s(x)}$	0.6		0.65		0.7		0.75		0.8		0.85		0.9	
		U.S.	L.S.	U.S.	L.S.										
0.2	-2.226	0.511	-3.488	0.491	-4.621	0.493	-4.570	0.470	-3.452	0.438	-2.645	0.395	-2.546	0.210	
0.4	-1.628	0.376	-2.341	0.366	-3.276	0.358	-3.674	0.338	-3.031	0.309	-2.020	0.273	-1.871	0.200	
0.6	-1.333	0.272	-1.809	0.273	-2.244	0.269	-2.381	0.263	-1.934	0.241	-1.413	0.220	-1.341	0.165	
0.8	-0.906	0.205	-1.134	0.209	-1.251	0.212	-1.305	0.216	-1.145	0.202	-0.809	0.195	-0.719	0.161	
0.9	-0.560	0.162	-0.680	0.163	-0.781	0.162	-0.830	0.166	-0.784	0.163	-0.616	0.163	-0.450	0.150	

TABLE 11—*continued*

WING A

 $\alpha = 31.65$ deg C_p

$\frac{x}{c_0}$	$\frac{y}{s(x)}$	0		0.1		0.2		0.3		0.4		0.5		0.55	
		U.S.	L.S.	U.S.	L.S.										
0.2	-0.748	0.710	-0.750	0.696	-0.745	0.679	-0.766	0.669	-0.885	0.641	-1.509	0.615	-2.311	0.590	
0.4	-0.639	0.513	-0.666	0.511	-0.664	0.504	-0.696	0.497	-0.794	0.490	-1.197	0.488	-1.716	0.467	
0.6	-0.632	0.365	-0.652	0.358	-0.664	0.364	-0.734	0.367	-0.871	0.371	-1.239	0.374	-1.544	0.361	
0.8	-0.480	0.245	-0.482	0.246	-0.510	0.251	-0.556	0.258	-0.675	0.272	-0.892	0.279	-1.047	0.273	
0.9	—	—	-0.224	0.208	-0.247	0.209	-0.296	0.213	-0.387	0.216	-0.530	0.222	-0.642	0.213	

38

$\frac{x}{c_0}$	$\frac{y}{s(x)}$	0.6		0.65		0.7		0.75		0.8		0.85		0.9	
		U.S.	L.S.	U.S.	L.S.										
0.2	-3.580	0.593	-4.958	0.548	-5.936	0.553	-5.600	0.513	-4.102	0.465	-3.099	0.399	-3.030	0.126	
0.4	-2.406	0.481	-3.199	0.450	-3.787	0.431	-3.642	0.411	-2.594	0.367	-2.120	0.311	-2.125	0.207	
0.6	-1.861	0.387	-2.189	0.362	-2.293	0.358	-2.128	0.340	-1.647	0.314	-1.401	0.272	-1.383	0.193	
0.8	-1.176	0.299	-1.315	0.289	-1.324	0.288	-1.258	0.284	-1.029	0.269	-0.819	0.248	-0.800	0.200	
0.9	-0.718	0.233	-0.823	0.216	-0.854	0.222	-0.843	0.220	-0.741	0.220	-0.598	0.213	-0.517	0.182	

WING B

TABLE 12
Pressure Coefficients at Zero Yaw

$\alpha = 0$ deg

C_p

$\frac{x}{c_0}$	$\frac{y}{s(x)}$	0		0.1		0.2		0.3		0.4		0.5		0.55	
		U.S.	L.S.	U.S.	L.S.										
0.10	+0.108	+0.094	+0.099	+0.094	+0.095	+0.091	+0.095	+0.086	+0.094	+0.094	+0.092	+0.088	+0.094	+0.093	
0.20	+0.048	+0.040	+0.042	+0.041	+0.041	+0.039	+0.044	+0.044	+0.046	0.045	+0.044	+0.042	0.048	0.047	
0.30	-0.007	-0.009	-0.011	-0.012	-0.010	-0.013	-0.006	0	0	+0.021	0	-0.008	+0.006	+0.014	
0.40	-0.052	-0.059	-0.056	-0.058	-0.058	-0.060	-0.054	-0.059	-0.049	-0.051	-0.046	-0.051	-0.039	-0.043	
0.50	-0.099	-0.099	-0.099	-0.106	-0.103	-0.105	-0.103	-0.102	-0.100	-0.102	-0.097	-0.098	-0.089	-0.090	
0.60	-0.137	-0.137	-0.141	-0.142	-0.146	-0.144	-0.144	-0.145	-0.147	-0.148	-0.144	-0.144	-0.137	-0.139	
0.70	-0.154	-0.149	-0.160	-0.156	-0.169	-0.162	-0.174	-0.165	-0.176	-0.174	-0.184	-0.177	-0.181	-0.176	
0.80	-0.137	-0.125	-0.140	-0.129	-0.155	-0.141	-0.162	-0.146	-0.172	-0.163	-0.187	-0.182	-0.194	-0.185	
0.90	-0.012	—	-0.032	-0.015	-0.045	-0.029	-0.057	-0.042	-0.076	-0.067	-0.100	-0.099	-0.113	-0.105	
0.95	+0.100	—	+0.087	—	+0.076	—	+0.065	—	+0.048	—	+0.019	—	+0.008	—	
0.98	—	—	+0.192	—	+0.175	—	+0.170	—	+0.162	—	+0.149	—	+0.144	—	

TABLE 12—*continued*WING B $\alpha = 0 \text{ deg}$ C_p

$\frac{x}{c_0}$	$\frac{y}{s(x)}$	0·6		0·65		0·7		0·75		0·8		0·85		0·9	
		U.S.	L.S.	U.S.	L.S.										
0·10	+0·094	+0·103	+0·094	+0·091	+0·094	+0·093	+0·094	+0·095	+0·095	+0·097	+0·101	+0·100	+0·106	+0·108	
0·20	0·048	0·050	0·054	0·050	0·053	0·052	0·064	0·054	0·060	0·059	0·065	0·061	0·059	0·065	
0·30	+0·014	+0·007	+0·012	+0·018	+0·016	+0·019	+0·020	+0·022	+0·029	+0·029	+0·032	+0·030	0·035	0·038	
0·40	-0·037	-0·040	-0·030	-0·034	-0·024	-0·025	-0·013	-0·021	-0·009	-0·011	-0·001	-0·005	+0·007	+0·008	
0·50	-0·084	-0·088	-0·075	-0·076	-0·071	-0·068	-0·059	-0·059	-0·046	-0·048	-0·038	-0·039	-0·024	-0·022	
0·60	-0·133	-0·137	-0·127	-0·126	-0·119	-0·122	-0·105	-0·109	-0·087	-0·091	-0·074	-0·076	-0·052	-0·059	
0·70	-0·181	-0·177	-0·176	-0·173	-0·170	-0·165	-0·158	-0·158	-0·141	-0·141	-0·123	-0·125	-0·093	-0·095	
0·80	-0·202	-0·195	-0·205	-0·199	-0·205	-0·201	-0·202	-0·202	-0·195	-0·196	-0·180	-0·178	-0·145	-0·151	
0·90	-0·133	-0·125	-0·147	-0·137	-0·169	-0·161	-0·184	-0·185	-0·206	-0·197	-0·213	-0·213	-0·209	-0·214	
0·95	-0·013	—	-0·036	—	-0·062	—	-0·197	—	-0·124	—	-0·164	—	-0·206	—	
0·98	+0·132	—	+0·117	—	+0·206	—	+0·080	—	+0·046	—	+0·003	—	-0·075	—	

TABLE 12—*continued*WING B $\alpha = 2.02 \text{ deg}$ C_p

$\frac{x}{c_0}$	$\frac{y}{s(x)}$	0		0.1		0.2		0.3		0.4		0.5		0.55	
		U.S.	L.S.	U.S.	L.S.										
0.10	+0.082	+0.120	+0.077	+0.121	+0.076	+0.117	+0.073	+0.104	+0.073	+0.115	+0.075	+0.110	+0.073	+0.114	
0.20	+0.030	0.063	+0.023	0.065	+0.024	0.064	+0.022	0.065	+0.024	0.067	+0.028	0.064	+0.029	0.068	
0.30	-0.029	+0.011	-0.028	+0.012	-0.026	+0.012	-0.028	+0.020	-0.024	+0.044	-0.022	+0.010	-0.018	+0.038	
0.40	-0.070	-0.038	-0.073	-0.037	-0.076	-0.036	-0.077	-0.037	-0.073	-0.026	-0.067	-0.025	-0.065	-0.017	
0.50	-0.115	-0.081	-0.115	-0.086	-0.120	-0.085	-0.124	-0.082	-0.122	-0.078	-0.119	-0.069	-0.114	-0.065	
0.60	-0.150	-0.122	-0.151	-0.124	-0.159	-0.123	-0.163	-0.127	-0.166	-0.125	-0.165	-0.114	-0.164	-0.112	
0.70	-0.162	-0.141	-0.165	-0.146	-0.175	-0.149	-0.185	-0.153	-0.193	-0.155	-0.199	-0.154	-0.201	-0.154	
0.80	-0.136	-0.124	-0.137	-0.124	-0.153	-0.133	-0.165	-0.141	-0.180	-0.153	-0.198	-0.164	-0.209	-0.167	
0.90	+0.005	—	-0.020	-0.021	-0.033	-0.033	-0.049	-0.047	-0.070	-0.070	-0.100	-0.096	-0.112	-0.105	
0.95	+0.110	—	+0.103	—	+0.094	—	+0.076	—	+0.060	—	+0.034	—	+0.018	—	
0.98	—	—	+0.194	—	+0.186	—	+0.179	—	+0.172	—	+0.160	—	+0.156	—	

TABLE 12—*continued*

WING B

 $\alpha = 2.02 \text{ deg}$ C_p

$\frac{x}{c_0}$	$\frac{y}{s(x)}$	C_p													
		0.6		0.65		0.7		0.75		0.8		0.85		0.9	
		U.S.	L.S.												
42	0.10	+0.074	+0.112	+0.077	+0.110	+0.078	+0.113	+0.074	+0.111	+0.075	+0.115	+0.086	+0.118	+0.088	+0.120
	0.20	+0.029	0.071	+0.032	0.072	+0.037	0.073	+0.042	0.075	0.041	0.077	0.044	0.079	0.052	0.079
	0.30	-0.012	+0.035	-0.014	+0.041	-0.010	+0.040	-0.003	0.045	+0.004	0.050	+0.009	0.048	+0.015	0.053
	0.40	-0.064	-0.014	-0.059	-0.008	-0.049	-0.001	-0.042	+0.003	-0.037	+0.013	-0.028	+0.018	-0.021	0.029
	0.50	-0.112	-0.051	-0.103	-0.048	-0.101	-0.036	-0.090	-0.034	-0.079	-0.022	-0.070	-0.011	-0.053	+0.001
	0.60	-0.159	-0.108	-0.158	-0.100	-0.151	-0.090	-0.140	-0.076	-0.124	-0.058	-0.110	-0.043	-0.093	-0.029
	0.70	-0.206	-0.151	-0.203	-0.146	-0.201	-0.135	-0.194	-0.124	-0.181	-0.105	-0.163	-0.085	-0.136	-0.056
	0.80	-0.219	-0.176	-0.227	-0.176	-0.231	-0.175	-0.236	-0.170	-0.237	-0.157	-0.227	-0.133	-0.200	-0.102
	0.90	-0.133	-0.121	-0.155	-0.127	-0.178	-0.149	-0.202	-0.165	-0.232	-0.171	-0.250	-0.173	-0.268	-0.157
	0.95	-0.002	—	-0.027	—	-0.055	—	-0.088	—	-0.129	—	-0.180	—	-0.238	—
	0.98	+0.145	—	+0.133	—	+0.114	—	+0.085	—	+0.057	—	+0.011	—	-0.075	—

TABLE 12—*continued*

WING B

 $\alpha = 4.05 \text{ deg}$ C_p

43

$\frac{x}{c_0}$	$\frac{y}{s(x)}$	0		0.1		0.2		0.3		0.4		0.5		0.55	
		U.S.	L.S.	U.S.	L.S.										
0.10	+0.058	+0.120	+0.061	+0.146	+0.057	+0.141	+0.058	+0.127	+0.052	+0.138	+0.052	+0.128	+0.052	+0.130	
0.20	+0.007	0.063	0	0.089	-0.001	0.088	0	0.092	0	0.092	+0.004	0.086	+0.006	0.090	
0.30	-0.049	+0.038	-0.049	+0.036	-0.048	+0.036	-0.048	+0.046	-0.048	+0.067	-0.046	+0.052	-0.044	0.056	
0.40	-0.088	-0.014	-0.093	-0.012	-0.097	-0.012	-0.097	-0.012	-0.098	-0.001	-0.094	-0.002	-0.091	+0.008	
0.50	-0.130	-0.060	-0.132	-0.065	-0.138	-0.061	-0.143	-0.057	-0.145	-0.054	-0.144	-0.054	-0.142	-0.039	
0.60	-0.163	-0.104	-0.166	-0.107	-0.171	-0.103	-0.178	-0.102	-0.187	-0.100	-0.190	-0.089	-0.188	-0.085	
0.70	-0.171	-0.126	-0.177	-0.132	-0.184	-0.132	-0.196	-0.134	-0.207	-0.136	-0.221	-0.131	-0.226	-0.128	
0.80	-0.141	-0.115	-0.143	-0.118	-0.157	-0.122	-0.174	-0.130	-0.191	-0.139	-0.214	-0.146	-0.226	-0.147	
0.90	-0.017	—	-0.021	-0.020	-0.032	-0.032	-0.051	-0.044	-0.075	-0.067	-0.105	-0.091	-0.120	-0.100	
0.95	+0.034	—	+0.102	0	+0.097	—	+0.080	—	+0.057	—	+0.031	—	+0.018	—	
0.98	—	—	+0.197	—	+0.192	—	+0.183	—	+0.173	—	+0.160	—	+0.154	—	

TABLE 12—*continued*WING B $\alpha = 4.05 \text{ deg}$ C_p

$\frac{x}{c_0}$	$\frac{y}{s(x)}$	0.6		0.65		0.7		0.75		0.8		0.85		0.9	
		U.S.	L.S.	U.S.	L.S.										
0.10	+0.051	+0.128	+0.055	+0.126	+0.057	+0.129	+0.051	+0.129	+0.053	+0.130	+0.054	+0.129	+0.045	+0.129	
0.20	+0.006	0.090	+0.008	0.092	+0.013	0.093	+0.020	0.095	+0.023	0.095	+0.031	0.093	-0.024	0.091	
0.30	-0.037	0.062	-0.038	0.059	-0.034	0.060	-0.028	0.064	-0.016	0.065	-0.011	0.065	-0.064	0.066	
0.40	-0.091	+0.010	-0.084	+0.015	-0.077	+0.026	-0.067	+0.025	-0.061	+0.033	-0.054	0.036	-0.080	0.041	
0.50	-0.138	-0.032	-0.134	-0.020	-0.131	-0.012	-0.120	-0.007	-0.107	0	-0.097	+0.011	-0.112	+0.019	
0.60	-0.187	-0.079	-0.189	-0.069	-0.182	-0.058	-0.172	-0.042	-0.158	-0.029	-0.146	-0.017	-0.137	-0.006	
0.70	-0.230	-0.122	-0.233	-0.115	-0.232	-0.101	-0.227	-0.091	-0.220	-0.070	-0.204	-0.053	-0.185	-0.026	
0.80	-0.239	-0.153	-0.252	-0.149	-0.257	-0.142	-0.268	-0.136	-0.274	-0.120	-0.280	-0.096	-0.255	-0.064	
0.90	-0.142	-0.112	-0.165	-0.115	-0.189	-0.131	-0.219	-0.142	-0.255	-0.142	-0.286	-0.137	-0.318	-0.111	
0.95	-0.003	—	-0.028	—	-0.055	—	-0.091	—	-0.134	—	-0.194	—	-0.271	—	
0.98	+0.141	—	+0.128	—	+0.112	—	+0.087	—	+0.057	—	+0.011	—	-0.078	—	

TABLE 12—*continued*WING B $\alpha = 6.09 \text{ deg}$ C_p

$\frac{x}{c_0}$	$\frac{y}{s(x)}$	0		0.1		0.2		0.3		0.4		0.5		0.55	
		U.S.	L.S.	U.S.	L.S.	U.S.	L.S.	U.S.	L.S.	U.S.	L.S.	U.S.	L.S.	U.S.	L.S.
0.10	+0.035	+0.178	+0.038	+0.173	+0.035	+0.166	+0.036	+0.148	+0.030	+0.160	+0.031	+0.150	+0.029	+0.150	
0.20	-0.011	0.116	-0.020	0.119	-0.023	0.114	-0.023	0.118	-0.022	0.116	-0.022	0.110	-0.019	0.113	
0.30	-0.067	0.063	-0.069	0.062	-0.071	0.062	-0.072	0.072	-0.072	0.091	-0.071	0.069	-0.067	0.080	
0.40	-0.106	+0.012	-0.110	+0.015	-0.117	+0.013	-0.120	+0.015	-0.120	+0.024	-0.120	+0.028	-0.116	+0.033	
0.50	-0.147	-0.039	-0.149	-0.041	-0.152	-0.033	-0.164	-0.032	-0.167	-0.024	-0.169	-0.016	-0.168	-0.011	
0.60	-0.177	-0.084	-0.176	-0.085	-0.187	-0.081	-0.197	-0.079	-0.206	-0.074	-0.214	-0.061	-0.213	-0.056	
0.70	-0.183	-0.110	-0.186	-0.115	-0.196	-0.110	-0.211	-0.112	-0.226	-0.111	-0.244	-0.105	-0.249	-0.099	
0.80	-0.148	-0.105 ^b	-0.151	-0.106	-0.163	-0.109	-0.183	-0.113	-0.204	-0.120	-0.232	-0.126	-0.249	-0.125	
0.90	-0.004	—	-0.024	-0.011	-0.033	-0.026	-0.056	-0.039	-0.082	-0.058	-0.121	-0.079	-0.137	-0.085	
0.95	+0.109	—	+0.101	—	+0.100	—	+0.083	—	+0.050	—	+0.015	—	-0.002	—	
0.98	—	—	+0.198	—	+0.197	—	+0.191	—	+0.171	—	+0.147	—	+0.138	—	

TABLE 12—*continued*WING B $\alpha = 6.09 \text{ deg}$ C_p

$\frac{x}{c_0}$	$\frac{y}{s(x)}$	0.6		0.65		0.7		0.75		0.8		0.85		0.9	
		U.S.	L.S.	U.S.	L.S.										
0.10	+0.030	+0.148	+0.034	+0.145	+0.042	+0.146	+0.035	+0.141	+0.039	+0.141	-0.046	+0.137	-0.089	+0.130	
0.20	-0.017	0.111	-0.014	0.112	-0.002	0.109	+0.013	0.110	+0.009	0.107	-0.126	0.100	-0.148	0.096	
0.30	-0.060	0.079	-0.059	0.081	-0.052	0.084	-0.033	0.080	-0.038	0.079	-0.167	0.075	-0.190	0.072	
0.40	-0.116	+0.034	-0.105	0.040	-0.091	0.048	-0.075	0.046	-0.096	0.049	-0.201	0.049	-0.229	0.048	
0.50	-0.166	-0.005	-0.154	+0.006	-0.147	+0.016	-0.135	+0.015	-0.148	+0.023	-0.239	0.029	-0.251	0.028	
0.60	-0.211	-0.051	-0.210	-0.038	-0.200	-0.029	-0.196	-0.017	-0.208	-0.005	-0.252	+0.007	-0.298	+0.009	
0.70	-0.258	-0.094	-0.259	-0.083	-0.259	-0.070	-0.258	-0.058	-0.251	-0.042	-0.292	-0.022	-0.351	-0.004	
0.80	-0.263	-0.125	-0.276	-0.121	-0.281	-0.111	-0.294	-0.104	-0.314	-0.089	-0.340	-0.058	-0.403	-0.034	
0.90	-0.159	-0.096	-0.188	-0.098	-0.218	-0.109	-0.250	-0.118	-0.293	-0.113	-0.348	-0.098	-0.469	-0.070	
0.95	-0.028	—	-0.056	—	-0.087	—	-0.120	—	-0.165	—	-0.270	—	-0.502	—	
0.98	+0.119	—	+0.105	—	+0.084	—	+0.064	—	+0.031	—	-0.095	—	-0.459	—	

TABLE 12—*continued*WING B $\alpha = 8.13 \text{ deg}$ C_p

$\frac{x}{c_0}$	$\frac{y}{s(x)}$	0		0.1		0.2		0.3		0.4		0.5		0.55	
		U.S.	L.S.	U.S.	L.S.										
0.10	+0.017	+0.211	+0.017	+0.204	+0.016	+0.195	+0.010	+0.171	+0.007	+0.183	+0.004	+0.169	+0.005	+0.171	
0.20	-0.036	0.147	-0.040	0.148	-0.042	0.142	-0.045	0.144	-0.043	0.141	-0.044	0.130	-0.041	0.131	
0.30	-0.084	0.093	-0.086	0.093	-0.088	0.091	-0.095	0.100	-0.096	0.117	-0.095	0.085	-0.089	0.100	
0.40	-0.122	+0.041	-0.128	+0.044	-0.133	+0.042	-0.140	+0.043	-0.140	0.054	-0.142	0.053	-0.138	0.057	
0.50	-0.158	-0.011	-0.162	-0.012	-0.168	-0.008	-0.183	-0.004	-0.189	+0.003	-0.191	+0.014	-0.188	+0.016	
0.60	-0.188	-0.059	-0.190	-0.058	-0.198	-0.054	-0.212	-0.051	-0.227	-0.045	-0.232	-0.034	-0.232	-0.028	
0.70	-0.191	-0.088	-0.193	-0.094	-0.204	-0.089	-0.222	-0.089	-0.241	-0.086	-0.260	-0.077	-0.263	-0.072	
0.80	-0.153	-0.091	-0.159	-0.089	-0.171	-0.095	-0.189	-0.097	-0.214	-0.099	-0.241	-0.105	-0.257	-0.101	
0.90	-0.004	—	-0.025	-0.005	-0.034	-0.020	-0.055	-0.031	-0.083	-0.049	-0.121	-0.067	-0.139	-0.072	
0.95	+0.109	—	+0.104	—	+0.107	—	+0.094	—	+0.062	—	+0.015	—	-0.005	—	
0.98	—	—	+0.198	—	+0.195	—	+0.194	—	+0.183	—	+0.148	—	+0.136	—	

TABLE 12—*continued*WING B $\alpha = 8.13 \text{ deg}$ C_p

$\frac{x}{c_0}$	$\frac{y}{s(x)}$	0.6		0.65		0.7		0.75		0.8		0.85		0.9	
		U.S.	L.S.	U.S.	L.S.										
0.10	+0.009	+0.166	+0.018	+0.158	+0.017	+0.159	-0.070	+0.153	-0.071	+0.154	-0.128	+0.142	-0.168	+0.129	
0.20	-0.035	0.129	-0.026	0.127	-0.004	0.126	+0.001	0.122	-0.170	0.118	-0.303	0.106	-0.218	0.096	
0.30	-0.079	0.095	-0.071	0.100	-0.054	0.103	-0.052	0.098	-0.203	0.093	-0.348	0.083	-0.273	0.072	
0.40	-0.134	0.059	-0.115	0.062	-0.090	0.070	-0.105	0.067	-0.267	0.064	-0.387	0.060	-0.313	0.051	
0.50	-0.180	+0.021	-0.158	+0.031	-0.144	+0.031	-0.181	0.041	-0.336	0.041	-0.412	0.042	-0.355	0.033	
0.60	-0.222	-0.022	-0.211	-0.011	-0.202	-0.002	-0.280	+0.011	-0.392	+0.020	-0.430	0.020	-0.406	0.019	
0.70	-0.262	-0.063	-0.257	-0.055	-0.283	-0.038	-0.357	-0.024	-0.436	-0.120	-0.479	+0.001	-0.467	+0.010	
0.80	-0.265	-0.100	-0.284	-0.092	-0.328	-0.081	-0.414	-0.066	-0.499	-0.163	-0.529	-0.029	-0.534	-0.008	
0.90	-0.159	-0.079	-0.199	-0.078	-0.279	-0.088	-0.409	-0.089	-0.536	-0.191	-0.597	-0.067	-0.575	-0.034	
0.95	-0.028	—	-0.066	—	-0.145	—	-0.322	—	-0.532	—	-0.569	—	-0.469	—	
0.98	+0.115	—	+0.092	—	+0.036	—	-0.151	—	-0.392	—	-0.370	—	-0.197	—	

TABLE 12—*continued*WING B $\alpha = 10.17 \text{ deg}$ C_p

$\frac{x}{c_0}$	$\frac{y}{s(x)}$	0		0.1		0.2		0.3		0.4		0.5		0.55	
		U.S.	L.S.	U.S.	L.S.										
0.10	-0.004	+0.242	-0.009	+0.238	-0.009	+0.223	-0.014	+0.192	-0.021	+0.206	-0.018	+0.191	-0.014	+0.190	
0.20	-0.047	0.178	-0.063	0.182	-0.063	0.172	-0.067	0.170	-0.064	0.165	-0.064	0.155	-0.056	0.153	
0.30	-0.102	0.125	-0.106	0.126	-0.110	0.122	-0.115	0.128	-0.116	0.141	-0.113	0.118	-0.103	0.118	
0.40	-0.139	0.071	-0.144	0.060	-0.153	0.071	-0.160	0.073	-0.161	0.082	-0.160	0.080	-0.151	0.083	
0.50	-0.175	+0.018	-0.180	+0.016	-0.187	+0.021	-0.201	+0.026	-0.206	+0.033	-0.206	+0.042	-0.198	0.043	
0.60	-0.201	-0.033	-0.205	-0.032	-0.215	-0.028	-0.229	-0.023	-0.241	-0.018	-0.245	-0.002	-0.239	+0.002	
0.70	-0.201	-0.066	-0.207	-0.070	-0.220	-0.065	-0.239	-0.052	-0.253	-0.056	-0.272	-0.047	-0.263	-0.044	
0.80	-0.161	-0.075	-0.168	-0.073	-0.181	-0.077	-0.199	-0.077	-0.222	-0.077	-0.244	-0.079	-0.251	-0.077	
0.90	+0.002	—	-0.031	+0.002	-0.039	-0.013	-0.056	-0.023	-0.086	-0.039	-0.119	-0.056	-0.128	-0.058	
0.95	+0.114	—	+0.104	—	+0.108	—	+0.096	—	+0.066	—	+0.016	—	-0.002	—	
0.98	—	—	+0.193	—	+0.186	—	+0.189	—	+0.186	—	+0.150	—	+0.134	—	

TABLE 12—*continued*WING B $\alpha = 10.17 \text{ deg}$ C_p

$\frac{x}{c_0}$	$\frac{y}{s(x)}$	0.6		0.65		0.7		0.75		0.8		0.85		0.9	
		U.S.	L.S.												
50	0.10	-0.008	+0.182	-0.013	+0.175	-0.096	+0.171	-0.248	+0.161	-0.247	+0.165	-0.230	+0.142	-0.259	+0.122
	0.20	-0.044	0.150	-0.024	0.147	-0.016	0.141	-0.175	0.131	-0.422	0.126	-0.448	0.108	-0.283	0.094
	0.30	-0.086	0.112	-0.070	0.119	-0.072	0.117	-0.211	0.108	-0.462	0.103	-0.498	0.087	-0.337	0.070
	0.40	-0.138	0.083	-0.110	0.085	-0.119	0.086	-0.294	0.081	-0.522	0.076	-0.535	0.065	-0.386	0.050
	0.50	-0.179	0.049	-0.147	0.058	-0.179	0.054	-0.374	0.058	-0.576	0.057	-0.578	0.051	-0.432	0.034
	0.60	-0.218	+0.008	-0.198	+0.019	-0.263	+0.025	-0.483	+0.032	-0.631	0.040	-0.602	0.034	-0.497	0.024
	0.70	-0.249	-0.034	-0.249	-0.023	-0.374	-0.009	-0.580	-0.001	-0.682	+0.015	-0.639	+0.024	-0.556	0.023
	0.80	-0.245	-0.073	-0.278	-0.063	-0.465	-0.052	-0.671	-0.041	-0.732	-0.132	-0.675	0	-0.612	+0.014
	0.90	-0.137	-0.063	-0.197	-0.059	-0.454	-0.066	-0.711	-0.069	-0.777	-0.165	-0.690	-0.036	-0.596	-0.003
	0.95	-0.021	—	-0.075	—	-0.325	—	-0.652	—	-0.734	—	-0.569	—	-0.424	—
	0.98	+0.107	—	+0.064	—	-0.127	—	-0.433	—	-0.502	—	-0.311	—	-0.186	—

TABLE 12—*continued*

WING B

 $\alpha = 15.29 \text{ deg}$ C_p

$\frac{x}{c_0}$	$\frac{y}{s(x)}$	0		0.1		0.2		0.3		0.4		0.5		0.55	
		U.S.	L.S.												
0.10		-0.060	+0.336	-0.065	+0.316	-0.069	+0.297	-0.075	+0.261	-0.073	+0.259	-0.069	+0.238	-0.100	+0.236
0.20		-0.102	0.270	-0.090	0.264	-0.111	0.253	-0.115	0.238	-0.111	0.229	-0.088	0.211	-0.077	0.206
0.30		-0.146	0.215	-0.152	0.208	-0.155	0.205	-0.163	0.202	-0.159	0.200	-0.136	0.180	-0.123	0.175
0.40		-0.181	0.159	-0.187	0.156	-0.195	0.159	-0.205	0.156	-0.203	0.156	-0.172	0.152	-0.165	0.146
0.50		-0.212	0.103	-0.219	0.100	-0.224	0.107	-0.244	0.106	-0.242	0.108	-0.211	0.117	-0.203	0.117
0.60		-0.240	0.047	-0.244	+0.046	-0.254	0.052	-0.267	0.058	-0.271	0.064	-0.245	0.071	-0.244	0.081
0.70		-0.238	+0.003	-0.246	-0.002	-0.256	+0.008	-0.276	+0.008	-0.282	+0.017	-0.270	+0.027	-0.280	+0.039
0.80		-0.198	-0.021	-0.204	-0.025	-0.214	-0.021	-0.240	-0.021	-0.255	-0.019	-0.261	-0.013	-0.294	-0.011
0.90		-0.030	—	-0.060	0.027	-0.065	+0.016	-0.094	+0.006	-0.130	-0.013	-0.178	-0.017	-0.236	-0.019
0.95		+0.101	—	+0.089	—	+0.094	—	+0.073	—	+0.016	—	-0.065	—	-0.134	—
0.98		—	—	+0.185	—	+0.184	—	+0.179	—	+0.160	—	+0.088	—	+0.031	—

51

TABLE 12—*continued*

WING B

 $\alpha = 15.29 \text{ deg}$ C_p

52

$\frac{x}{c_0}$	$\frac{y}{s(x)}$	0.6		0.65		0.7		0.75		0.8		0.85		0.9	
		U.S.	L.S.	U.S.	L.S.	U.S.	L.S.	U.S.	L.S.	U.S.	L.S.	U.S.	L.S.	U.S.	L.S.
0.10	-0.225	+0.223	-0.451	+0.205	-0.566	+0.198	-0.548	+0.184	-0.546	0.182	-0.514	0.131	-0.473	0.085	
0.20	-0.098	0.196	-0.264	0.179	-0.590	0.169	-0.899	0.157	-0.820	0.138	-0.562	0.102	-0.514	0.079	
0.30	-0.136	0.167	-0.289	0.160	-0.609	0.149	-0.932	0.136	-0.891	0.115	-0.613	0.081	-0.585	0.044	
0.40	-0.207	0.142	-0.380	0.137	-0.713	0.129	-1.008	0.119	-0.928	0.102	-0.650	0.071	-0.631	0.031	
0.50	-0.246	0.115	-0.449	0.118	-0.805	0.106	-1.081	0.104	-0.960	0.086	-0.696	0.065	-0.688	0.021	
0.60	-0.309	0.081	-0.553	0.087	-0.918	0.087	-1.164	0.088	-0.951	0.081	-0.751	0.056	-0.744	0.021	
0.70	-0.380	+0.042	-0.661	0.054	-1.026	0.061	-1.215	0.069	-0.953	0.073	-0.792	0.058	-0.788	0.031	
0.80	-0.419	-0.006	-0.723	+0.012	-1.079	+0.021	-1.213	+0.035	-0.910	0.048	-0.792	0.054	-0.797	0.042	
0.90	-0.380	-0.025	-0.661	-0.017	-0.974	-0.017	-1.056	-0.013	-0.757	0	-0.638	0.023	-0.642	0.046	
0.95	-0.273	—	-0.513	—	-0.738	—	-0.761	—	-0.489	—	-0.368	—	-0.356	—	
0.98	-0.079	—	-0.245	—	-0.399	—	-0.422	—	-0.255	—	-0.184	—	-0.167	—	

TABLE 12—*continued*WING B $\alpha = 20.42 \text{ deg}$ C_p

53

$\frac{x}{c_0}$	$\frac{y}{s(x)}$	0		0.1		0.2		0.3		0.4		0.5		0.55	
		U.S.	L.S.	U.S.	L.S.										
0.10	-0.119	0.434	-0.129	0.400	-0.124	0.369	-0.132	0.320	-0.157	0.315	-0.343	0.283	-0.566	0.272	
0.20	-0.154	0.368	-0.163	0.351	-0.160	0.326	-0.159	0.306	-0.147	0.291	-0.191	0.262	-0.343	0.249	
0.30	-0.196	0.312	-0.206	0.301	-0.206	0.290	-0.211	0.280	-0.201	0.267	-0.243	0.237	-0.372	0.226	
0.40	-0.232	0.253	-0.244	0.249	-0.249	0.242	-0.253	0.237	-0.245	0.233	-0.309	0.219	-0.466	0.211	
0.50	-0.272	0.197	-0.279	0.191	-0.285	0.198	-0.294	0.195	-0.287	0.195	-0.364	0.185	-0.539	0.182	
0.60	-0.307	0.138	-0.314	0.135	-0.318	0.142	-0.327	0.143	-0.335	0.150	-0.435	0.158	-0.634	0.153	
0.70	-0.315	0.086	-0.323	0.080	-0.333	0.085	-0.353	0.091	-0.366	0.102	-0.495	0.118	-0.715	0.120	
0.80	-0.285	0.043	-0.310	0.045	-0.310	0.043	-0.338	0.045	-0.376	0.050	-0.529	0.060	-0.742	0.066	
0.90	-0.104	—	-0.142	0.066	-0.160	0.054	-0.205	0.045	-0.280	0.031	-0.464	0.026	-0.645	0.028	
0.95	+0.053	—	+0.041	—	+0.026	—	-0.024	—	-0.113	—	-0.489	—	-0.435	—	
0.98	—	—	+0.189	—	+0.181	—	+0.158	—	+0.091	—	-0.049	—	-0.152	—	

TABLE 12—*continued*

WING B

 $\alpha = 20.42 \text{ deg}$ C_p

$\frac{x}{c_0}$	$\frac{y}{s(x)}$	0.6		0.65		0.7		0.75		0.8		0.85		0.9	
		U.S.	L.S.												
54	0.10	-0.852	0.254	-0.948	0.231	-0.925	0.209	-0.898	0.186	-0.888	0.181	-0.787	0.108	-0.740	+0.029
	0.20	-0.683	0.235	-1.123	0.212	-1.391	0.192	-1.233	0.164	-0.888	0.129	-0.793	0.089	-0.771	+0.020
	0.30	-0.650	0.216	-1.092	0.197	-1.416	0.177	-1.337	0.149	-0.919	0.114	-0.858	0.070	-0.840	-0.003
	0.40	-0.785	0.196	-1.217	0.179	-1.467	0.164	-1.295	0.135	-0.929	0.104	-0.898	0.056	-0.890	-0.009
	0.50	-0.879	0.177	-1.308	0.172	-1.529	0.154	-1.264	0.134	-0.952	0.100	-0.944	0.052	-0.931	-0.015
	0.60	-0.975	0.148	-1.387	0.145	-1.544	0.144	-1.218	0.132	-0.984	0.104	-0.986	0.064	-0.967	-0.009
	0.70	-1.057	0.122	-1.435	0.120	-1.515	0.119	-1.166	0.120	-0.986	0.110	-0.986	0.085	-0.973	+0.027
	0.80	-1.052	0.075	-1.358	0.081	-1.389	0.087	-1.064	0.091	-0.915	0.095	-0.923	0.091	-0.921	0.052
	0.90	-0.867	0.027	-1.038	0.031	-1.025	0.035	-0.763	0.037	-0.625	0.049	-0.616	0.070	-0.625	+0.083
	0.95	-0.585	—	-0.688	—	-0.647	—	-0.462	—	-0.337	—	-0.314	—	-0.302	—
	0.98	-0.257	—	-0.332	—	-0.335	—	-0.258	—	-0.203	—	-0.218	—	-0.211	—

TABLE 12—*continued*WING B $\alpha = 25.56 \text{ deg}$ C_p

x c_0	y $s(x)$	0		0.1		0.2		0.3		0.4		0.5		0.55	
		U.S.	L.S.												
5	0.10	-0.195	0.535	-0.201	0.492	-0.219	0.447	-0.263	0.387	-0.489	0.369	-1.038	0.327	-1.264	0.305
	0.20	-0.130	0.473	-0.230	0.450	-0.234	0.414	-0.232	0.382	-0.320	0.350	-0.775	0.312	-1.219	0.292
	0.30	-0.270	0.417	-0.274	0.398	-0.282	0.384	-0.284	0.362	-0.368	0.333	-0.782	0.296	-1.154	0.276
	0.40	-0.313	0.361	-0.318	0.354	-0.338	0.337	-0.344	0.326	-0.456	0.310	-0.905	0.287	-1.233	0.269
	0.50	-0.370	0.302	-0.372	0.298	-0.384	0.293	-0.407	0.291	-0.525	0.281	-0.973	0.266	-1.302	0.247
	0.60	-0.420	0.241	-0.422	0.241	-0.440	0.237	-0.467	0.245	-0.600	0.245	-1.051	0.243	-1.381	0.234
	0.70	-0.440	0.181	-0.443	0.179	-0.472	0.182	-0.513	0.191	-0.665	0.200	-1.088	0.206	-1.404	0.207
	0.80	-0.416	0.126	-0.414	0.126	-0.457	0.122	-0.513	0.132	-0.673	0.139	-1.051	0.149	-1.308	0.153
	0.90	-0.195	—	-0.245	0.124	-0.292	0.110	-0.369	0.101	-0.533	0.091	-0.811	0.085	-0.974	0.084
	0.95	-0.003	—	-0.028	—	-0.076	—	-0.153	—	-0.299	—	-0.510	—	-0.612	—
	0.98	—	—	+0.175	—	+0.139	—	+0.085	—	-0.024	—	-0.176	—	-0.261	—

TABLE 12—*continued*

WING B

 $\alpha = 25.56 \text{ deg}$ C_p

$\frac{x}{c_0}$	$\frac{y}{s(x)}$	0.6		0.65		0.7		0.75		0.8		0.85		0.9	
		U.S.	L.S.	U.S.	L.S.										
0.10	-1.376	0.274	-1.304	0.238	-1.273	0.212	-1.317	0.174	-1.299	0.174	-1.105	0.062	-1.055	-0.053	
0.20	-1.690	0.262	-1.965	0.232	-1.771	0.199	-1.278	0.158	-1.140	0.112	-1.101	0.045	-1.055	-0.053	
0.30	-1.634	0.253	-2.002	0.219	-1.917	0.193	-1.415	0.149	-1.145	0.103	-1.128	0.031	-1.098	-0.063	
0.40	-1.702	0.247	-1.984	0.219	-1.827	0.191	-1.346	0.145	-1.182	0.099	-1.180	0.028	-1.138	-0.073	
0.50	-1.728	0.232	-1.930	0.211	-1.732	0.187	-1.273	0.155	-1.199	0.104	-1.220	0.030	-1.171	-0.073	
0.60	-1.723	0.224	-1.849	0.209	-1.588	0.185	-1.226	0.153	-1.203	0.108	-1.239	0.043	-1.188	-0.067	
0.70	-1.688	0.208	-1.755	0.201	-1.494	0.189	-1.194	0.170	-1.178	0.137	-1.207	0.078	-1.171	-0.019	
0.80	-1.525	0.157	-1.560	0.163	-1.334	0.168	-1.065	0.164	-1.040	0.154	-1.059	0.118	-1.055	+0.039	
0.90	-1.076	0.087	-1.057	0.095	-0.886	0.099	-0.663	0.105	-0.627	0.122	-0.608	0.126	-0.612	+0.112	
0.95	-0.676	—	-0.660	—	-0.551	—	-0.415	—	-0.397	—	-0.395	—	-0.396	—	
0.98	-0.322	—	-0.344	—	-0.319	—	-0.276	—	-0.266	—	-0.297	—	-0.292	—	

TABLE 12—*continued*WING B $\alpha = 30.70 \text{ deg}$ C_p

$\frac{x}{c_0}$	$\frac{y}{s(x)}$	0		0.1		0.2		0.3		0.4		0.5		0.55	
		U.S.	L.S.	U.S.	L.S.										
0.10	-0.278	0.636	-0.307	0.575	-0.383	0.518	-0.574	0.461	-1.096	0.413	-1.716	0.347	-1.795	0.322	
0.20	-0.318	0.574	-0.336	0.537	-0.387	0.500	-0.487	0.457	-0.874	0.409	-1.768	0.347	-2.080	0.317	
0.30	-0.356	0.525	-0.374	0.498	-0.409	0.470	-0.500	0.453	-0.895	0.400	-1.708	0.347	-2.227	0.317	
0.40	-0.394	0.469	-0.421	0.452	-0.448	0.435	-0.543	0.422	-0.878	0.379	-1.695	0.343	-2.244	0.322	
0.50	-0.468	0.409	-0.476	0.405	-0.517	0.396	-0.608	0.388	-0.912	0.370	-1.670	0.335	-2.179	0.313	
0.60	-0.521	0.353	-0.540	0.342	-0.578	0.340	-0.678	0.345	-0.985	0.332	-1.674	0.322	-2.123	0.304	
0.70	-0.556	0.286	-0.573	0.287	-0.617	0.297	-0.729	0.306	-1.019	0.289	-1.619	0.309	-1.989	0.296	
0.80	-0.531	0.220	-0.548	0.215	-0.608	0.210	-0.725	0.228	-0.993	0.225	-1.444	0.232	-1.701	0.240	
0.90	-0.272	—	-0.340	0.181	-0.413	0.171	-0.530	0.167	-0.737	0.161	-1.023	0.156	-1.157	0.158	
0.95	-0.051	—	-0.082	—	-0.149	—	-0.266	—	-0.433	—	-0.631	—	-0.709	—	
0.98	—	—	+0.160	—	+0.089	—	+0.020	—	-0.109	—	-0.253	—	-0.317	—	

TABLE 12—*continued*WING B $\alpha = 30.70 \text{ deg}$ C_p

$\frac{x}{c_0}$	$\frac{y}{s(x)}$	0.6		0.65		0.7		0.75		0.8		0.85		0.9	
		U.S.	L.S.	U.S.	L.S.	U.S.	L.S.								
0.10	-1.707	0.285	-1.702	0.226	-1.712	0.186	-1.813	0.136	-1.789	0.138	-1.457	-0.018	-1.386	-0.156	
0.20	-1.998	0.276	-1.985	0.226	-1.746	0.186	-1.675	0.132	-1.565	0.062	-1.482	-0.022	-1.404	-0.156	
0.30	-2.446	0.280	-2.371	0.226	-1.882	0.194	-1.576	0.132	-1.501	0.071	-1.478	-0.039	-1.395	-0.147	
0.40	-2.570	0.285	-2.543	0.239	-1.959	0.203	-1.554	0.140	-1.463	0.075	-1.444	-0.027	-1.391	-0.147	
0.50	-2.532	0.276	-2.500	0.247	-2.036	0.220	-1.511	0.149	-1.412	0.079	-1.419	-0.014	-1.404	-0.138	
0.60	-2.404	0.285	-2.380	0.252	-2.057	0.220	-1.507	0.175	-1.434	0.104	-1.444	0	-1.416	-1.130	
0.70	-2.216	0.285	-2.174	0.264	-1.793	0.245	-1.455	0.214	-1.383	0.160	-1.398	+0.062	-1.378	-0.061	
0.80	-1.844	0.242	-1.783	0.239	-1.482	0.237	-1.244	0.222	-1.196	0.193	-1.204	0.125	-1.211	+0.020	
0.90	-1.186	0.161	-1.096	0.161	-0.908	0.169	-0.713	0.171	-0.679	0.181	-0.659	+0.167	-0.651	+0.131	
0.95	-0.737	—	-0.697	—	-0.576	—	-0.476	—	-0.480	—	-0.482	—	-0.476	—	
0.98	-0.361	—	-0.375	—	-0.351	—	-0.368	—	-0.319	—	-0.343	—	-0.335	—	

WING C

TABLE 13

Pressure Coefficients at Zero Yaw

 $\alpha = 0 \text{ deg}$ C_p

59

$\frac{x}{c_0}$	$\frac{y}{s(x)}$	0.		0.1		0.2		0.3		0.4	
		U.S.	L.S.								
0.10	+0.092	+0.092	+0.090	+0.082	+0.083	+0.083	+0.082	+0.080	+0.081	+0.080	+0.080
0.20	+0.033	+0.033	+0.028	—	+0.029	—	+0.028	—	+0.028	—	—
0.30	-0.004	-0.004	-0.012	-0.008	-0.009	-0.005	-0.012	-0.011	-0.012	-0.009	-0.009
0.40	-0.052	-0.052	-0.052	-0.058	-0.053	-0.059	-0.052	-0.059	-0.051	-0.054	-0.054
0.50	-0.082	-0.081	-0.080	-0.082	-0.082	-0.084	-0.085	-0.083	-0.083	-0.084	-0.084
0.60	-0.094	-0.107	-0.102	-0.104	-0.104	-0.107	-0.112	-0.110	-0.107	-0.107	-0.107
0.70	-0.103	-0.110	-0.110	-0.106	-0.112	-0.108	-0.121	-0.116	-0.118	-0.114	-0.114
0.80	-0.082	-0.081	-0.084	-0.083	-0.091	-0.089	-0.103	-0.095	-0.102	-0.101	-0.101
0.90	—	—	+0.002	+0.001	-0.012	-0.013	-0.025	-0.026	-0.036	-0.039	-0.039
0.95	—	—	0.096	0.091	+0.076	+0.070	+0.058	+0.054	+0.037	+0.033	+0.033
0.98	—	—	+0.169	+0.171	+0.154	+0.153	+0.140	+0.135	+0.117	+0.110	+0.110

TABLE 13—*continued*WING C $\alpha = 0 \text{ deg}$ C_p

09

$\frac{x}{c_0}$	$\frac{y}{s(x)}$	0.5		0.6		0.7		0.8		0.9	
		U.S.	L.S.	U.S.	L.S.	U.S.	L.S.	U.S.	L.S.	U.S.	L.S.
0.10	+0.080	+0.081	+0.084	+0.081	+0.083	+0.080	+0.089	+0.090	+0.100	+0.099	
0.20	+0.029	—	+0.038	—	+0.042	—	+0.047	—	0.053	—	
0.30	-0.003	-0.006	-0.003	+0.005	-0.007	+0.003	+0.012	+0.013	+0.018	+0.025	
0.40	-0.045	-0.051	-0.042	-0.042	-0.034	-0.038	-0.026	-0.027	-0.013	-0.008	
0.50	-0.080	-0.081	-0.069	-0.073	-0.066	-0.066	-0.049	-0.054	-0.038	-0.041	
0.60	-0.110	-0.105	-0.094	-0.094	-0.089	-0.092	-0.083	-0.078	-0.058	-0.058	
0.70	-0.126	-0.114	-0.110	-0.107	-0.106	-0.107	-0.091	-0.086	-0.069	-0.071	
0.80	-0.106	-0.100	-0.102	-0.100	-0.106	-0.098	-0.086	-0.082	-0.069	-0.071	
0.90	-0.046	-0.045	-0.050	-0.050	-0.055	-0.025	-0.057	-0.038	-0.045	-0.048	
0.95	+0.017	+0.016	+0.006	+0.002	-0.004	-0.010	-0.015	-0.017	-0.019	-0.038	
0.98	+0.096	+0.082	+0.080	+0.060	—	—	—	—	—	—	

TABLE 13—*continued*WING C $\alpha = 2.03 \text{ deg}$ C_p

$\frac{x}{c_0}$	$\frac{y}{s(x)}$	0		0.1		0.2		0.3		0.4	
		U.S.	L.S.	U.S.	L.S.	U.S.	L.S.	U.S.	L.S.	U.S.	L.S.
0.10	+0.066	+0.119	+0.064	+0.105	+0.063	+0.104	+0.062	+0.103	+0.061	+0.103	
0.20	+0.013	0.055	+0.008	—	+0.010	—	+0.009	—	+0.007	—	
0.30	-0.033	+0.011	-0.035	+0.014	-0.032	+0.014	-0.035	+0.011	-0.035	+0.012	
0.40	-0.070	-0.034	-0.073	-0.038	-0.073	-0.039	-0.073	-0.036	-0.066	-0.030	
0.50	-0.099	-0.066	-0.099	-0.062	-0.101	-0.070	-0.104	-0.061	-0.103	-0.066	
0.60	-0.109	-0.091	-0.116	-0.089	-0.121	-0.090	-0.128	-0.089	-0.126	-0.086	
0.70	-0.112	-0.098	-0.118	-0.093	-0.123	-0.094	-0.135	-0.099	-0.135	-0.096	
0.80	-0.090	-0.077	-0.093	-0.075	-0.101	-0.081	-0.113	-0.082	-0.115	-0.087	
0.90	—	—	-0.003	0	-0.014	-0.013	-0.028	-0.022	-0.042	-0.030	
0.95	—	—	+0.094	+0.088	+0.079	+0.069	+0.060	+0.051	+0.036	+0.035	
0.98	—	—	+0.167	+0.167	+0.158	+0.147	+0.144	+0.128	+0.118	+0.108	

TABLE 13—*continued*WING C $\alpha = 2.03 \text{ deg}$ C_p

$\frac{x}{c_0}$	$\frac{y}{s(x)}$	0.5		0.6		0.7		0.8		0.9	
		U.S.	L.S.	U.S.	L.S.	U.S.	L.S.	U.S.	L.S.	U.S.	L.S.
0.10	+0.059	+0.102		+0.071	+0.104	+0.058	+0.101	+0.071	+0.105	+0.080	+0.112
0.20	+0.012	—		+0.014	—	+0.018	—	+0.022	—	+0.030	—
0.30	-0.025	+0.015		-0.026	+0.027	-0.035	+0.027	-0.015	+0.035	-0.008	0.039
0.40	-0.067	-0.028		-0.066	-0.016	-0.061	-0.014	-0.056	-0.003	-0.044	+0.017
0.50	-0.102	-0.061		-0.093	-0.049	-0.094	-0.044	-0.080	-0.030	-0.073	-0.015
0.60	-0.131	-0.082		-0.119	-0.070	-0.118	-0.061	-0.118	-0.047	-0.102	-0.024
0.70	-0.148	-0.092		-0.133	-0.081	-0.134	-0.078	-0.122	-0.055	-0.100	-0.037
0.80	-0.124	-0.082		-0.125	-0.079	-0.133	-0.069	-0.114	-0.051	-0.110	-0.031
0.90	-0.058	-0.037		-0.066	-0.037	-0.072	-0.005	-0.079	-0.016	-0.091	-0.018
0.95	+0.015	+0.016		-0.003	+0.008	-0.015	+0.005	-0.031	-0.001	-0.080	-0.012
0.98	+0.095	+0.081		+0.072	+0.065	—	—	—	—	—	—

TABLE 13—*continued*WING C $\alpha = 4.07 \text{ deg}$ C_p

63

$\frac{x}{c_0}$	$\frac{y}{s(x)}$	0		0.1		0.2		0.3		0.4	
		U.S.	L.S.	U.S.	L.S.	U.S.	L.S.	U.S.	L.S.	U.S.	L.S.
0.10	+0.046	+0.148	+0.045	+0.134	+0.044	+0.131	+0.037	+0.125	+0.043	+0.126	
0.20	-0.008	0.084	-0.013	—	-0.013	—	-0.014	—	-0.015	—	
0.30	-0.050	+0.034	-0.052	+0.038	-0.052	+0.039	-0.056	+0.038	-0.055	+0.037	
0.40	-0.087	-0.010	-0.090	-0.016	-0.092	-0.014	-0.093	-0.011	-0.081	-0.004	
0.50	-0.115	-0.040	-0.115	-0.043	-0.116	-0.045	-0.126	-0.048	-0.124	-0.038	
0.60	-0.122	-0.073	-0.131	-0.070	-0.135	-0.068	-0.148	-0.066	-0.145	-0.060	
0.70	-0.125	-0.082	-0.130	-0.079	-0.137	-0.078	-0.152	-0.080	-0.152	-0.072	
0.80	-0.098	-0.063	-0.106	-0.063	-0.110	-0.066	-0.126	-0.067	-0.130	-0.067	
0.90	—	—	-0.004	+0.006	-0.016	-0.006	-0.033	-0.015	-0.047	-0.019	
0.95	—	—	+0.094	0.091	+0.082	+0.070	+0.060	+0.053	+0.033	+0.039	
0.98	—	—	+0.169	+0.170	+0.165	+0.144	+0.148	+0.127	+0.122	+0.112	

TABLE 13—*continued*

WING C

 $\alpha = 4.07 \text{ deg}$ C_p

$\frac{x}{c_0}$	$\frac{y}{s(x)}$	0.5		0.6		0.7		0.8		0.9	
		U.S.	L.S.	U.S.	L.S.	U.S.	L.S.	U.S.	L.S.	U.S.	L.S.
0.10	+0.030	+0.125	+0.048	+0.122	+0.033	+0.118	+0.045	+0.229	+0.011	+0.119	
0.20	-0.015	—	-0.055	—	-0.002	—	+0.009	—	-0.102	—	
0.30	-0.050	+0.028	-0.049	0.049	-0.056	0.050	-0.024	0.052	-0.160	0.058	
0.40	-0.092	-0.005	-0.079	+0.005	-0.080	+0.015	-0.069	+0.018	-0.206	0.034	
0.50	-0.128	-0.037	-0.118	-0.024	-0.113	-0.013	-0.096	-0.008	-0.254	0.010	
0.60	-0.157	-0.058	-0.143	-0.046	-0.132	-0.031	-0.144	-0.019	-0.306	+0.005	
0.70	-0.172	-0.070	-0.155	-0.058	-0.146	-0.045	-0.149	-0.026	-0.328	-0.004	
0.80	-0.142	-0.066	-0.140	-0.058	-0.134	-0.041	-0.151	-0.024	-0.343	0	
0.90	-0.067	-0.024	-0.074	-0.019	-0.063	+0.016	-0.130	+0.006	-0.304	+0.010	
0.95	+0.007	+0.026	-0.003	+0.018	-0.003	+0.020	-0.082	+0.014	-0.248	+0.010	
0.98	+0.091	+0.088	+0.071	+0.072	—	—	—	—	—	—	

WING C

TABLE 13—*continued* $\alpha = 6.11 \text{ deg}$ C_p

$\frac{x}{c_0}$	$\frac{y}{s(x)}$	0		0.1		0.2		0.3		0.4	
		U.S.	L.S.	U.S.	L.S.	U.S.	L.S.	U.S.	L.S.	U.S.	L.S.
0.10	+0.023	+0.180	+0.021	+0.162	+0.019	+0.157	+0.012	+0.150	+0.017	+0.147	
0.20	-0.031	0.117	-0.035	—	-0.035	—	-0.039	—	-0.040	—	
0.30	-0.067	0.065	-0.074	0.064	-0.074	0.064	-0.080	0.063	-0.080	0.061	
0.40	-0.102	+0.015	-0.111	+0.011	-0.113	+0.009	-0.116	+0.013	-0.092	+0.021	
0.50	-0.130	-0.020	-0.133	-0.019	-0.137	-0.019	-0.147	-0.023	-0.147	-0.013	
0.60	-0.136	-0.050	-0.148	-0.046	-0.155	-0.045	-0.168	-0.043	-0.167	-0.036	
0.70	-0.138	-0.063	-0.145	-0.059	-0.154	-0.057	-0.170	-0.058	-0.169	-0.048	
0.80	-0.107	-0.048	-0.112	-0.049	-0.122	-0.051	-0.139	-0.051	-0.143	-0.047	
0.90	—	—	-0.008	+0.016	-0.020	0	-0.039	-0.006	-0.056	-0.008	
0.95	—	—	+0.094	0.094	+0.083	+0.071	+0.060	+0.057	+0.030	+0.047	
0.98	—	—	+0.168	+0.171	+0.166	+0.140	+0.162	+0.125	+0.123	+0.113	

TABLE 13—*continued*WING C $\alpha = 6.11 \text{ deg}$ C_p

$\frac{x}{c_0}$	$\frac{y}{s(x)}$	0.5		0.6		0.7		0.8		0.9	
		U.S.	L.S.	U.S.	L.S.	U.S.	L.S.	U.S.	L.S.	U.S.	L.S.
0.10	+0.007	+0.143		+0.026	+0.139	+0.016	+0.133	+0.013	0.132	-0.128	0.120
0.20	-0.036	—		-0.034	—	-0.013	—	-0.066	—	-0.200	—
0.30	-0.071	0.062		-0.070	0.070	-0.067	0.072	-0.134	0.073	-0.258	0.069
0.40	-0.114	+0.019		-0.108	+0.028	-0.085	0.037	-0.217	0.040	-0.306	0.047
0.50	-0.150	-0.008		-0.135	-0.016	-0.112	0.013	-0.287	0.025	-0.350	0.028
0.60	-0.179	-0.030		-0.156	-0.018	-0.124	+0.014	-0.384	0.009	-0.397	0.024
0.70	-0.190	-0.046		-0.162	-0.030	-0.137	-0.018	-0.423	0.002	-0.408	0.019
0.80	-0.154	-0.041		-0.145	-0.035	-0.121	-0.014	-0.440	0.004	-0.403	0.028
0.90	-0.070	-0.007		-0.081	-0.004	-0.044	+0.031	-0.415	0.028	-0.331	0.034
0.95	+0.008	+0.032		-0.005	+0.028	+0.017	+0.031	-0.349	0.027	-0.239	0.024
0.98	+0.092	+0.094		+0.076	+0.079	—	—	—	—	—	—

WING C

TABLE 13—*continued* $\alpha = 8.15 \text{ deg}$ C_p

$\frac{x}{c_0}$	$\frac{y}{s(x)}$	0		0.1		0.2		0.3		0.4	
		U.S.	L.S.	U.S.	L.S.	U.S.	L.S.	U.S.	L.S.	U.S.	L.S.
0.10	+0.001	+0.214	+0.001	+0.192	-0.003	+0.184	-0.011	+0.165	-0.005	+0.172	
0.20	-0.051	0.148	-0.056	—	-0.056	—	-0.060	—	-0.063	—	
0.30	-0.086	0.095	-0.094	0.094	-0.095	0.094	-0.103	0.092	-0.100	0.089	
0.40	-0.120	0.041	-0.127	0.040	-0.133	0.040	-0.136	0.042	-0.109	0.047	
0.50	-0.144	+0.005	-0.149	+0.009	-0.155	+0.005	-0.168	+0.004	-0.168	+0.015	
0.60	-0.150	-0.025	-0.164	-0.020	-0.171	-0.019	-0.188	-0.016	-0.186	-0.007	
0.70	-0.149	-0.040	-0.161	-0.035	-0.167	-0.034	-0.188	-0.031	-0.187	-0.023	
0.80	-0.118	-0.029	-0.125	-0.030	-0.132	-0.033	-0.153	-0.029	-0.156	-0.025	
0.90	—	—	-0.017	+0.027	-0.025	+0.013	-0.045	+0.007	-0.063	+0.006	
0.95	—	—	+0.092	0.096	+0.084	0.075	+0.059	0.064	+0.028	0.055	
0.98	—	—	+0.167	+0.173	+0.168	+0.141	+0.154	+0.130	+0.121	+0.119	

WING C

TABLE 13—*continued* $\alpha = 8.15 \text{ deg}$ C_p

89

$\frac{x}{c_0}$	$\frac{y}{s(x)}$	0.5		0.6		0.7		0.8		0.9	
		U.S.	L.S.	U.S.	L.S.	U.S.	L.S.	U.S.	L.S.	U.S.	L.S.
0.10	-0.016	+0.161		+0.005	+0.158	+0.009	0.145	-0.221	0.139	-0.193	0.117
0.20	-0.058	—		-0.048	—	-0.014	—	-0.318	—	-0.267	—
0.30	-0.093	0.087		-0.083	0.092	-0.072	0.090	-0.396	0.086	-0.322	0.072
0.40	-0.134	0.048		-0.121	0.055	-0.099	0.057	-0.492	0.058	-0.374	0.054
0.50	-0.166	+0.018		-0.144	0.030	-0.146	0.038	-0.577	0.043	-0.419	0.040
0.60	-0.193	-0.004		-0.158	+0.009	-0.176	0.022	-0.684	0.030	-0.463	0.041
0.70	-0.203	-0.016		-0.164	-0.003	-0.218	0.009	-0.711	0.028	-0.479	0.043
0.80	-0.158	-0.017		-0.137	-0.007	-0.219	0.009	-0.725	0.029	-0.460	0.049
0.90	-0.071	+0.008		-0.062	+0.015	-0.151	0.049	-0.645	0.048	-0.362	0.056
0.95	+0.008	0.046		+0.005	0.039	-0.089	0.040	-0.533	0.036	-0.248	0.035
0.98	+0.094	+0.101		+0.082	+0.083	—	—	—	—	—	—

WING C

TABLE 13—*continued* $\alpha = 10.20 \text{ deg}$ C_p

69

$\frac{x}{c_0}$	$\frac{y}{s(x)}$	0		0.1		0.2		0.3		0.4	
		U.S.	L.S.	U.S.	L.S.	U.S.	L.S.	U.S.	L.S.	U.S.	L.S.
0.10	-0.024	+0.248	-0.023	+0.223	-0.025	+0.211	-0.034	+0.201	-0.030	+0.196	
0.20	-0.075	0.180	-0.077	—	-0.075	—	-0.082	—	-0.083	—	
0.30	-0.109	0.125	-0.115	0.124	-0.114	0.122	-0.124	0.119	-0.121	0.116	
0.40	-0.140	0.075	-0.147	0.072	-0.152	0.068	-0.158	0.069	-0.154	0.076	
0.50	-0.165	+0.036	-0.168	0.040	-0.175	0.031	-0.189	0.034	-0.185	0.056	
0.60	-0.172	-0.001	-0.183	+0.007	-0.188	+0.007	-0.207	+0.013	-0.199	0.023	
0.70	-0.170	-0.018	-0.177	-0.012	-0.181	-0.009	-0.204	-0.006	-0.198	+0.004	
0.80	-0.133	-0.014	-0.136	-0.014	-0.145	-0.014	-0.168	-0.007	-0.165	-0.002	
0.90	—	—	-0.024	+0.038	-0.036	+0.023	-0.056	+0.020	-0.067	+0.021	
0.95	—	—	+0.092	0.104	+0.082	0.079	+0.052	0.070	+0.024	0.065	
0.98	—	—	+0.168	+0.174	+0.167	+0.142	—	+0.133	+0.119	+0.126	

TABLE 13—*continued*WING C $\alpha = 10 \cdot 20 \text{ deg}$ C_p

$\frac{x}{c_0}$	$\frac{y}{s(x)}$	0.5		0.6		0.7		0.8		0.9	
		U.S.	L.S.	U.S.	L.S.	U.S.	L.S.	U.S.	L.S.	U.S.	L.S.
0.10	-0.034	0.183	-0.006	0.174	-0.078	0.156	-0.379	0.143	-0.282	0.110	
0.20	-0.075	—	-0.058	—	-0.083	—	-0.571	—	-0.350	—	
0.30	-0.110	0.113	-0.092	0.114	-0.167	0.106	-0.664	0.097	-0.407	0.073	
0.40	-0.147	0.076	-0.127	0.081	-0.229	0.078	-0.759	0.073	-0.464	0.060	
0.50	-0.179	0.049	-0.153	0.056	-0.331	0.061	-0.827	0.062	-0.459	0.053	
0.60	-0.203	0.028	-0.172	0.038	-0.382	0.048	-0.908	0.053	-0.556	0.055	
0.70	-0.211	0.013	-0.178	0.026	-0.454	0.037	-0.899	0.052	-0.561	0.062	
0.80	-0.163	0.008	-0.159	0.017	-0.459	0.034	-0.869	0.052	-0.524	0.072	
0.90	-0.073	0.027	-0.087	0.030	-0.374	0.053	-0.734	0.066	-0.396	0.075	
0.95	+0.008	0.056	-0.021	0.047	-0.282	0.050	-0.568	0.044	-0.260	0.049	
0.98	+0.095	0.107	+0.064	0.085	—	—	—	—	—	—	

TABLE 13—*continued*WING C $\alpha = 15 \cdot 33 \text{ deg}$ C_p

$\frac{x}{c_0}$	$\frac{y}{s(x)}$	0		0·1		0·2		0·3		0·4	
		U.S.	L.S.	U.S.	L.S.	U.S.	L.S.	U.S.	L.S.	U.S.	L.S.
0·10	—0·080	0·340	—0·082	0·302	—0·081	0·283	—0·088	0·268	—0·081	0·250	
0·20	—0·124	0·275	—0·169	—	—0·129	—	—0·138	—	—0·135	—	
0·30	—0·155	0·215	—0·171	0·204	—0·167	0·198	—0·175	0·195	—0·170	0·182	
0·40	—0·188	0·165	—0·203	0·156	—0·205	0·152	—0·210	0·154	—	0·149	
0·50	—0·220	0·122	—0·226	0·119	—0·234	0·112	—0·240	0·116	—0·215	0·118	
0·60	—0·223	0·082	—0·240	0·085	—0·242	0·085	—0·258	0·094	—0·257	0·097	
0·70	—0·220	0·056	—0·236	0·058	—0·238	0·064	—0·254	0·069	—0·256	0·076	
0·80	—0·185	0·046	—0·194	0·041	—0·196	0·044	—0·212	0·054	—0·221	0·058	
0·90	—	—	—0·065	0·069	—0·073	0·056	—0·090	0·060	—0·112	0·058	
0·95	—	—	+0·069	0·123	0·064	0·100	+0·029	0·094	—0·010	0·083	
0·98	—	—	+0·171	0·185	0·169	0·152	+0·144	0·146	+0·097	0·130	

WING C

TABLE 13—*continued* $\alpha = 15.33 \text{ deg}$ C_p

$\frac{x}{c_0}$	$\frac{y}{s(x)}$	0.5		0.6		0.7		0.8		0.9	
		U.S.	L.S.	U.S.	L.S.	U.S.	L.S.	U.S.	L.S.	U.S.	L.S.
0.10	-0.085	0.232	-0.224	0.227	-0.719	0.184	-0.600	0.153	-0.524	0.071	
0.20	-0.118	—	-0.245	—	-0.857	—	-0.751	—	-0.613	—	
0.30	-0.148	0.176	-0.261	0.170	-0.924	0.150	-0.926	0.122	-0.673	0.062	
0.40	-0.204	0.147	-0.342	0.149	-1.007	0.134	-0.963	0.113	-0.727	0.062	
0.50	-0.249	0.122	-0.437	0.128	-1.153	0.126	-0.950	0.111	-0.779	0.068	
0.60	-0.283	0.102	-0.508	0.116	-1.155	0.117	-0.957	0.109	-0.800	0.075	
0.70	-0.307	0.085	-0.535	0.102	-1.151	0.109	-0.923	0.113	-0.769	0.095	
0.80	-0.256	0.070	-0.508	0.087	-1.078	0.106	-0.830	0.117	-0.677	0.112	
0.90	-0.162	0.068	-0.392	0.083	-0.817	0.113	-0.624	0.113	-0.455	0.116	
0.95	-0.071	0.077	-0.270	0.068	-0.614	0.072	-0.430	0.077	-0.274	0.081	
0.98	+0.046	0.106	-0.122	0.070	—	—	—	—	—	—	

WING CTABLE 13—*continued* $\alpha = 20.48 \text{ deg}$ C_p

$\frac{x}{c_0}$	$\frac{y}{s(x)}$	0		0.1		0.2		0.3		0.4	
		U.S.	L.S.	U.S.	L.S.	U.S.	L.S.	U.S.	L.S.	U.S.	L.S.
0.10	-0.140	0.444	-0.146	0.387	-0.149	0.360	-0.156	0.333	-0.168	0.310	
0.20	-0.185	0.372	-0.194	—	-0.194	—	-0.195	—	-0.209	—	
0.30	-0.219	0.318	-0.232	0.297	-0.235	0.282	-0.241	0.271	-0.253	0.256	
0.40	-0.260	0.268	-0.278	0.247	-0.283	0.239	-0.285	0.234	-0.316	0.231	
0.50	-0.296	0.220	-0.303	0.210	-0.309	0.204	-0.330	0.205	-0.370	0.200	
0.60	-0.307	0.173	-0.325	0.174	-0.330	0.179	-0.359	0.178	-0.405	0.183	
0.70	-0.310	0.140	-0.323	0.143	-0.328	0.148	-0.361	0.153	-0.416	0.162	
0.80	-0.271	0.116	-0.280	0.110	-0.283	0.117	-0.324	0.124	-0.376	0.135	
0.90	—	—	-0.132	0.120	-0.143	0.109	-0.175	0.107	-0.241	0.116	
0.95	—	—	+0.037	0.158	+0.014	0.136	-0.028	0.126	-0.095	0.118	
0.98	—	—	+0.176	0.214	+0.158	0.183	+0.120	0.163	+0.052	0.137	

TABLE 13—*continued*WING C $\alpha = 20.48 \text{ deg}$ C_p

$\frac{x}{c_0}$	$\frac{y}{s(x)}$	0.5		0.6		0.7		0.8		0.9	
		U.S.	L.S.	U.S.	L.S.	U.S.	L.S.	U.S.	L.S.	U.S.	L.S.
0.10	-0.378	0.275	-0.919	0.262	-0.966	0.189	-0.922	0.137	-0.808	0.010	
0.20	-0.299	—	-0.988	—	-1.502	—	-0.990	—	-0.891	—	
0.30	-0.389	0.237	-0.988	0.232	-1.642	0.182	-1.008	0.137	-0.969	0.029	
0.40	-0.518	0.218	-1.070	0.214	-1.615	0.178	-1.037	0.137	-1.027	0.037	
0.50	-0.597	0.195	-1.160	0.209	-1.663	0.178	-1.046	0.141	-1.055	0.064	
0.60	-0.660	0.181	-1.200	0.195	-1.573	0.176	-1.043	0.152	-1.044	0.085	
0.70	-0.685	0.170	-1.156	0.192	-1.487	0.166	-0.994	0.163	-0.956	0.125	
0.80	-0.587	0.148	-1.026	0.174	-1.325	0.162	-0.868	0.159	-0.795	0.146	
0.90	-0.420	0.123	-0.738	0.151	-0.929	0.160	-0.572	0.150	-0.477	0.142	
0.95	-0.251	0.102	-0.496	0.113	-0.654	0.102	-0.368	0.098	-0.281	0.104	
0.98	-0.070	0.099	-0.276	0.073	—	—	—	—	—	—	

TABLE 13—*continued*WING C $\alpha = 25.63 \text{ deg}$ C_p

$\frac{x}{c_0}$	$\frac{y}{s(x)}$	0		0.1		0.2		0.3		0.4	
		U.S.	L.S.	U.S.	L.S.	U.S.	L.S.	U.S.	L.S.	U.S.	L.S.
0.10	-0.226	0.543	-0.224	0.474	-0.235	0.434	-0.290	0.395	-0.512	0.358	
0.20	-0.271	0.475	-0.272	—	-0.273	—	-0.295	—	-0.473	—	
0.30	-0.305	0.420	-0.317	0.393	-0.333	0.371	-0.376	0.349	-0.533	0.325	
0.40	-0.362	0.370	-0.372	0.345	-0.394	0.332	-0.413	0.320	-0.639	0.304	
0.50	-0.411	0.322	-0.409	0.309	-0.434	0.304	-0.517	0.293	-0.706	0.283	
0.60	-0.427	0.272	-0.440	0.272	-0.463	0.275	-0.559	0.270	-0.769	0.270	
0.70	-0.435	0.235	-0.442	0.233	-0.467	0.240	-0.561	0.243	-0.765	0.250	
0.80	-0.338	0.193	-0.390	0.193	-0.411	0.198	-0.503	0.208	-0.669	0.214	
0.90	—	—	-0.213	0.178	-0.233	0.169	-0.303	0.170	-0.441	0.174	
0.95	—	—	+0.003	0.199	-0.039	0.173	-0.107	0.164	-0.230	0.152	
0.98	—	—	+0.172	0.237	+0.137	0.208	+0.083	0.182	-0.022	0.145	

TABLE 13—*continued*

WING C

 $\alpha = 25.63$ deg C_p

$\frac{x}{c_0}$	$\frac{y}{s(x)}$	0.5		0.6		0.7		0.8		0.9	
		U.S.	L.S.	U.S.	L.S.	U.S.	L.S.	U.S.	L.S.	U.S.	L.S.
0.10	-1.155	0.313	-1.440	0.270	-1.360	0.191	-1.316	0.104	-1.138	-0.063	
0.20	-1.007	—	-1.861	—	-1.681	—	-1.281	—	-1.199	—	
0.30	-1.035	0.296	-1.979	0.262	-2.016	0.212	-1.274	0.137	-1.293	-0.020	
0.40	-1.150	0.285	-1.938	0.258	-1.920	0.214	-1.299	0.150	-1.332	-0.001	
0.50	-1.213	0.271	-1.911	0.239	-1.870	0.227	-1.293	0.173	-1.347	+0.043	
0.60	-1.254	0.266	1.825	0.257	-1.750	0.231	-1.251	0.182	-1.291	0.070	
0.70	-1.237	0.254	-1.686	0.260	-1.650	0.247	-1.170	0.217	-1.166	0.131	
0.80	-1.018	0.228	-1.436	0.239	-1.437	0.235	-0.948	0.234	-0.825	0.175	
0.90	-0.696	0.186	-0.974	0.203	-0.965	0.216	-0.584	0.215	-0.518	0.187	
0.95	-0.430	0.142	-0.655	0.137	-0.675	0.141	-0.394	0.145	-0.364	+0.135	
0.98	-0.186	0.104	-0.392	0.060	—	—	—	—	—	—	

TABLE 13—*continued*WING C $\alpha = 30.77 \text{ deg}$ C_p

$\frac{x}{c_0}$	$\frac{y}{s(x)}$	0		0.1		0.2		0.3		0.4	
		U.S.	L.S.	U.S.	L.S.	U.S.	L.S.	U.S.	L.S.	U.S.	L.S.
0.10	-0.305	0.645	-0.329	0.545	-0.409	0.503	-0.624	0.451	-1.199	0.400	
0.20	-0.370	0.580	-0.379	—	-0.431	—	-0.607	—	-1.143	—	
0.30	-0.405	0.530	-0.421	0.486	-0.478	0.460	-0.681	0.425	-1.169	0.387	
0.40	-0.457	0.485	-0.480	0.452	-0.561	0.430	-0.624	0.408	-1.191	0.374	
0.50	-0.510	0.435	-0.535	0.423	-0.617	0.409	-0.802	0.391	-1.234	0.365	
0.60	-0.531	0.385	-0.573	0.377	-0.669	0.374	-0.846	0.373	-1.247	0.356	
0.70	-0.545	0.335	-0.577	0.343	-0.660	0.340	-0.824	0.339	-1.169	0.343	
0.80	-0.489	0.295	-0.505	0.284	-0.574	0.289	-0.724	0.296	-0.985	0.304	
0.90	—	—	-0.279	0.242	-0.318	0.233	-0.433	0.248	-0.631	0.238	
0.95	—	—	-0.031	0.247	-0.080	0.229	-0.185	0.227	-0.343	0.199	
0.98	—	—	+0.167	0.268	+0.115	0.255	+0.037	0.244	-0.085	0.186	

TABLE 13—*continued*WING C $\alpha = 30.77 \text{ deg}$ C_p

$\frac{x}{c_0}$	$\frac{y}{s(x)}$	0.5		0.6		0.7		0.8		0.9	
		U.S.	L.S.	U.S.	L.S.	U.S.	L.S.	U.S.	L.S.	U.S.	L.S.
0.10	-1.887	0.340		-1.733	0.275	-1.732	0.173	-1.768	0.058	-1.513	-0.186
0.20	-1.934	—		-2.061	—	-1.888	—	-1.682	—	-1.586	—
0.30	-2.056	0.353		-2.695	0.309	-2.155	0.224	-1.619	0.113	-1.603	-0.083
0.40	-2.052	0.357		-2.716	0.318	-2.338	0.257	-1.542	0.160	-1.543	-0.023
0.50	-1.959	0.361		-2.610	0.318	-2.291	0.270	-1.503	0.185	-1.539	0.015
0.60	-1.887	0.357		-2.372	0.339	-2.116	0.292	-1.512	0.232	-1.526	0.071
0.70	-1.731	0.340		-2.087	0.343	-1.866	0.309	-1.383	0.274	-1.393	0.148
0.80	-1.364	0.319		-1.670	0.322	-1.508	0.313	-1.066	0.296	-1.058	0.213
0.90	-0.883	0.256		-1.057	0.271	-0.959	0.283	-0.611	0.274	-0.564	0.234
0.95	-0.541	0.205		-0.699	0.190	-0.670	0.202	-0.436	0.202	-0.422	0.191
0.98	-0.250	0.138		-0.419	0.096	—	—	—	—	—	—

WING C

TABLE 14

Pressure Coefficients at $\beta = -5 \text{ deg}$ $\alpha = 0 \text{ deg}$ C_p

$\frac{x}{c_0}$	$\frac{y}{s(x)}$	0		0.1		0.2		0.4		0.6		0.8		0.9	
		U.S.	L.S.												
0.20		—	—	-0.032	—	+0.009	—	+0.003	—	+0.005	—	+0.009	—	+0.006	—
0.40		-0.083	-0.098	-0.113	-0.120	-0.055	-0.062	-0.059	-0.059	-0.047	-0.052	-0.041	-0.043	-0.031	-0.027
0.60		-0.104	-0.114	-0.124	-0.126	-0.094	-0.098	-0.093	-0.092	-0.084	-0.086	-0.071	-0.072	-0.060	-0.059
0.80		-0.081	-0.077	-0.092	-0.089	-0.080	-0.075	-0.077	-0.075	-0.074	-0.074	-0.061	-0.060	-0.048	-0.054

$\frac{x}{c_0}$	$\frac{y}{s(x)}$	-0.1		-0.2		-0.4		-0.6		-0.8		-0.9			
		U.S.	L.S.	U.S.	L.S.										
0.20		+0.027	+0.078	+0.040	+0.074	+0.049	—	+0.063	—	+0.083	+0.059	+0.101	—		
0.40		-0.065	-0.075	-0.060	-0.061	-0.057	-0.051	-0.034	-0.038	-0.007	-0.011	+0.015	+0.016		
0.60		-0.118	-0.124	-0.120	-0.127	-0.121	-0.124	-0.107	-0.109	-0.080	-0.082	-0.056	-0.051		
0.80		-0.097	-0.097	-0.111	-0.109	-0.127	-0.127	-0.130	-0.123	-0.107	-0.110	-0.081	-0.084		

TABLE 14—*continued*WING C $\alpha = 2.03 \text{ deg}$ C_p

88

$\frac{x}{c_0}$	$\frac{y}{s(x)}$	0		0.1		0.2		0.4		0.6		0.8		0.9	
		U.S.	L.S.	U.S.	L.S.										
0.20	—	—	—	-0.083	—	-0.009	—	-0.015	—	-0.010	—	-0.006	—	-0.015	—
0.40	-0.095	-0.092	-0.116	-0.096	-0.074	-0.043	-0.075	-0.041	-0.064	-0.033	-0.061	-0.027	-0.053	-0.014	
0.60	-0.114	-0.104	-0.128	-0.113	-0.111	-0.082	-0.110	-0.076	-0.101	-0.064	-0.094	-0.051	-0.094	-0.036	
0.80	-0.087	-0.071	-0.092	-0.078	-0.091	-0.065	-0.091	-0.062	-0.089	-0.056	-0.082	-0.038	-0.103	-0.026	

$\frac{x}{c_0}$	$\frac{y}{s(x)}$	-0.1		-0.2		-0.4		-0.6		-0.8		-0.9	
		U.S.	L.S.										
0.20		+0.004	+0.080	+0.015	+0.079	+0.023	—	+0.037	—	+0.055	—	+0.071	—
0.40		-0.085	-0.047	-0.084	-0.039	-0.056	-0.026	-0.063	-0.006	-0.041	+0.026	-0.025	+0.049
0.60		-0.127	-0.104	-0.138	-0.107	-0.145	-0.101	-0.136	-0.077	-0.126	-0.040	-0.102	-0.004
0.80		-0.103	-0.089	-0.118	-0.101	-0.143	-0.112	-0.154	-0.084	-0.139	-0.067	-0.123	-0.029

WING CTABLE 14—*continued* $\alpha = 4.07 \text{ deg}$ C_p

$\frac{x}{c_0}$	$\frac{y}{s(x)}$	0		0.1		0.2		0.4		0.6		0.8		0.9	
		U.S.	L.S.	U.S.	L.S.										
0.20	—	—	—	-0.099	—	-0.028	—	-0.032	—	-0.029	—	-0.015	—	-0.143	—
0.40	-0.110	-0.076	-0.128	-0.073	-0.092	-0.024	-0.096	-0.019	-0.086	-0.014	-0.069	-0.007	-0.211	-0.001	
0.60	-0.128	-0.091	-0.142	-0.094	-0.127	-0.064	-0.129	-0.055	-0.122	-0.043	-0.108	-0.027	-0.274	-0.017	
0.80	-0.097	-0.062	-0.103	-0.067	-0.100	-0.052	-0.103	-0.047	-0.105	-0.038	-0.103	-0.015	-0.278	-0.005	

81

$\frac{x}{c_0}$	$\frac{y}{s(x)}$	-0.1		-0.2		-0.4		-0.6		-0.8		-0.9	
		U.S.	L.S.	U.S.	L.S.	U.S.	L.S.	U.S.	L.S.	U.S.	L.S.	U.S.	L.S.
0.20		-0.023	+0.084	-0.014	+0.077	-0.006	—	+0.007	—	+0.032	—	-0.048	—
0.40		-0.108	-0.020	-0.108	-0.012	-0.087	0.005	-0.093	0.023	-0.059	+0.054	-0.200	0.841
0.60		-0.148	-0.085	-0.160	-0.085	-0.169	0.061	-0.165	-0.045	-0.133	-0.004	-0.344	0.385
0.80		-0.111	-0.078	-0.129	-0.086	-0.158	0.081	-0.175	-0.068	-0.147	-0.033	-0.408	0.200

TABLE 14—*continued*

WING C

 $\alpha = 6.11 \text{ deg}$ C_p

$\frac{x}{c_0}$	$\frac{y}{s(x)}$	0		0.1		0.2		0.4		0.6		0.8		0.9	
		U.S.	L.S.	U.S.	L.S.										
0.20	—	—	—	-0.109	—	-0.053	—	-0.051	—	-0.047	—	-0.095	—	-0.191	—
0.40	-0.123	-0.058	-0.140	-0.041	-0.116	-0.004	-0.114	+0.003	-0.103	+0.005	-0.180	+0.005	-0.245	+0.006	
0.60	-0.141	-0.072	-0.154	-0.070	-0.146	-0.042	-0.146	-0.032	-0.140	-0.021	-0.280	-0.008	-0.299	-0.001	
0.80	-0.108	-0.049	-0.113	-0.052	-0.116	-0.037	-0.116	-0.029	-0.115	-0.017	-0.310	+0.006	-0.290	+0.015	

$\frac{x}{c_0}$	$\frac{y}{s(x)}$	-0.1		-0.2		-0.4		-0.6		-0.8		-0.9	
		U.S.	L.S.	U.S.	L.S.	U.S.	L.S.	U.S.	L.S.	U.S.	L.S.	U.S.	L.S.
0.20	-0.046	+0.081	-0.039	+0.074	-0.033	—	-0.019	—	-0.032	—	-0.185	—	—
0.40	-0.126	+0.009	-0.130	+0.017	-0.123	+0.035	-0.115	+0.053	-0.231	0.081	-0.321	0.094	0.060
0.60	-0.163	-0.058	-0.177	-0.057	-0.189	-0.040	-0.178	-0.012	-0.421	0.026	-0.455	0.047	—
0.80	-0.118	-0.061	-0.139	-0.068	-0.172	-0.066	-0.170	-0.040	-0.527	0.002	-0.498	0.047	—

TABLE 14—*continued*WING C $\alpha = 8.15 \text{ deg}$ C_p

58

$\frac{x}{c_0}$	$\frac{y}{s(x)}$	0		0.1		0.2		0.4		0.6		0.8		0.9	
		U.S.	L.S.	U.S.	L.S.										
0.20	—	—	—	-0.121	—	-0.079	—	-0.074	—	-0.068	—	-0.295	—	-0.239	—
0.40	-0.136	-0.034	-0.150	-0.006	-0.136	+0.020	-0.136	+0.024	-0.120	0.027	-0.418	0.019	-0.311	0.007	
0.60	-0.155	-0.048	-0.166	-0.038	-0.165	-0.019	-0.167	-0.008	-0.154	0.002	-0.514	0.009	-0.367	0.007	
0.80	-0.117	-0.031	-0.120	-0.031	-0.130	-0.019	-0.131	-0.010	-0.126	0.004	-0.514	0.027	-0.341	0.030	

$\frac{x}{c_0}$	$\frac{y}{s(x)}$	-0.1		-0.2		-0.4		-0.6		-0.8		-0.9	
		U.S.	L.S.	U.S.	L.S.	U.S.	L.S.	U.S.	L.S.	U.S.	L.S.	U.S.	L.S.
0.20		-0.071	+0.079	-0.065	+0.077	-0.061	—	-0.035	—	-0.303	—	-0.172	—
0.40		-0.146	+0.041	-0.151	+0.047	-0.156	+0.065	-0.122	+0.084	-0.494	0.105	-0.435	0.105
0.60		-0.178	-0.032	-0.195	-0.030	-0.209	-0.010	-0.166	+0.021	-0.706	0.059	-0.567	0.082
0.80		-0.127	-0.045	-0.151	-0.050	-0.183	-0.044	-0.141	-0.010	-0.795	0.035	-0.565	0.074

TABLE 14—*continued*WING C $\alpha = 10.20 \text{ deg}$ C_p

$\frac{x}{c_0}$	$\frac{y}{s(x)}$	0		0.1		0.2		0.4		0.6		0.8		0.9	
		U.S.	L.S.	U.S.	L.S.										
0.20	—	—	—	-0.138	—	-0.100	—	-0.096	—	-0.197	—	-0.382	—	-0.306	—
0.40	-0.155	-0.013	-0.168	+0.029	-0.156	0.047	-0.158	0.049	-0.140	0.049	-0.601	0.031	-0.385	0.011	
0.60	-0.174	-0.029	-0.183	-0.002	-0.183	0.006	-0.187	0.016	-0.180	0.026	-0.667	0.029	-0.439	0.016	
0.80	-0.132	-0.017	-0.136	-0.013	-0.141	0	-0.146	0.010	-0.155	0.026	-0.623	0.049	-0.387	0.047	

$\frac{x}{c_0}$	$\frac{y}{s(x)}$	-0.1		-0.2		-0.4		-0.6		-0.8		-0.9	
		U.S.	L.S.	U.S.	L.S.	U.S.	L.S.	U.S.	L.S.	U.S.	L.S.	U.S.	L.S.
0.20	-0.096	+0.081	-0.087	+0.071	-0.084	—	-0.034	—	-0.546	—	-0.384	—	
0.40	-0.168	+0.073	-0.175	0.081	-0.174	+0.097	-0.114	0.115	-0.764	0.128	-0.534	0.119	
0.60	-0.197	-0.006	-0.213	+0.003	-0.223	+0.021	-0.156	0.054	-0.977	0.091	-0.659	0.102	
0.80	-0.143	-0.027	-0.164	-0.028	-0.189	-0.018	-0.145	0.019	-1.016	0.065	-0.646	0.113	

TABLE 14—*continued*WING C $\alpha = 15 \cdot 33$ deg C_p

$\frac{x}{c_0}$	$\frac{y}{s(x)}$	0		0.1		0.2		0.4		0.6		0.8		0.9	
		U.S.	L.S.												
0.20		—	—	-0.196	—	-0.164	—	-0.160	—	-0.327	—	-0.592	—	-0.510	—
0.40		-0.215	0.048	-0.241	0.113	-0.226	0.116	-0.222	0.116	-0.402	0.100	-0.725	0.054	-0.579	0.010
0.60		-0.233	0.037	-0.253	0.070	-0.243	0.075	-0.253	0.085	-0.436	0.086	-0.834	0.068	-0.596	0.035
0.80		-0.185	0.033	-0.196	0.041	-0.197	0.050	-0.204	0.068	-0.375	0.084	-0.689	0.086	-0.464	0.069

$\frac{x}{c_0}$	$\frac{y}{s(x)}$	-0.1		-0.2		-0.4		-0.6		-0.8		-0.9	
		U.S.	L.S.										
0.20		-0.163	0.078	-0.151	0.062	-0.123	—	-0.126	—	-1.069	—	-0.661	—
0.40		-0.233	0.161	-0.234	0.172	-0.204	0.185	-0.333	0.186	-1.254	0.171	-0.830	0.125
0.60		-0.265	0.076	-0.270	0.083	-0.249	0.112	-0.536	0.138	-1.297	0.152	-0.953	0.131
0.80		-0.210	0.027	-0.218	0.031	-0.206	0.052	-0.616	0.092	-1.102	0.132	-0.847	0.163

WING CTABLE 14—*continued* $\alpha = 20.48 \text{ deg}$ C_p

$\frac{x}{c_0}$	$\frac{y}{s(x)}$	0		0.1		0.2		0.4		0.6		0.8		0.9	
		U.S.	L.S.	U.S.	L.S.	U.S.	L.S.	U.S.	L.S.	U.S.	L.S.	U.S.	L.S.	U.S.	L.S.
0.20	—	—	—	-0.305	—	-0.229	—	-0.299	—	-0.836	—	-0.786	—	-0.791	—
0.40	-0.316	0.137	-0.351	0.201	-0.287	0.199	-0.370	0.181	-0.959	0.153	-0.847	0.085	-0.749	-0.001	
0.60	-0.350	0.120	-0.353	0.157	-0.326	0.159	-0.426	0.162	-0.881	0.153	-0.813	0.113	-0.726	+0.033	
0.80	-0.283	0.099	-0.278	0.111	-0.285	0.118	-0.337	0.137	-0.661	0.151	-0.662	0.153	-0.528	+0.123	

$\frac{x}{c_0}$	$\frac{y}{s(x)}$	-0.1		-0.2		-0.4		-0.6		-0.8		-0.9	
		U.S.	L.S.										
0.20		-0.229	0.070	-0.210	0.053	-0.157	—	-0.884	—	-1.241	—	-1.002	—
0.40		-0.305	0.261	-0.293	0.271	-0.262	0.271	-1.223	0.256	-1.268	0.201	-1.191	0.106
0.60		-0.347	0.170	-0.341	0.182	-0.355	0.200	-1.481	0.220	-1.297	0.213	-1.289	0.146
0.80		-0.289	0.097	-0.291	0.109	-0.355	0.129	-1.408	0.174	-1.066	0.209	-1.042	0.204

TABLE 14—*continued*

WING C

 $\alpha = 25.63 \text{ deg}$ C_p

$\frac{x}{c_0}$	$\frac{y}{s(x)}$	0		0.1		0.2		0.4		0.6		0.8		0.9	
		U.S.	L.S.	U.S.	L.S.	U.S.	L.S.	U.S.	L.S.	U.S.	L.S.	U.S.	L.S.	U.S.	L.S.
0.20		—	—	-0.456	—	-0.334	—	-0.592	—	-1.455	—	-0.930	—	-0.938	—
0.40	-0.484	0.250	-0.487	0.306	-0.435	0.288	-0.713	0.252	-1.369	0.210	-0.953	0.100	-0.996	-0.040	
0.60	-0.542	0.222	-0.489	0.258	-0.498	0.251	-0.729	0.245	-1.201	0.229	-0.890	0.158	-0.886	+0.043	
0.80	-0.398	0.182	-0.381	0.195	-0.403	0.200	-0.529	0.212	-0.829	0.227	-0.666	0.212	-0.590	+0.153	

78

$\frac{x}{c_0}$	$\frac{y}{s(x)}$	-0.1		-0.2		-0.4		-0.6		-0.8		-0.9	
		U.S.	L.S.										
0.20		-0.293	0.064	-0.265	—	-0.301	—	-2.040	—	-1.469	—	-1.384	—
0.40		-0.387	0.367	-0.370	0.366	-0.529	0.354	-2.364	0.321	-1.578	0.217	-1.592	0.058
0.60		-0.441	0.275	-0.435	0.284	-0.708	0.293	-2.434	0.300	-1.584	0.252	-1.646	0.135
0.80		-0.379	0.185	-0.391	0.194	-0.706	0.222	-2.024	0.248	-1.222	0.273	-1.226	0.233

TABLE 14—*continued*

WING C

 $\alpha = 30.77 \text{ deg}$ C_p

$\frac{x}{c_0}$	$\frac{y}{s(x)}$	0		0.1		0.2		0.4		0.6		0.8		0.9	
		U.S.	L.S.	U.S.	L.S.	U.S.	L.S.	U.S.	L.S.	U.S.	L.S.	U.S.	L.S.	U.S.	L.S.
0.20	—	—	—	-0.648	—	-0.574	—	-1.115	—	-1.668	—	-1.141	—	-1.168	—
0.40	-0.721	0.360	-0.636	0.403	-0.681	0.379	-1.111	0.323	-1.429	0.272	-1.046	0.111	-1.082	-0.036	
0.60	-0.803	0.318	-0.665	0.343	-0.720	0.336	-0.981	0.319	-1.181	0.293	-0.911	0.193	-0.895	+0.058	
0.80	-0.565	0.236	-0.546	0.254	-0.570	0.255	-0.678	0.267	-0.814	0.285	-0.673	0.249	-0.614	+0.181	

88

$\frac{x}{c_0}$	$\frac{y}{s(x)}$	-0.1		-0.2		-0.4		-0.6		-0.8		-0.9	
		U.S.	L.S.										
0.20		-0.342	0.020	-0.318	—	-0.721	—	-3.199	—	-1.933	—	-1.780	—
0.40		-0.423	0.479	-0.425	0.468	-0.972	0.448	-3.211	0.400	-1.903	0.249	-1.848	0.049
0.60		-0.585	0.364	-0.656	0.379	-1.245	0.388	-1.784	0.383	-1.223	0.323	-1.197	0.215
0.80		-0.597	0.232	-0.703	0.246	-0.872	0.267	-0.959	0.315	-0.894	0.297	-0.819	0.267

TABLE 15

WING A

Local Cross-Load Coefficients $C_N(x)$

$\frac{x}{c_0}$	α	2.06	4.14	6.23	8.32	10.43	15.73	21.06	26.46	31.65
0.2		0.089	0.207	0.321	0.445	0.608	1.041	1.569	2.169	2.782
0.4		0.064	0.164	0.250	0.357	0.482	0.815	1.217	1.677	2.023
0.6		0.041	0.117	0.184	0.265	0.360	0.611	0.957	1.265	1.528
0.8		0.024	0.075	0.119	0.174	0.233	0.408	0.620	0.819	1.033
0.9		0.007	0.040	0.071	0.108	0.150	0.252	0.249	0.519	0.670

TABLE 16

WING B

Local Cross-Load Coefficients $C_N(x)$

$\frac{x}{c_0}$	α	2.02	4.05	6.09	8.13	10.17	15.29	20.42	25.56	30.70
0.1		0.036	0.077	0.127	0.191	0.254	0.452	0.703	1.041	1.430
0.2		0.036	0.085	0.137	0.194	0.258	0.461	0.709	1.040	1.428
0.3		0.043	0.097	0.148	0.204	0.270	0.476	0.723	1.062	1.469
0.4		0.043	0.093	0.148	0.209	0.276	0.494	0.745	1.086	1.480
0.5		0.046	0.097	0.152	0.215	0.281	0.507	0.758	1.090	1.484
0.6		0.047	0.093	0.151	0.216	0.292	0.515	0.769	1.088	1.474
0.7		0.047	0.094	0.151	0.194	0.290	0.514	0.765	1.073	1.430
0.8		0.044	0.087	0.130	0.208	0.260	0.473	0.704	0.976	1.252
0.9		0.028	0.054	0.094	0.146	0.204	0.359	0.510	0.675	0.838

TABLE 17

WING C

Local Cross-Load Coefficients $C_N(x)$

$\frac{x}{c_0}$	α	2.03	4.07	6.11	8.15	10.20	15.33	20.48	25.63	30.77
0.1		0.038	0.095	0.139	0.202	0.267	0.453	0.742	1.079	1.438
0.2	—	0.096	0.150	0.215	0.291	0.498	0.793	1.160	1.544	
0.3		0.048	0.098	0.160	0.226	0.311	0.537	0.838	1.222	1.619
0.4		0.043	0.100	0.168	0.236	0.326	0.566	0.875	1.262	1.669
0.5		0.047	0.102	0.175	0.245	0.340	0.587	0.902	1.279	1.684
0.6		0.047	0.104	0.180	0.252	0.348	0.596	0.903	1.260	1.648
0.7		0.046	0.104	0.176	0.253	0.350	0.583	0.867	1.203	1.512
0.8		0.043	0.095	0.162	0.233	0.318	0.521	0.758	1.047	1.274
0.9		0.031	0.069	0.124	0.170	0.227	0.365	0.532	0.699	0.845
0.95		0.014	0.042	0.078	0.109	0.144	0.228	0.335	0.450	0.484

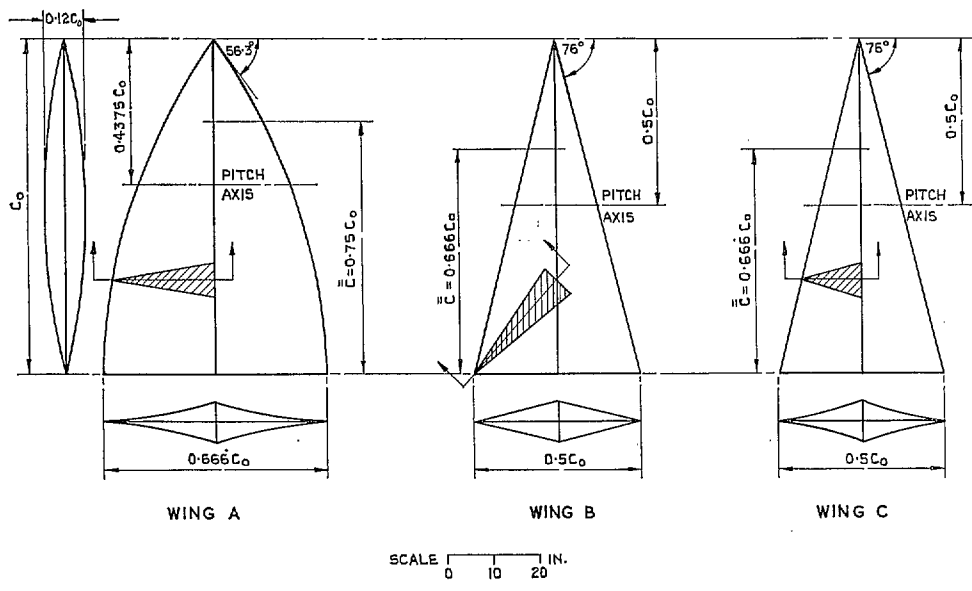


FIG. 1. Thick wings of aspect ratio 1.

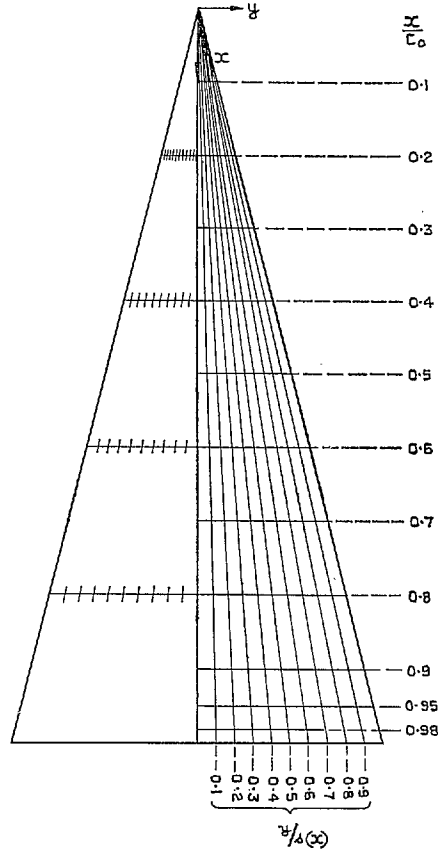
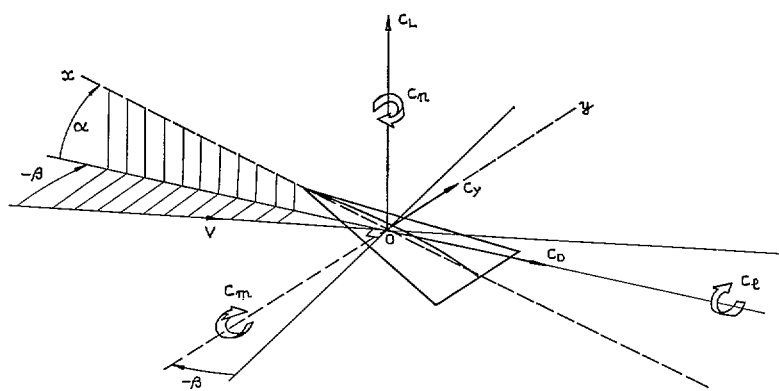


FIG. 2. Position of pressure holes on wing C. Pressure-plotting holes at intersections of spanwise rows (constant x/c_0) and rays (constant $y/s(x)$).



O_X, O_Y BODY AXES
O MEAN QUARTER-CHORD POINT

FIG. 3. Force and moment axes system.

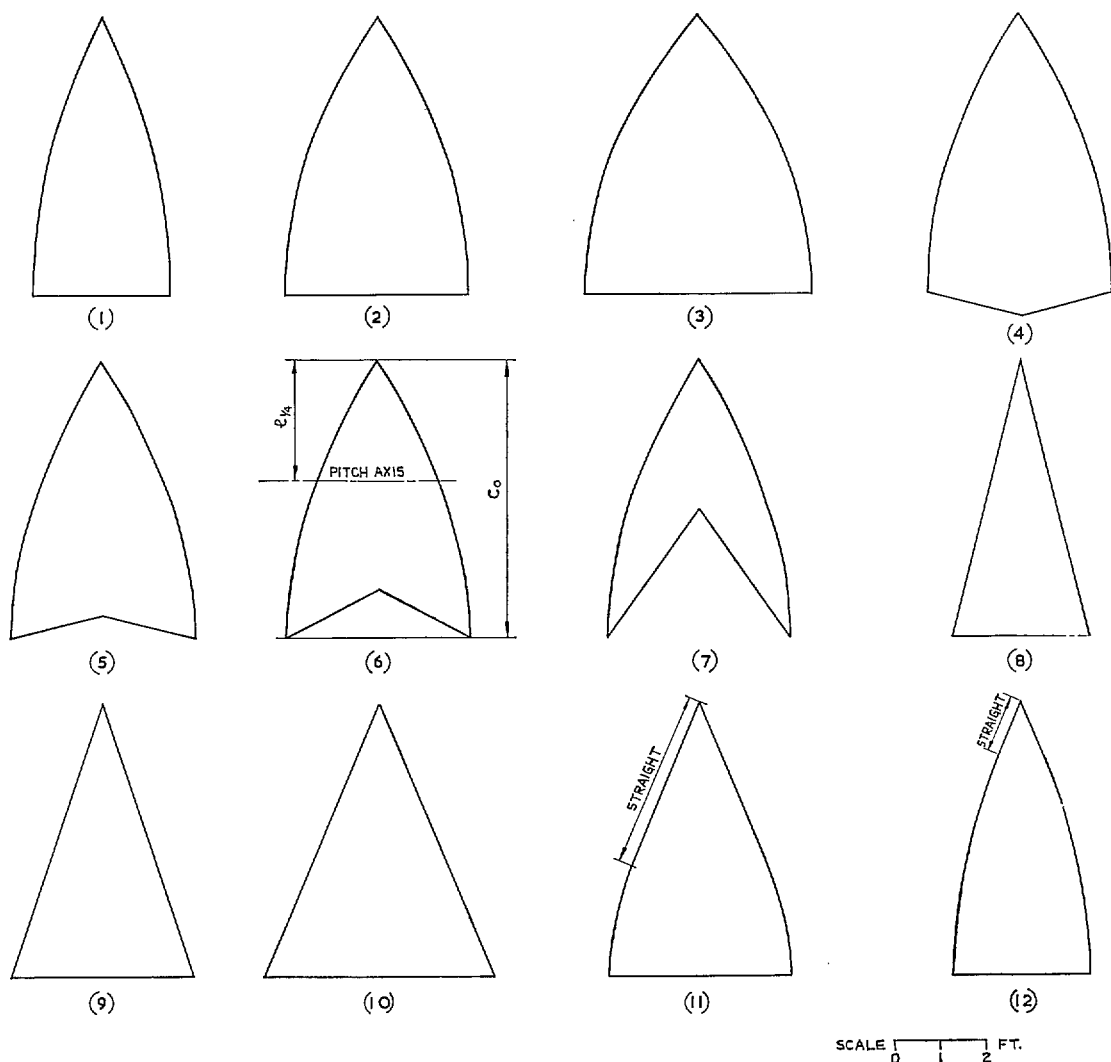
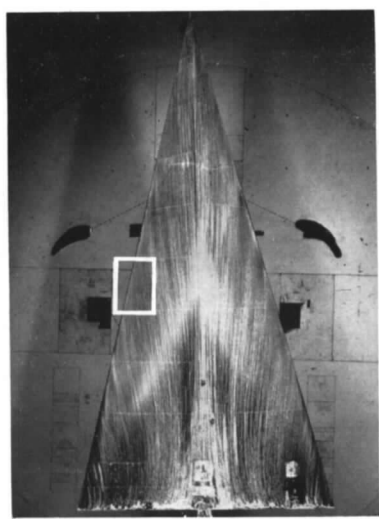


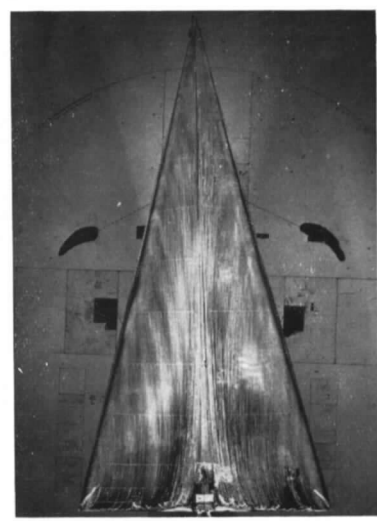
FIG. 4. Flat-plate models. (See Table 1 for geometric details.)



$\alpha = 2.02$ deg

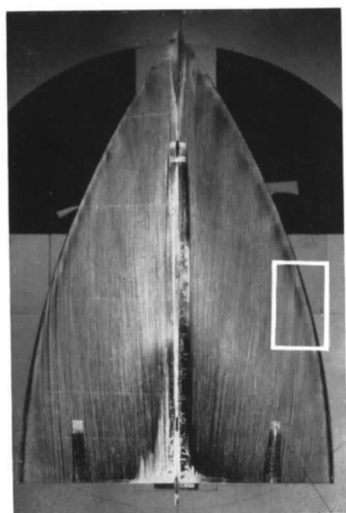


$\alpha = 2.02$ deg

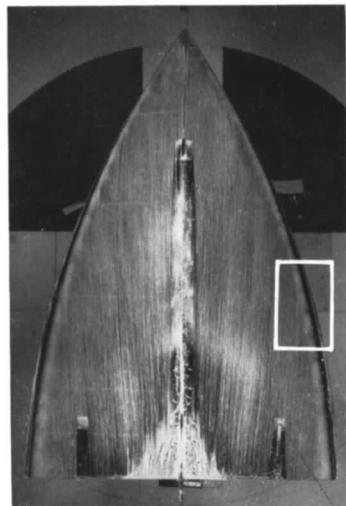


$\alpha = 5.07$ deg

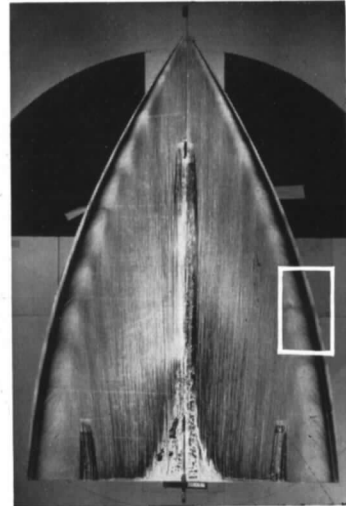
FIG. 5. Wing B. Oil-flow patterns at low incidences.



$\alpha = 1.03$ deg



$\alpha = 2.07$ deg



$\alpha = 5.19$ deg

FIG. 6. Wing A. Oil-flow patterns at low incidences.

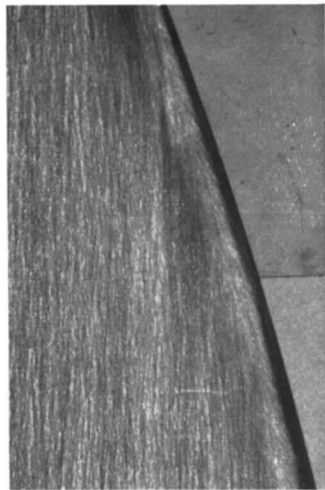
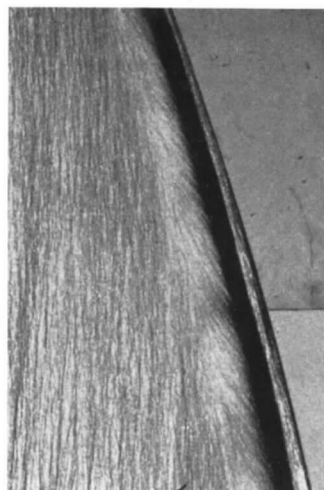
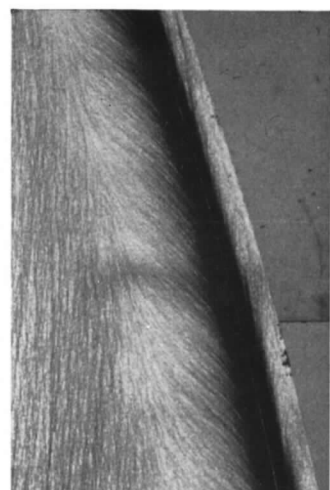
 $\alpha = 1.03 \text{ deg}$  $\alpha = 2.07 \text{ deg}$  $\alpha = 5.19 \text{ deg}$

FIG. 7. Wing A. Enlargements of areas marked in Fig. 6.

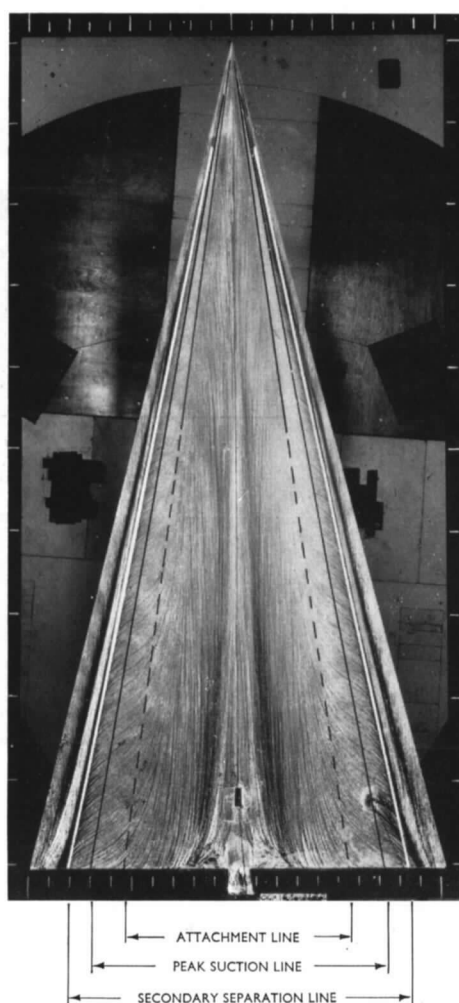


FIG. 8. Typical surface oil-flow pattern, wing C. $\alpha = 15.33 \text{ deg.}$

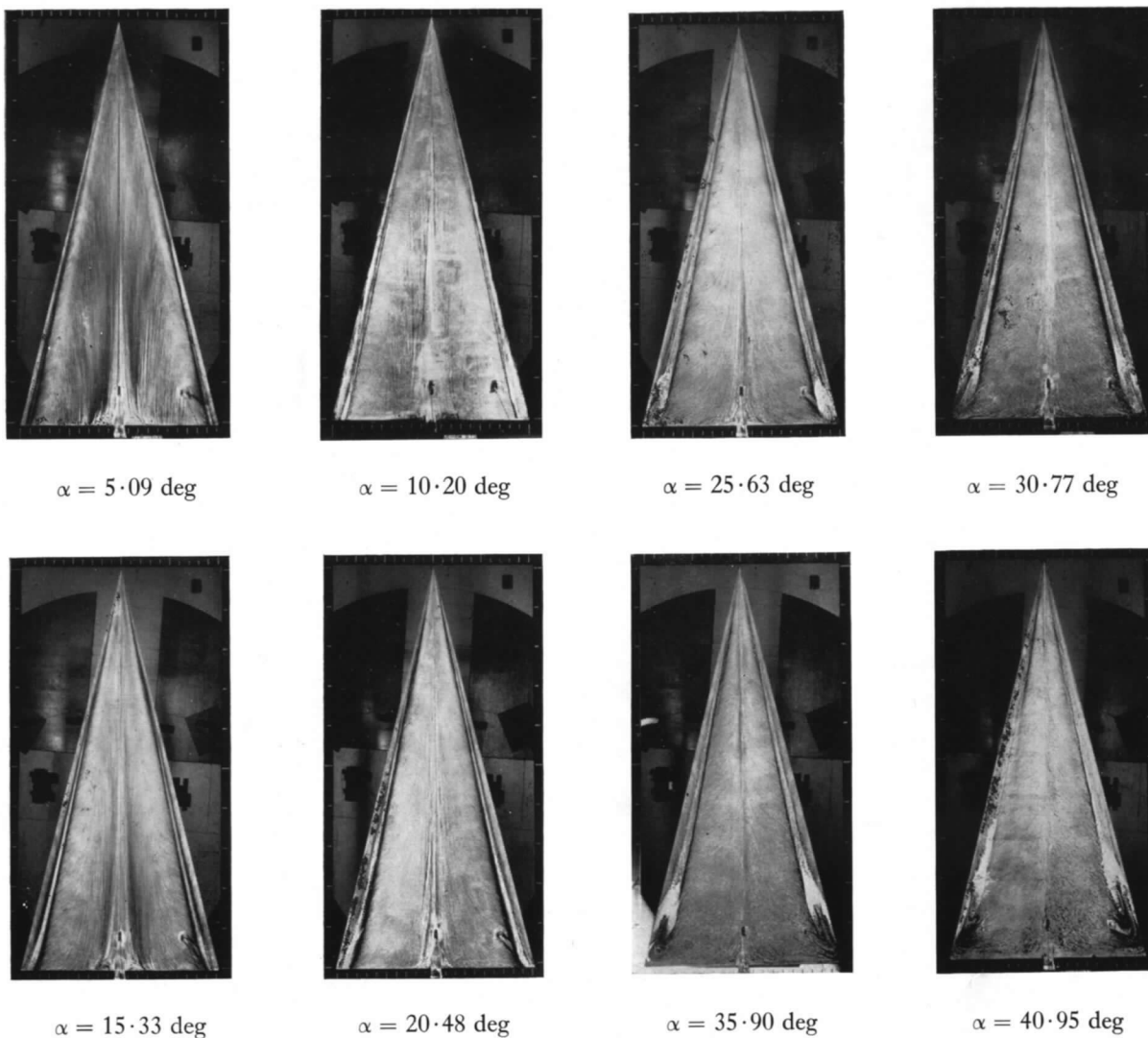


FIG. 9. Variation of surface oil-flow pattern with incidence, wing C.

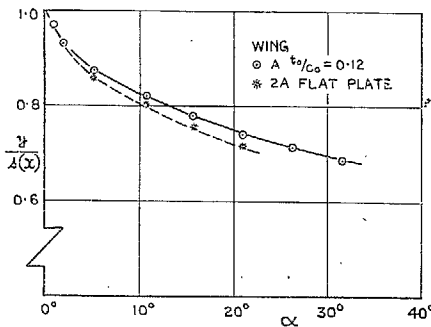


FIG. 10. Effect of thickness on spanwise position of suction peaks on gothic wing of aspect ratio 1.

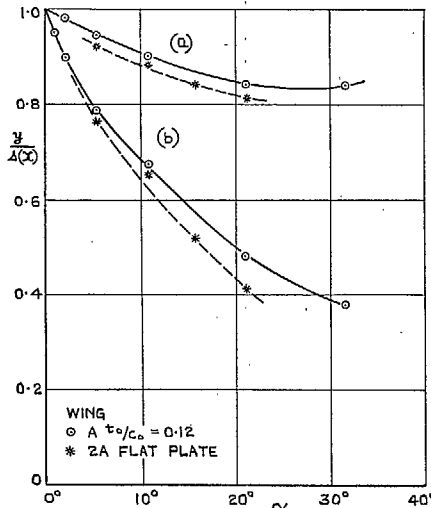


FIG. 11. Effect of thickness on position of secondary separation (a) and attachment line (b) on gothic wing of aspect ratio 1.

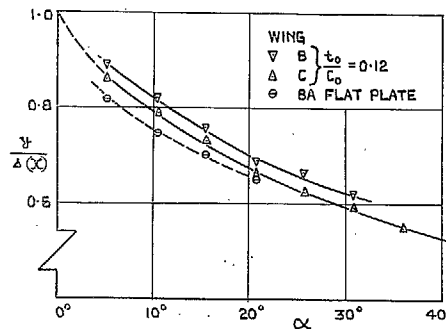


FIG. 12. Effect of thickness on spanwise position of suction peaks on delta wings of aspect ratio 1.

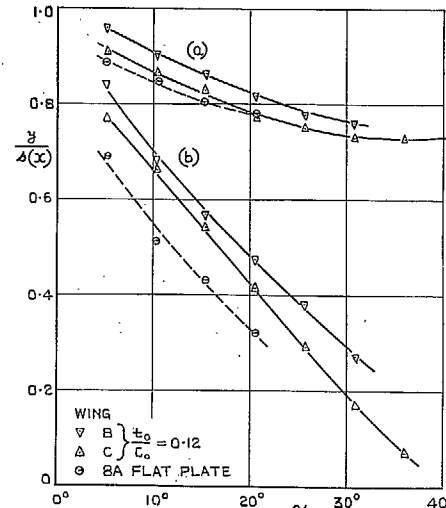


FIG. 13. Effect of thickness on position of secondary separation (a) and attachment line (b) on delta wings of aspect ratio 1.

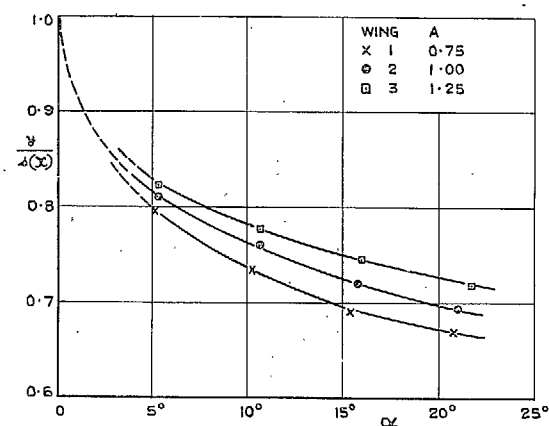


FIG. 14. Spanwise position of points of inflection on flat-plate gothic wings.

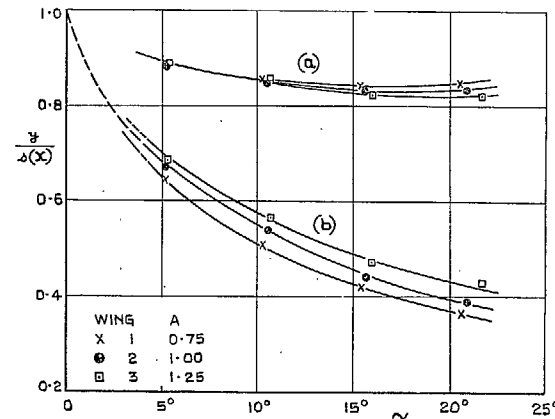


FIG. 15. Spanwise position of secondary separation (a) and attachment line (b) on flat-plate gothic wings.

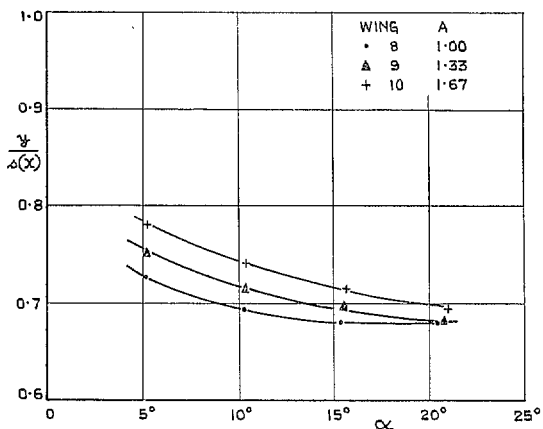


FIG. 16. Spanwise position of points of inflection on flat-plate delta wings.

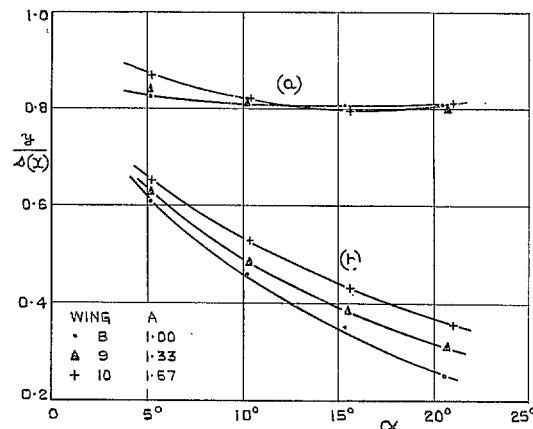


FIG. 17. Spanwise position of secondary separation (a) and attachment line (b) on flat-plate delta wings.

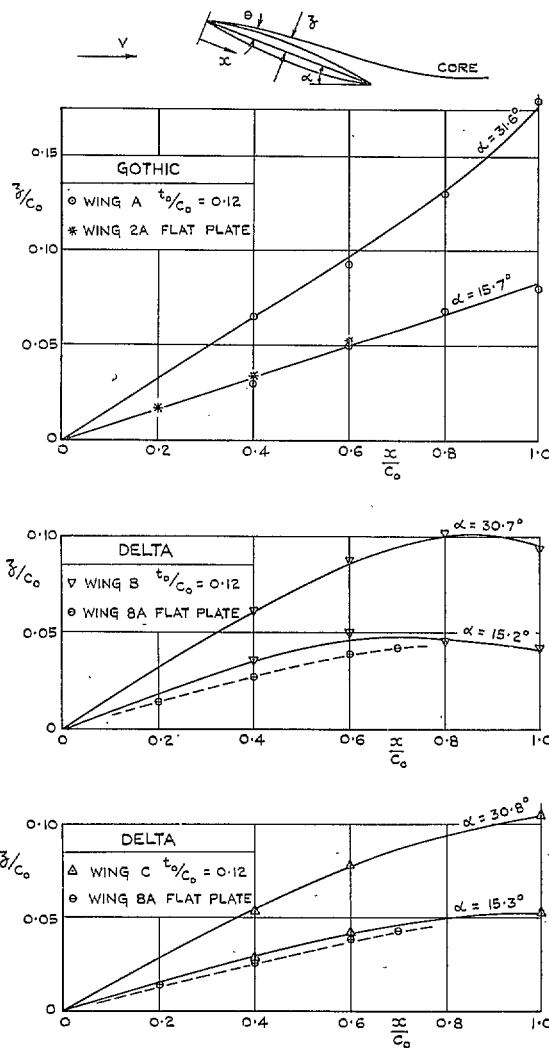


FIG. 18. Side elevation of vortex-core path on wings A, B and C. Aspect ratio = 1.

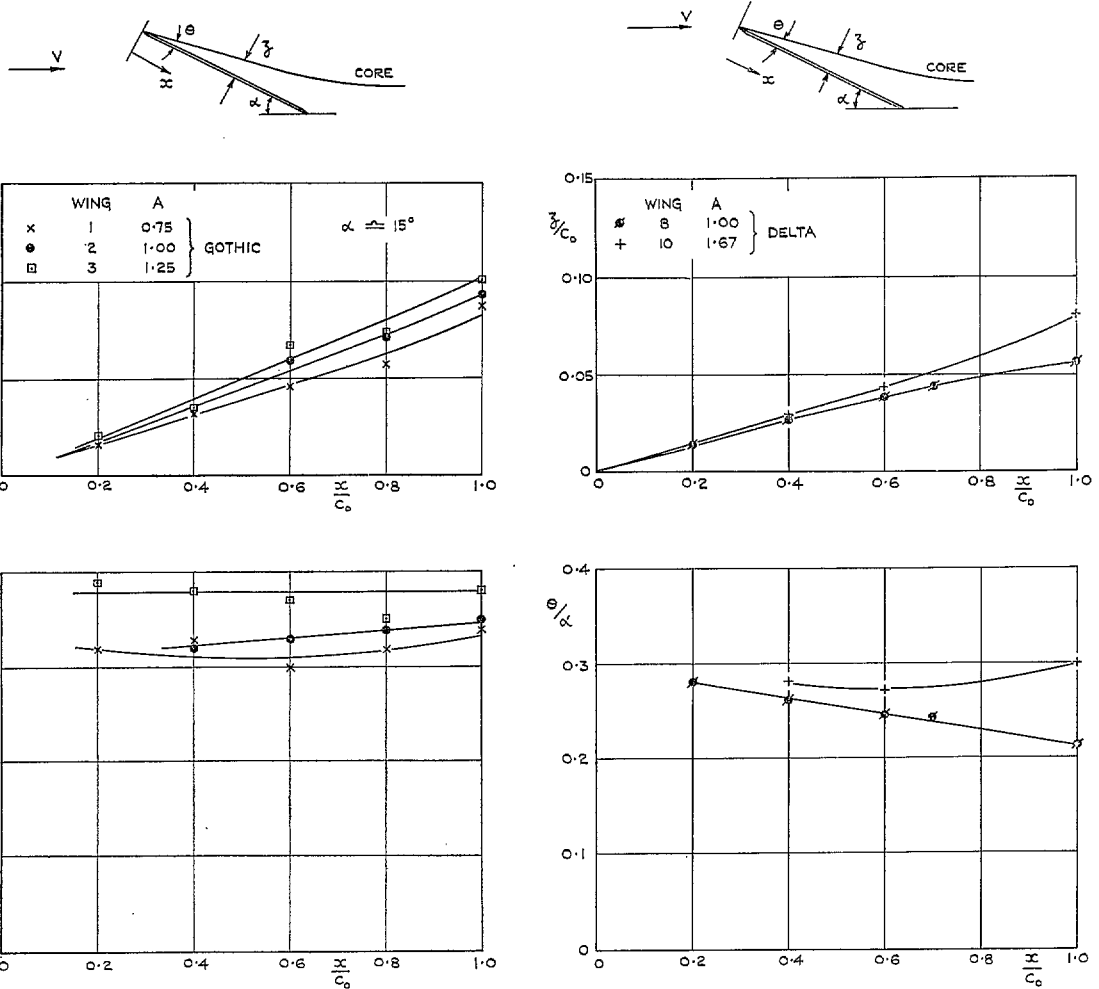


FIG. 19. Side elevation of vortex-core path on flat-plate gothic wings of various aspect ratios. $\alpha \approx 15$ deg.

FIG. 20. Side elevation of vortex-core path on flat-plate delta wings of various aspect ratios. $\alpha \approx 15$ deg.

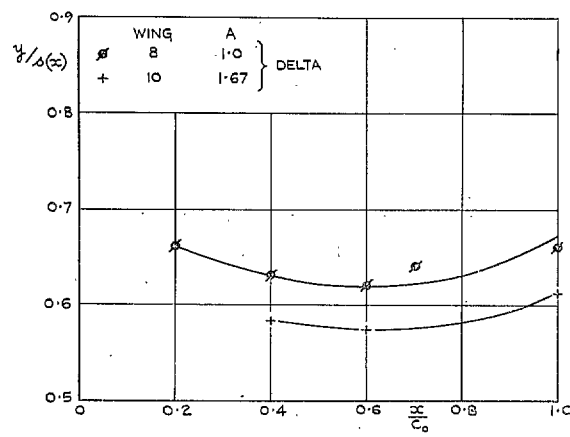
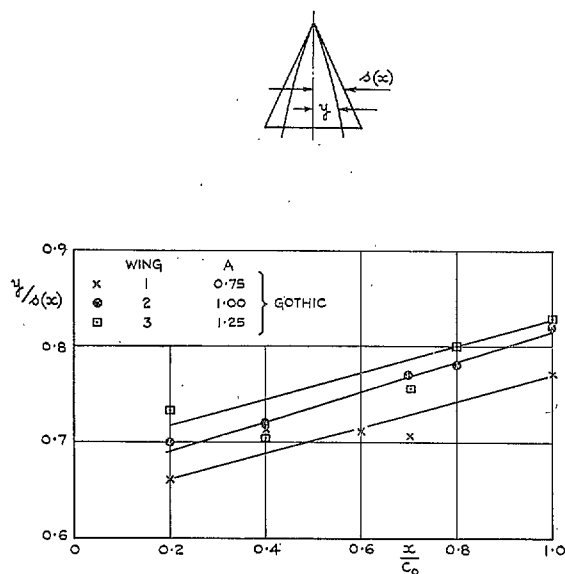


FIG. 21. Plan view of vortex paths on flat-plate wings. $\alpha \approx 15$ deg.

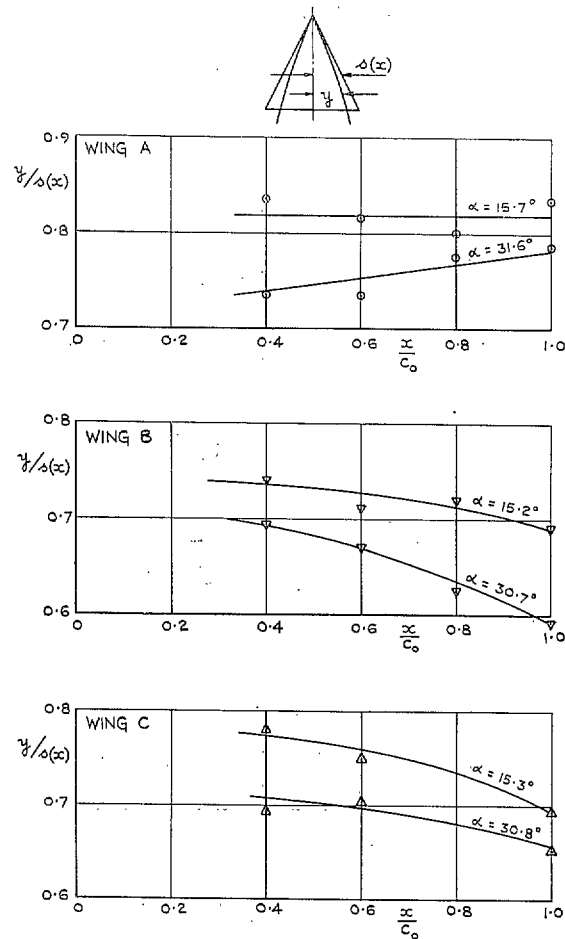
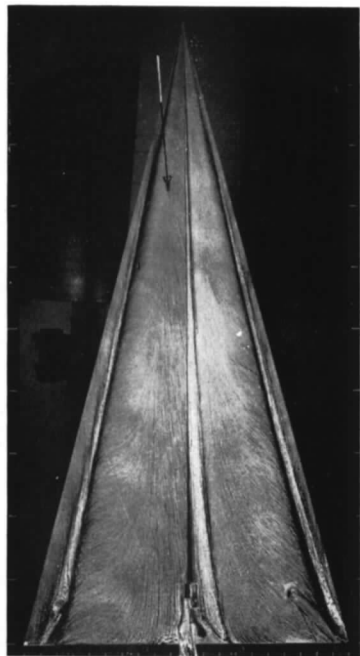
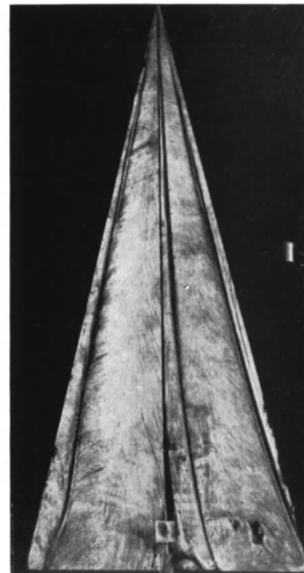


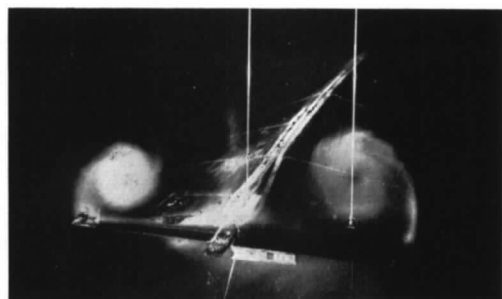
FIG. 22. Plan view of vortex-core path on wings A, B and C. Aspect ratio = 1.



$\alpha = 20.48 \text{ deg}$, $\psi = 5 \text{ deg}$

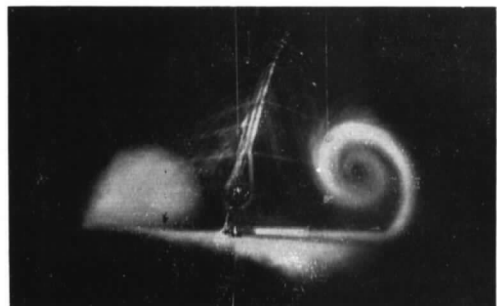


$\alpha = 20.48 \text{ deg}$, $\psi = 10 \text{ deg}$



$\alpha = 20.48 \text{ deg}$, $\psi = 5 \text{ deg}$

FIG. 23. Wing C. Flow patterns on yawed model.



$\alpha = 20.48 \text{ deg}$, $\psi = 10 \text{ deg}$

FIG. 24. Wing C. Flow patterns on yawed model.

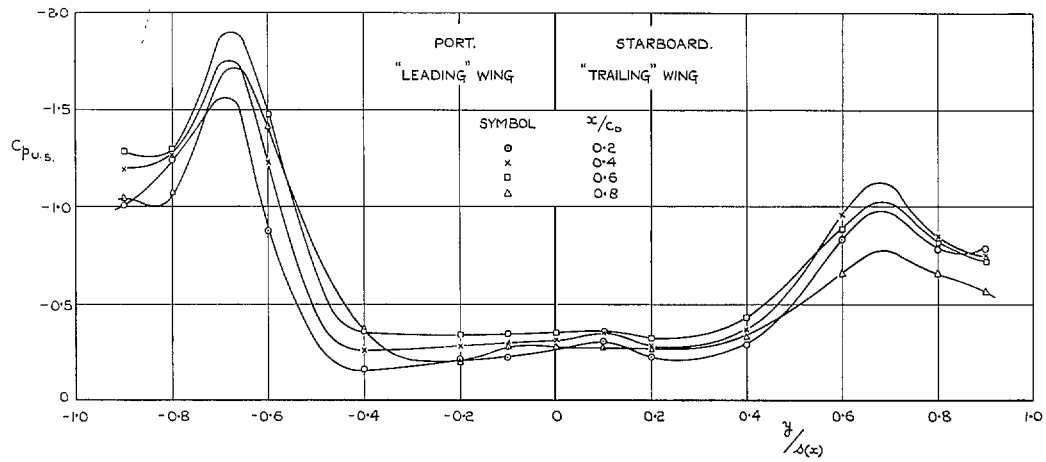


FIG. 25. Typical upper-surface pressure distribution on yawed wing (Wing C).
 $\alpha = 20.48$ deg; $\psi = 5$ deg.

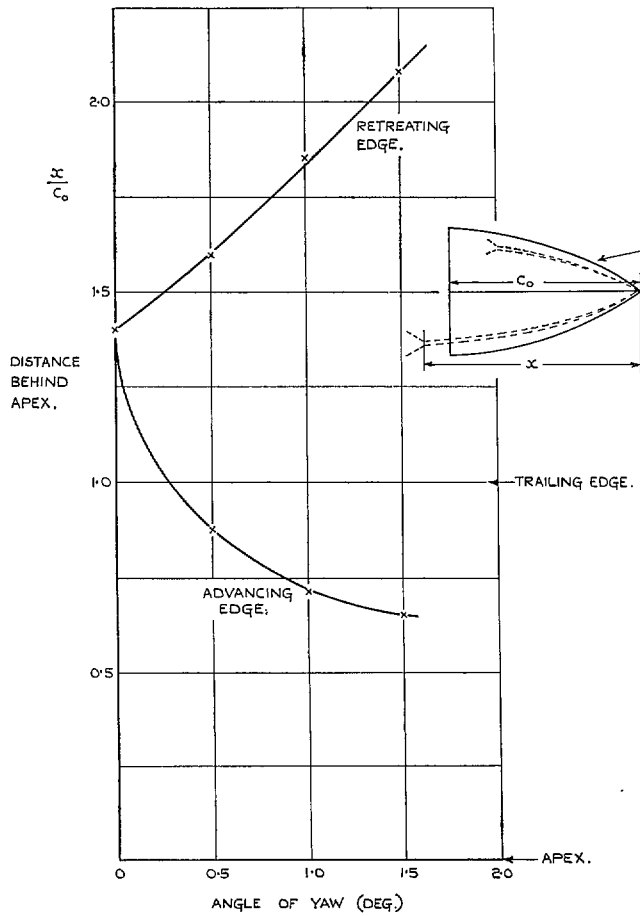


FIG. 26. Wing A. $\alpha = 23$ deg. Position of breakdown of vortex core.

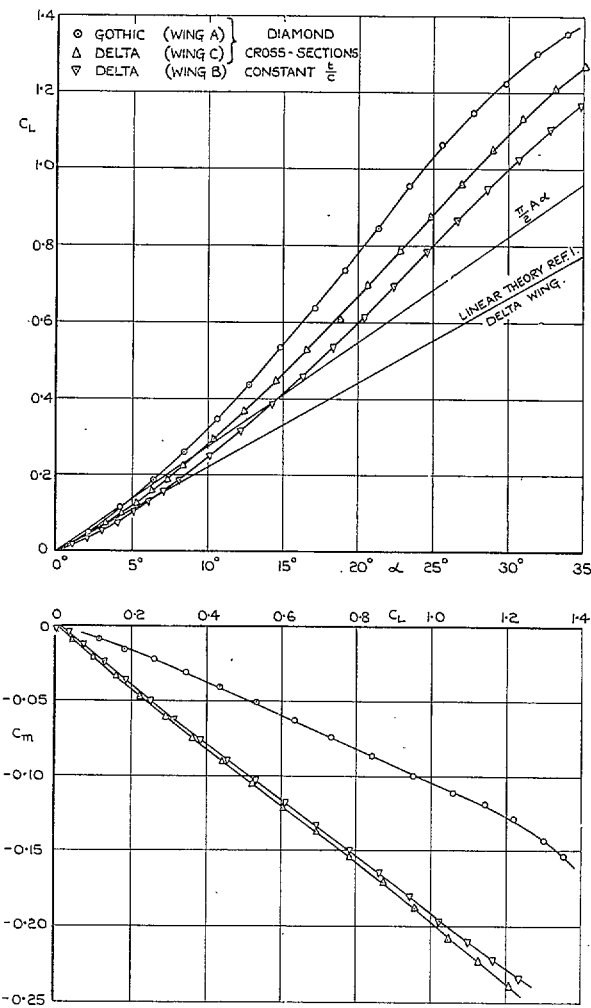


FIG. 27. Lift and pitching-moment characteristics of thick wings of aspect ratio 1. Wings A, B and C. $t_0/c_0 = 0.12$.

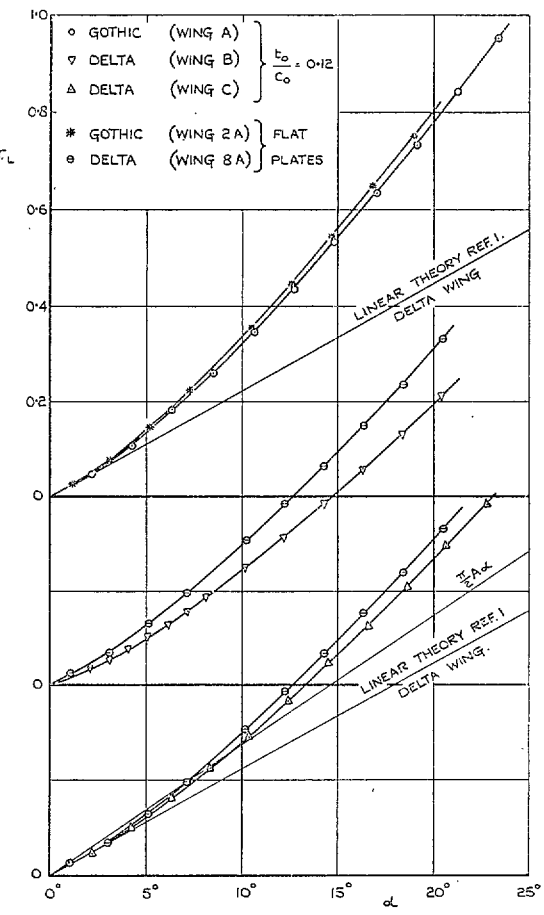


FIG. 28. Effect of wing thickness on lift characteristics of gothic and delta wings.
Aspect ratio = 1.

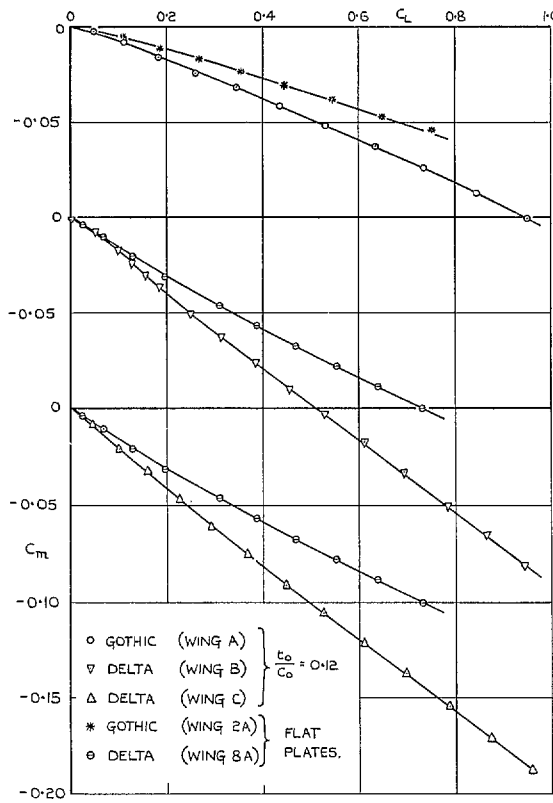


FIG. 29. Effect of wing thickness on pitching-moment characteristics of gothic and delta wings. Aspect ratio = 1.

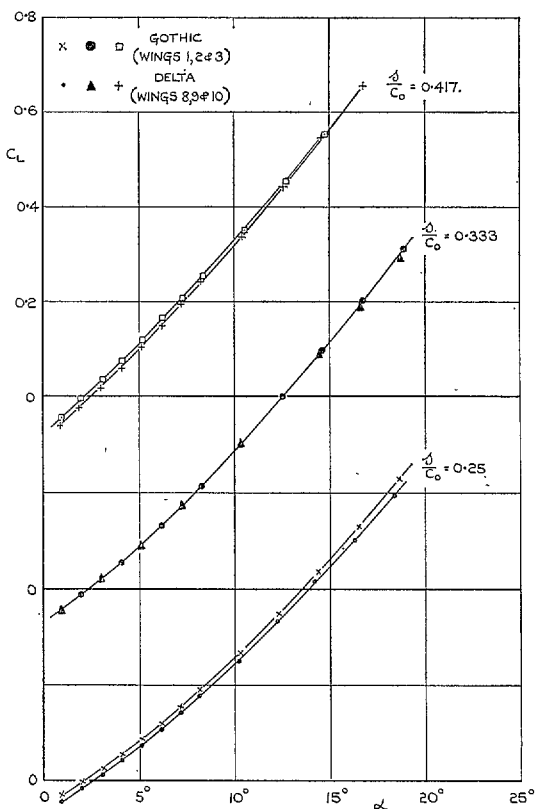


FIG. 30. Lift curves for flat-plate gothic and delta wings of the same slenderness ratio s/c_0 .

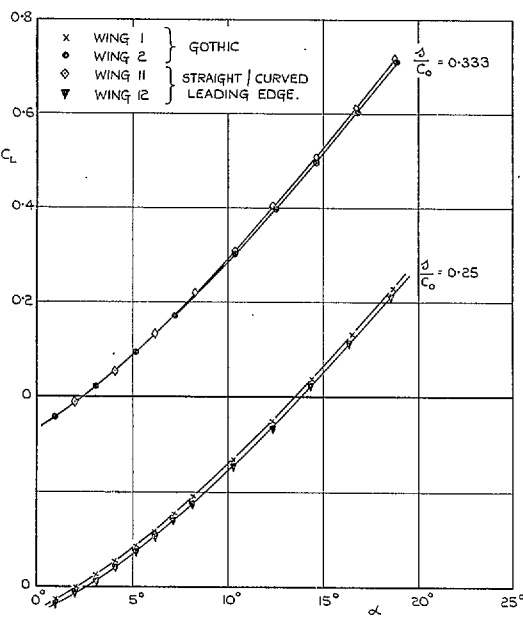


FIG. 31. Lift curves for flat-plate wings of different leading-edge plan-form shape but same slenderness ratio s/c_0 .

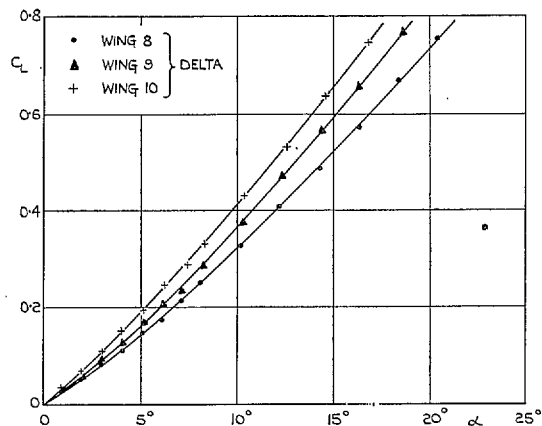
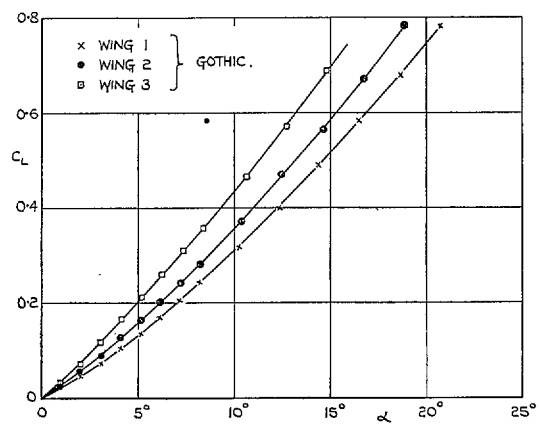


FIG. 32. Lift curves for flat-plate wings with zero-lift angle correction.

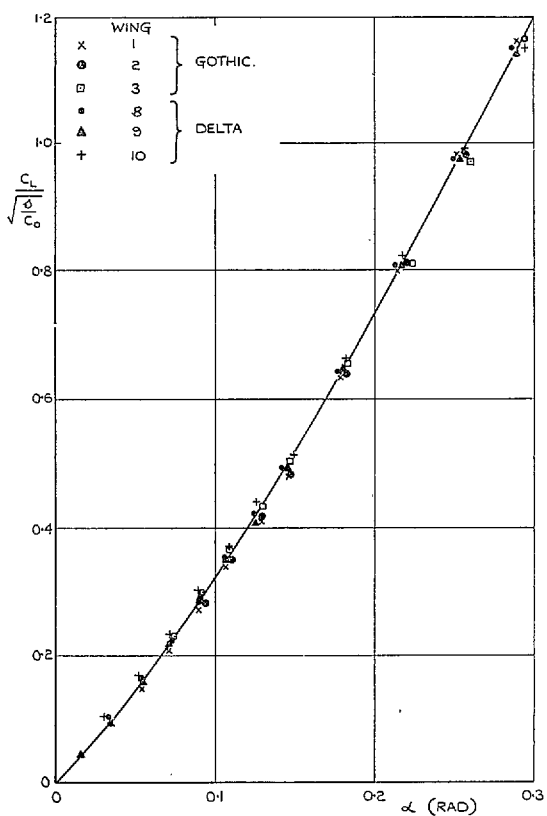


FIG. 33. Collapse of lift curves for flat gothic and delta wings.

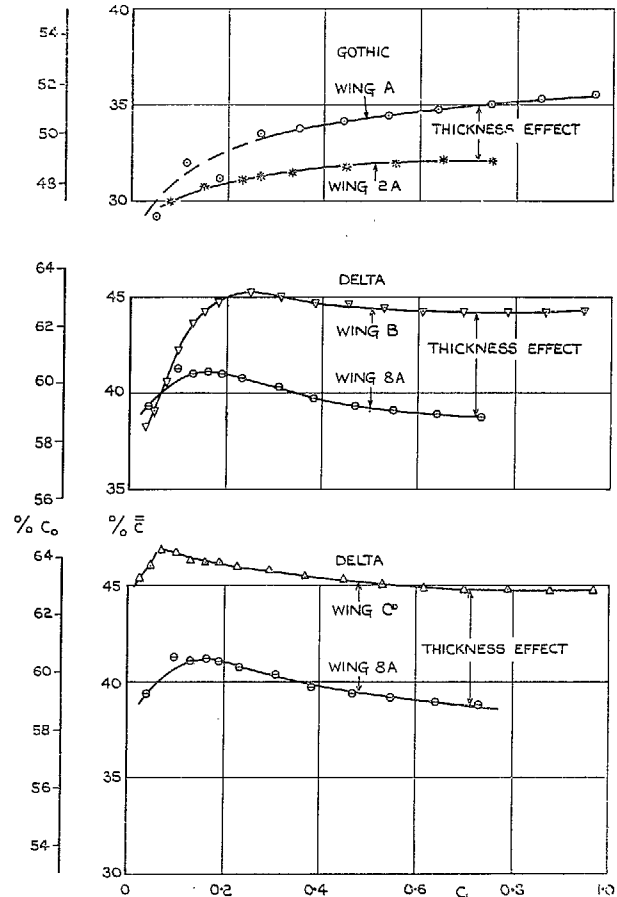
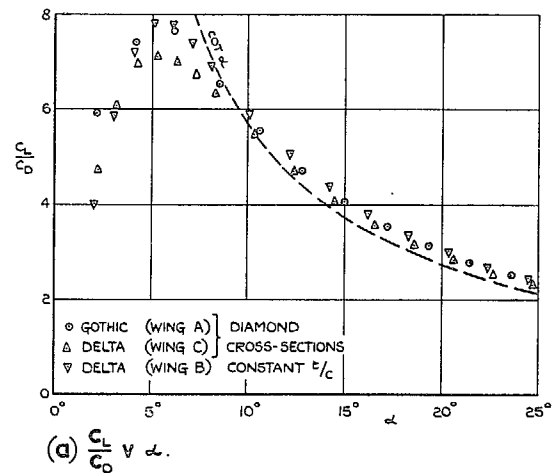
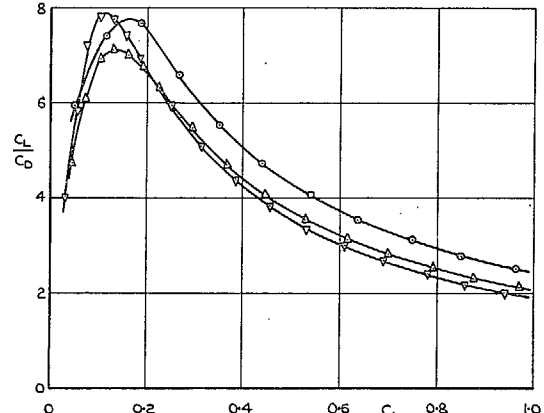


FIG. 34. Centre-of-pressure position on gothic and delta wings of aspect ratio 1.



(a) C_L/C_D v α .



(b) C_L/C_D v C_L

FIGS. 35a and 35b. Lift/drag ratio of wings A, B and C. $A = 1$; $t_0/c_0 = 0.12$.

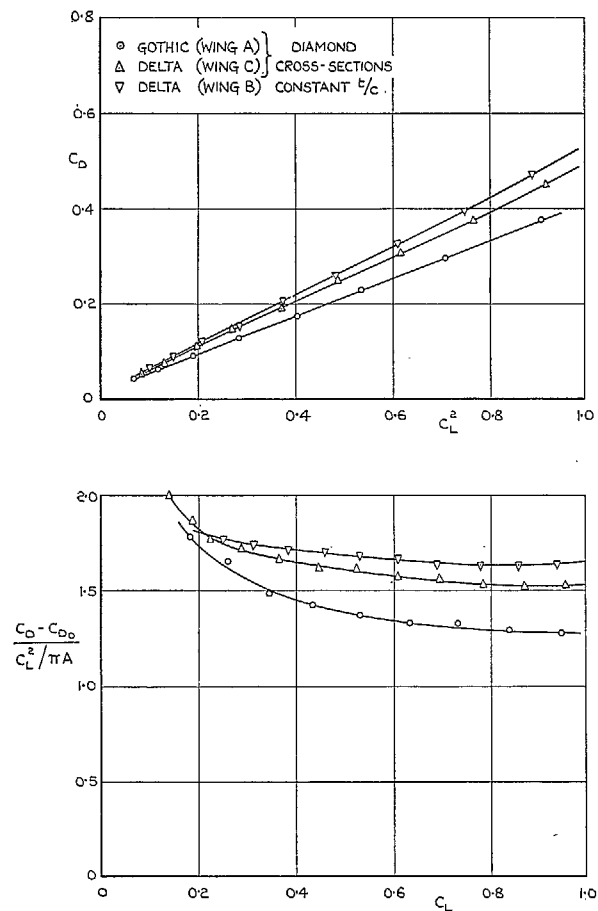


FIG. 36. Drag characteristics of wings A, B and C. $A = 1$; $t_0/c_0 = 0.12$.

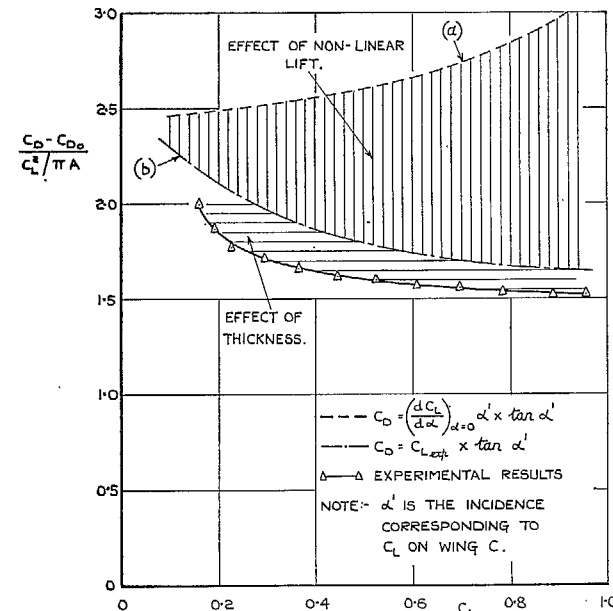
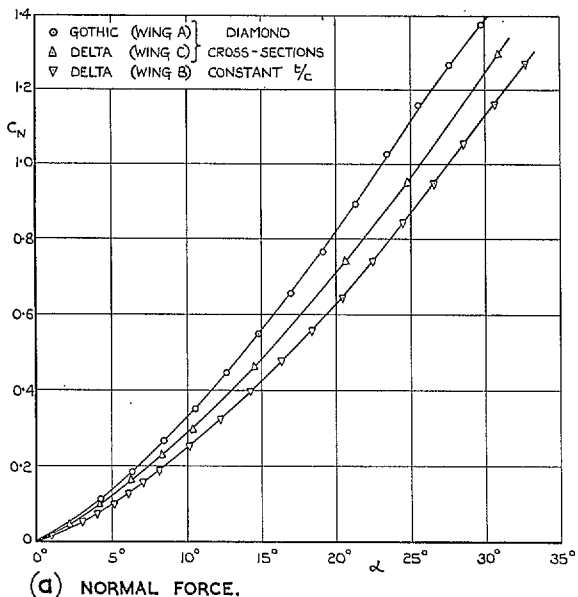
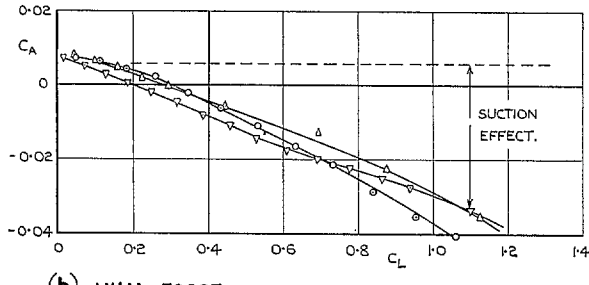


FIG. 37. Wing C. Reduction of drag factor due to effects of vortex sheets. $A = 1$; $t_0/c_0 = 0.12$.

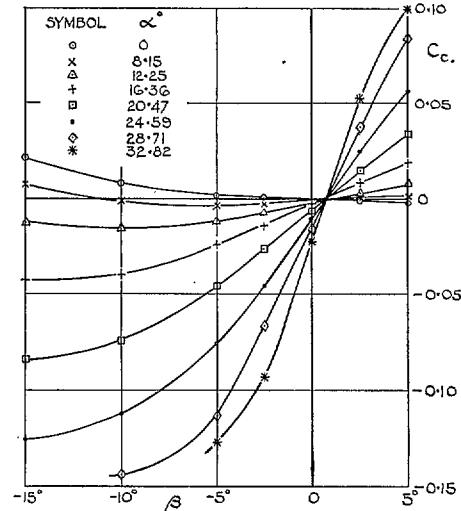


(a) NORMAL FORCE.

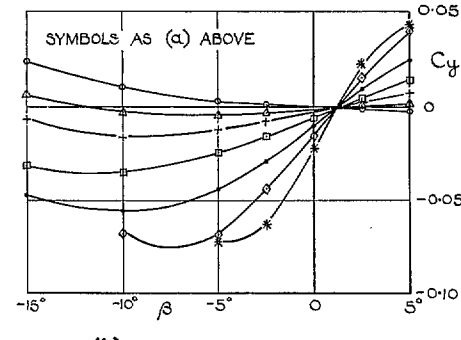


(b) AXIAL FORCE.

FIGS. 38a and 38b. Overall normal force and axial force on wings A, B and C. $A = 1$; $t_0/c_0 = 0.12$.

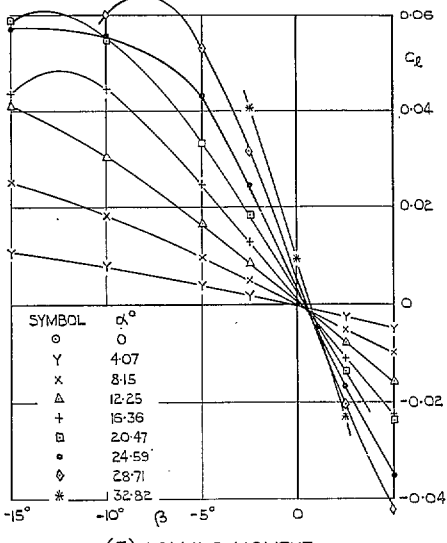


(a) CROSS-WIND FORCE.

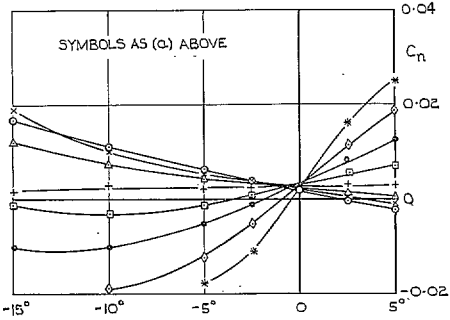


(b) SIDE FORCE.

FIGS. 39a and 39b. Typical variation of cross-wind force (a), and side force (b), with sideslip. Wing C. $A = 1$; $t_0/c_0 = 0.12$.



(a) ROLLING MOMENT.



(b) YAWING MOMENT.

Figs. 40a and 40b. Typical variation of rolling moment (a) and yawing moment (b) with sideslip.

Wing C. $A = 1$; $t_0/c_0 = 0.12$.

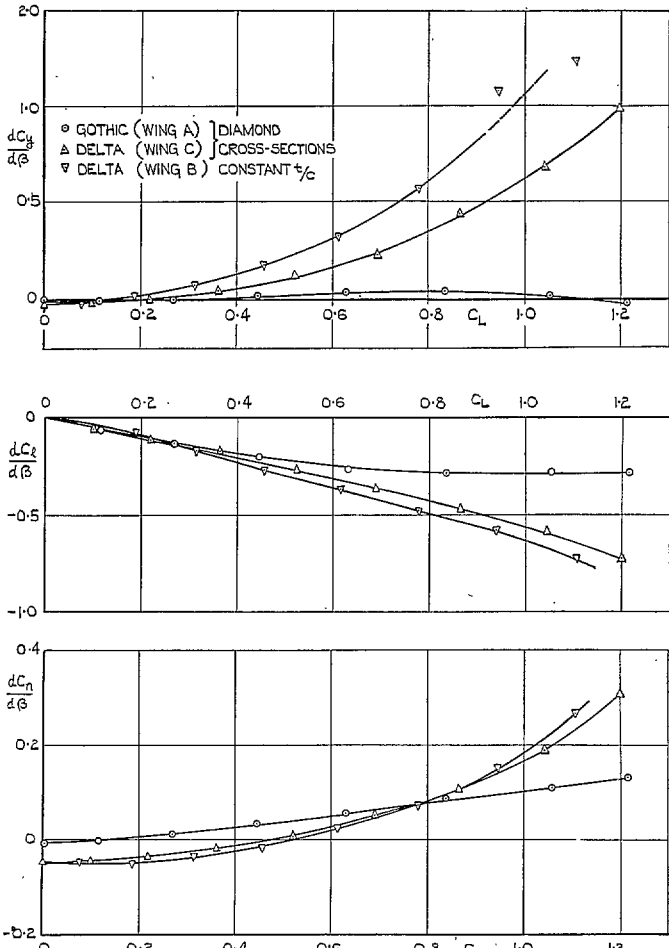
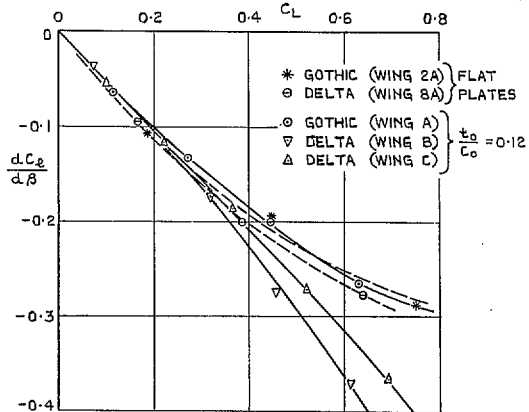
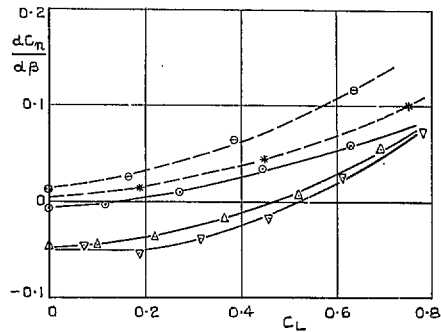


FIG. 41. Static sideslip derivatives for thick wings of aspect ratio 1. Wings A, B and C. $t_0/c_0 = 0.12$.



(a) ROLLING MOMENT DERIVATIVE.



(b) YAWING MOMENT DERIVATIVE.

FIGS. 42a and 42b. Effect of thickness on static sideslip derivatives of gothic and delta wings. Aspect ratio = 1.

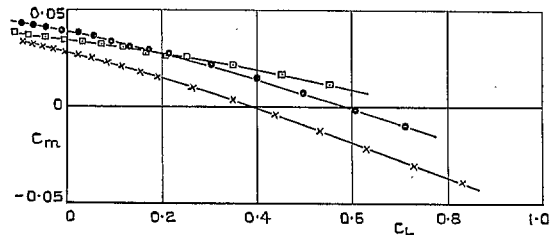
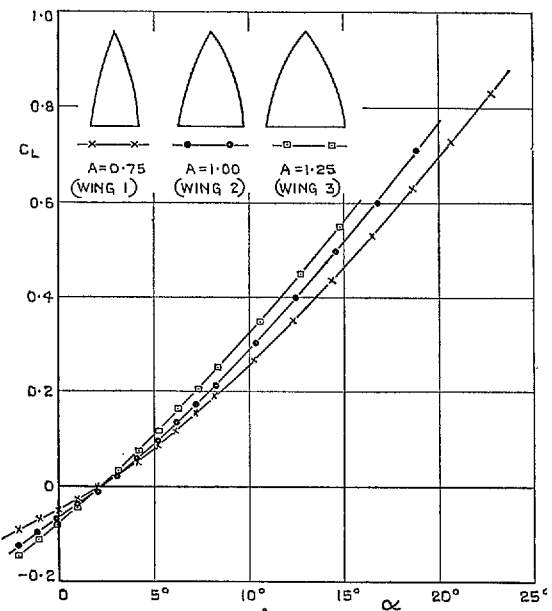


FIG. 43. Effect of aspect ratio on lift and pitching-moment characteristics of flat-plate gothic wings.

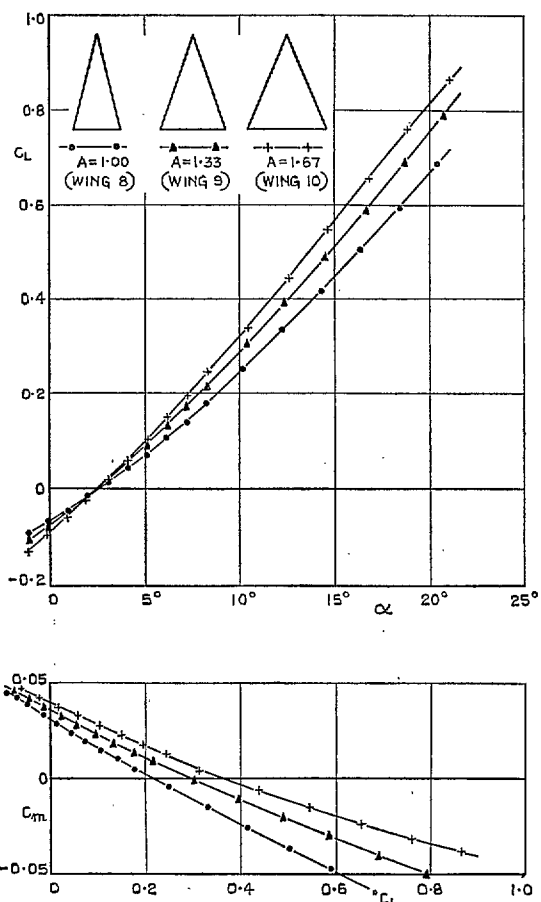


FIG. 44. Effect of aspect ratio on lift and pitching-moment characteristics of flat-plate delta wings.

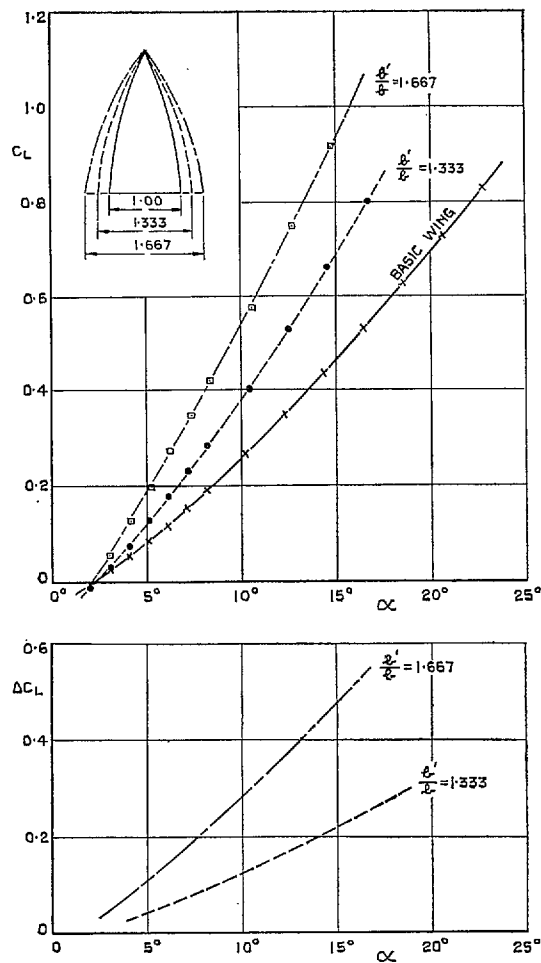


FIG. 45. Effect of extending leading edges on lift of flat-plate gothic wing of aspect ratio 0.75 (C_L based on basic wing area).

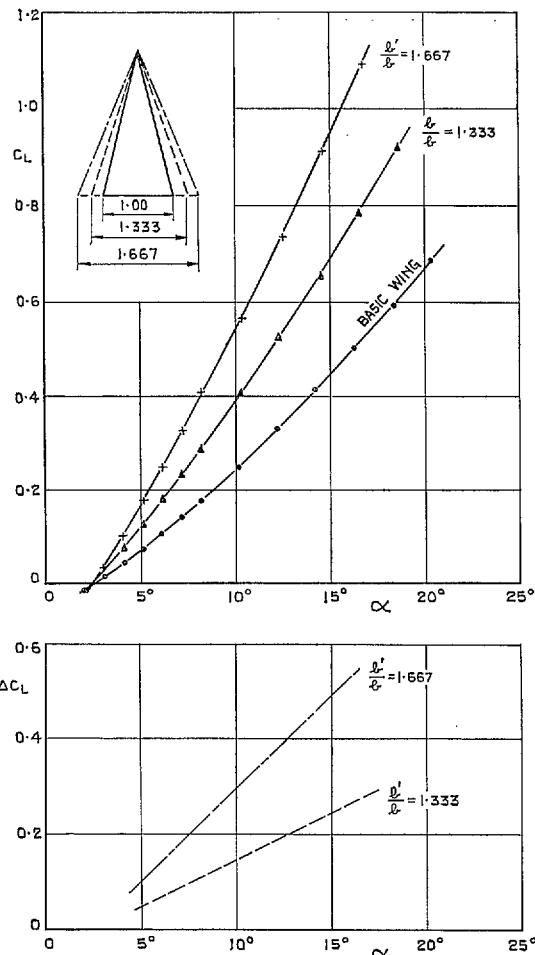


FIG. 46. Effect of extending leading edges on lift of flat-plate delta wing of aspect ratio 1 (C_L based on basic wing area).

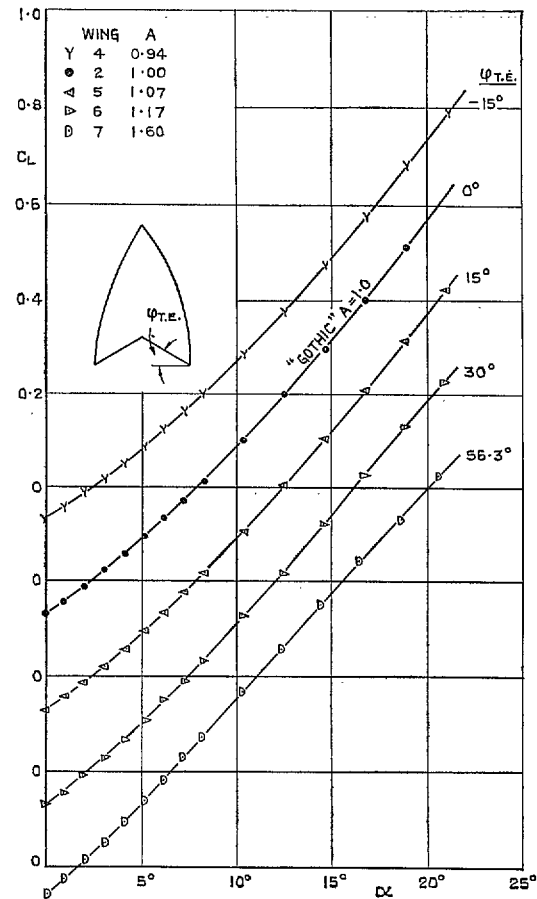


FIG. 47. Effect of trailing-edge sweep on lift of wing with ' $A = 1$ gothic' leading-edge shape (Flat-plate models).

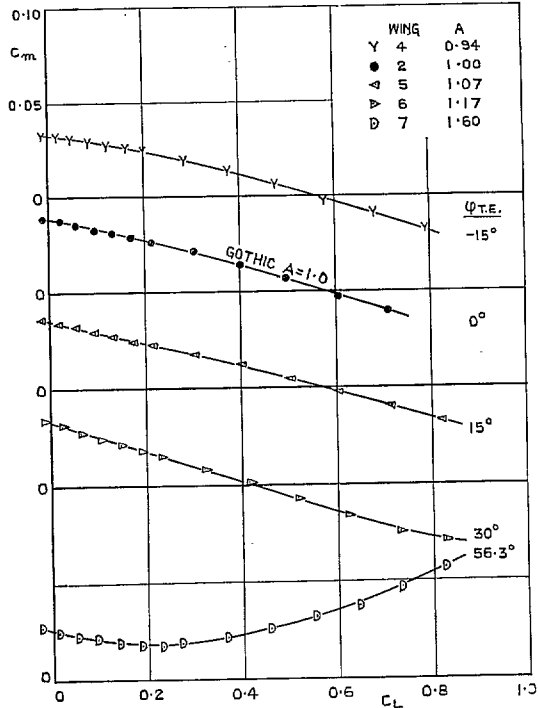


FIG. 48. Effect of trailing-edge sweep on pitching moment of wing with ' $A = 1.0$ ' gothic' leading-edge shape (Flat-plate models).

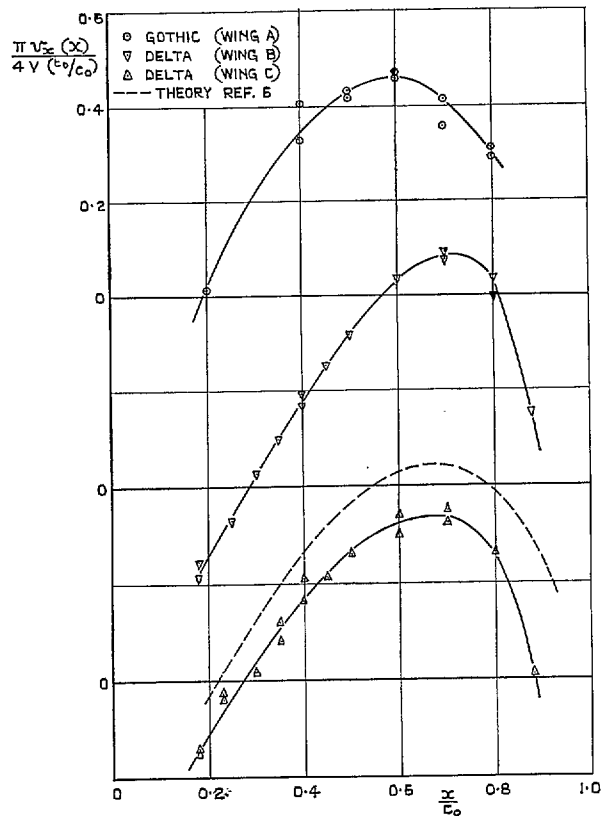


FIG. 49. Wings A, B and C, centre-line supersonic velocity distributions at zero incidence.
 $A = 1.$

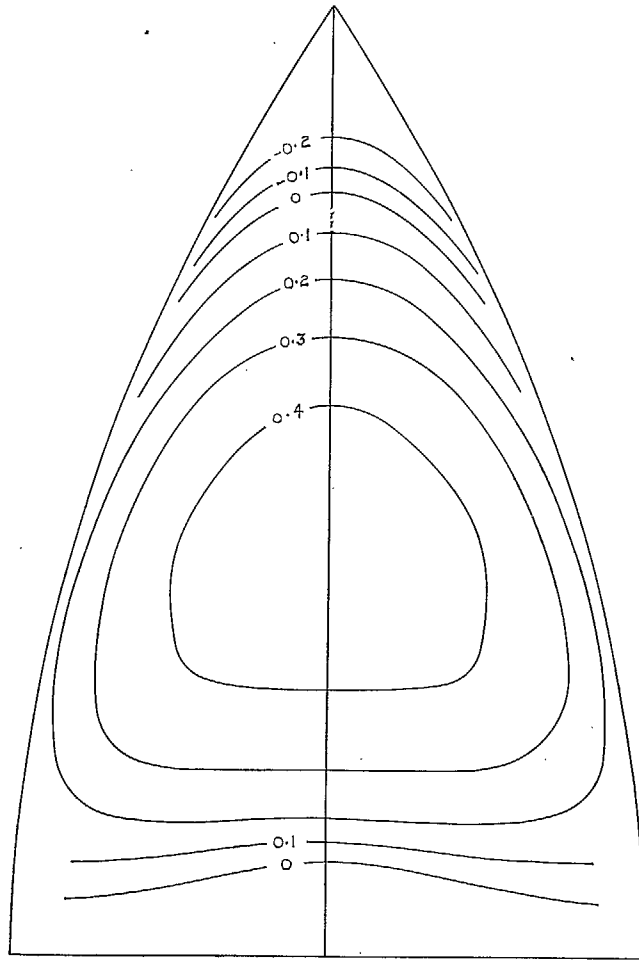


FIG. 50. Wing A. Isobar pattern at zero incidence.
Values plotted: $\{\pi v_x(x)\}/\{4V(t_0/c_0)\}$.

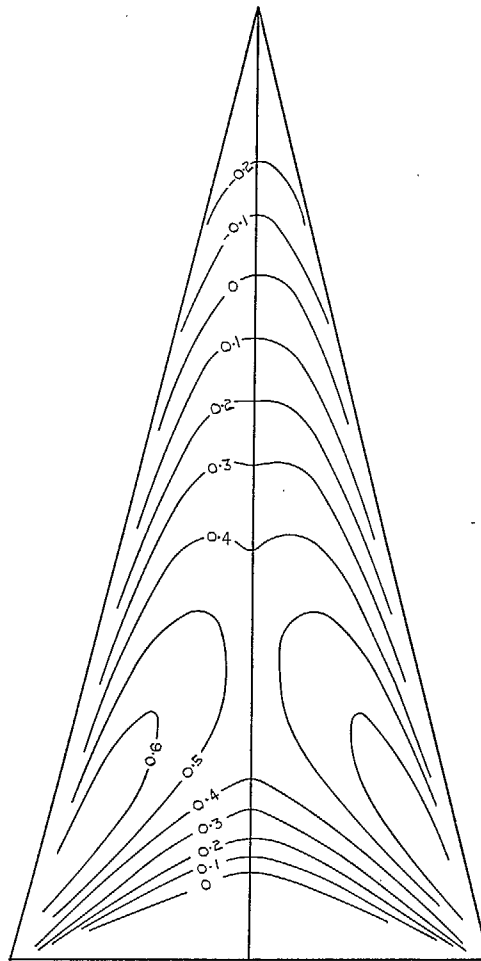


FIG. 51. Wing B. Isobar pattern at zero incidence.
Values plotted: $\{\pi v_x(x)\}/\{4V(t_0/c_0)\}$.

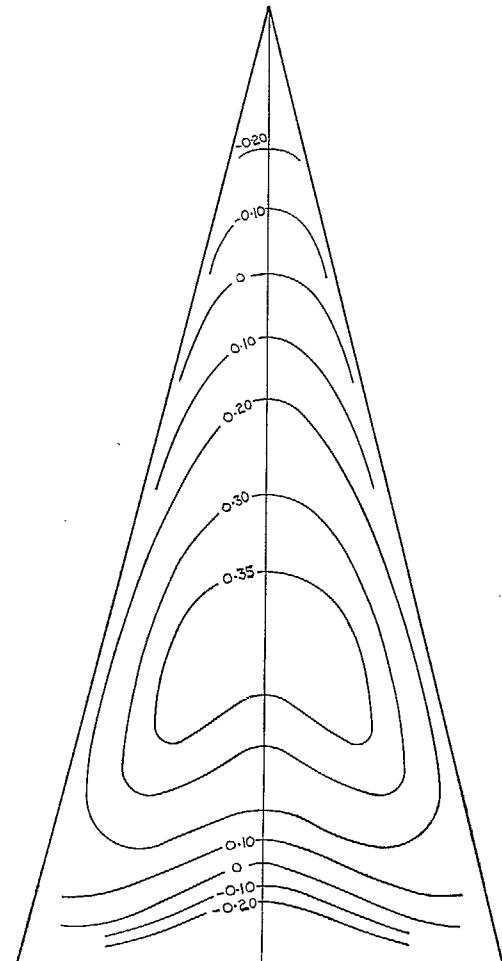
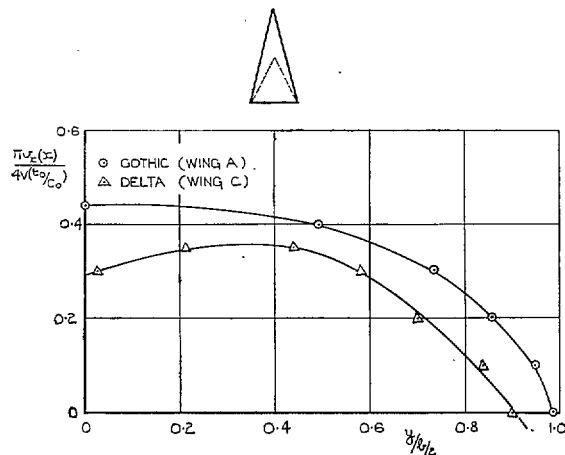
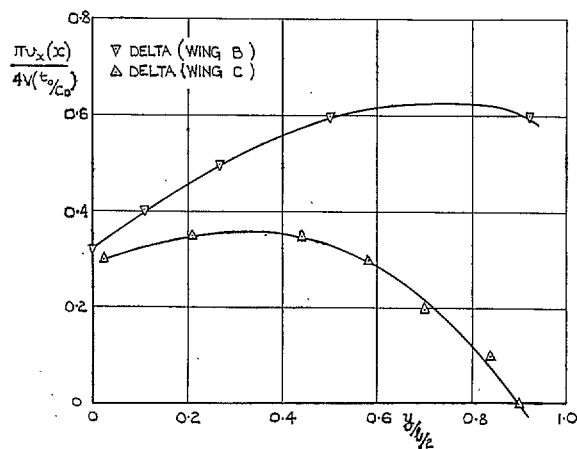


FIG. 52. Wing C. Isobar pattern at zero incidence.
Values plotted: $\{\pi v_x(x)\}/\{4V(t_0/c_0)\}$.

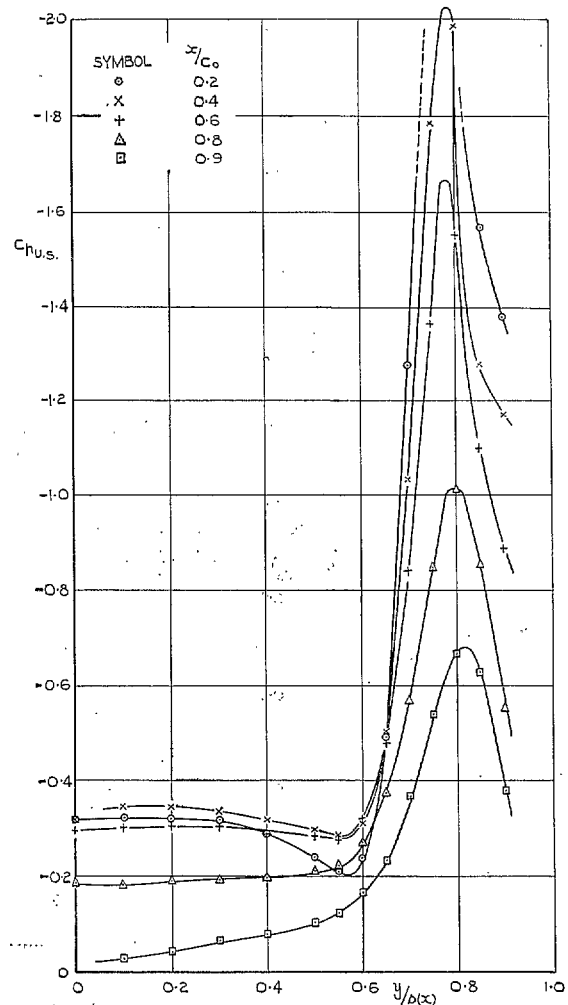
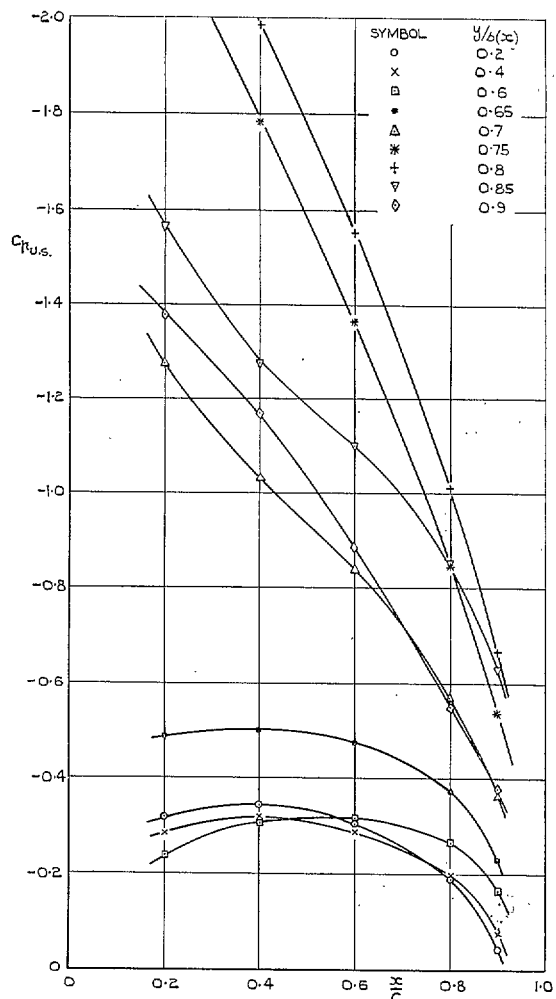


(a) GOTHIC AND DELTA WINGS WITH
DIAMOND CROSS-SECTIONS



(b) DELTA WINGS

Figs. 53a and 53b. Comparison of super-velocities on 50 per cent chord-line at zero incidence.



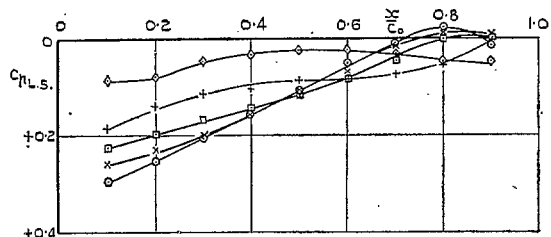
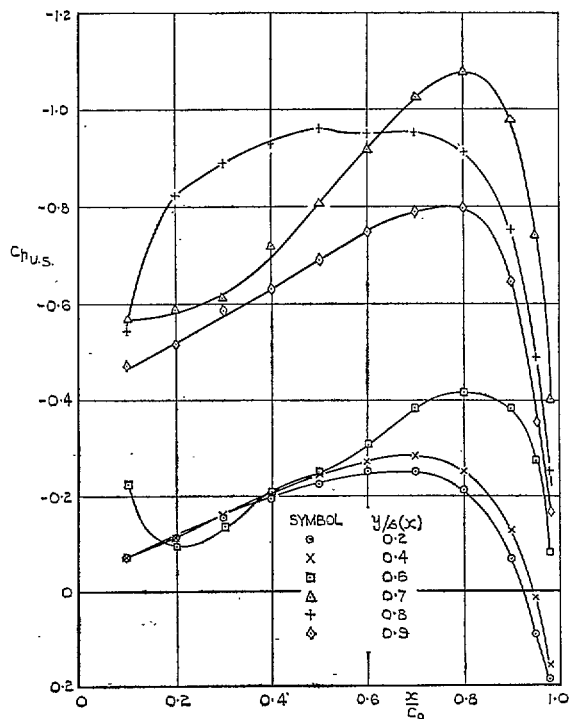


FIG. 56. Wing B. Upper and lower surface pressure coefficients on rays from apex.
 $\alpha = 15 \cdot 29$ deg.

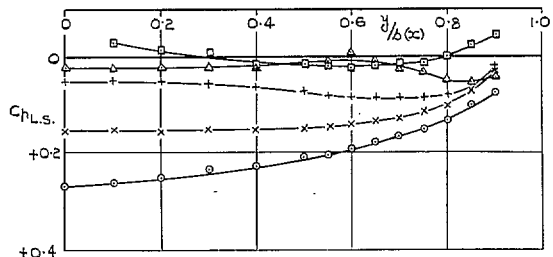
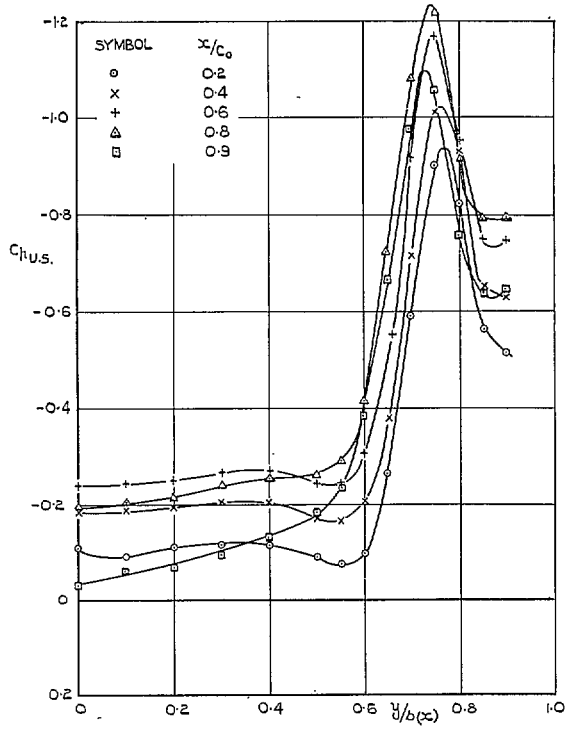


FIG. 57. Wing B. Upper and lower surface pressure coefficients along lines of constant x/c_0 .
 $\alpha = 15 \cdot 29$ deg.

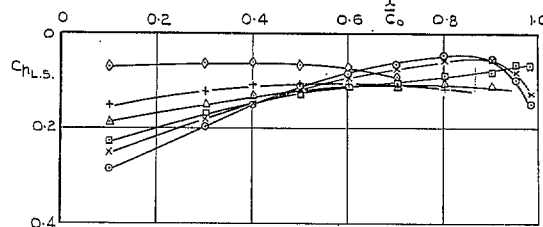
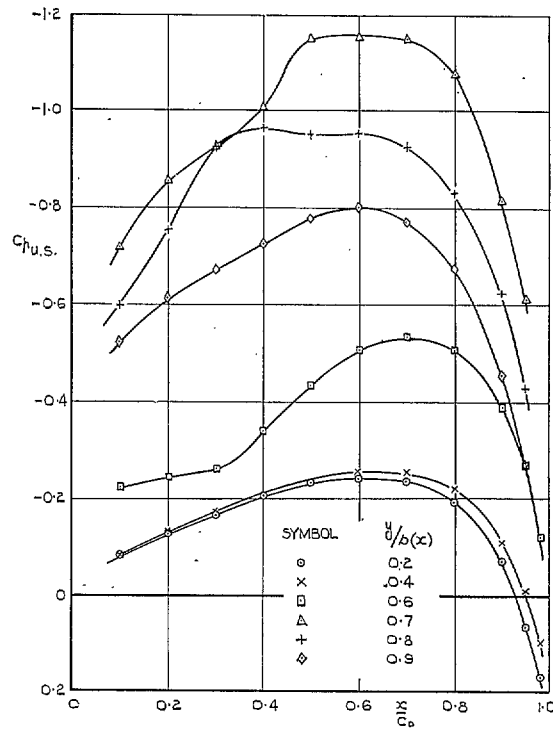


FIG. 58. Wing C. Upper and lower surface pressure coefficients on rays from apex.
 $\alpha = 15 \cdot 33$ deg.

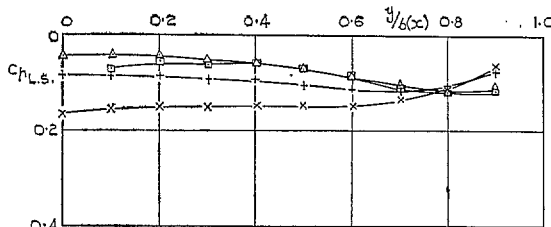
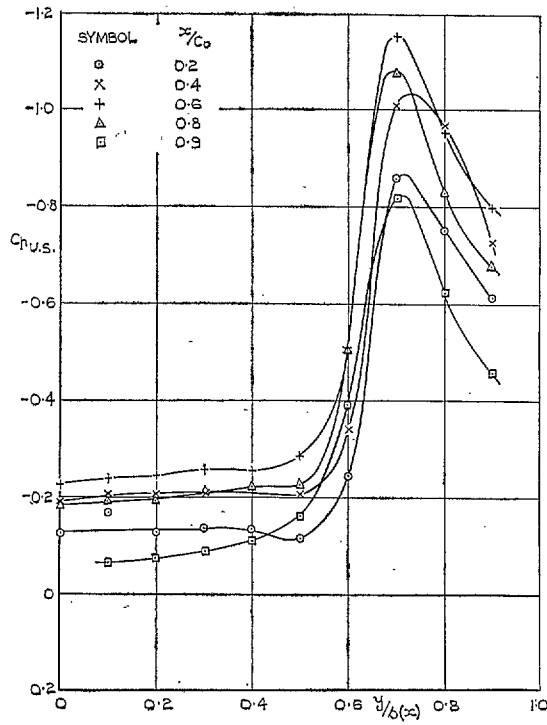


FIG. 59. Wing C. Upper and lower surface pressure coefficients along lines of constant x/c_0 .
 $\alpha = 15 \cdot 33$ deg.

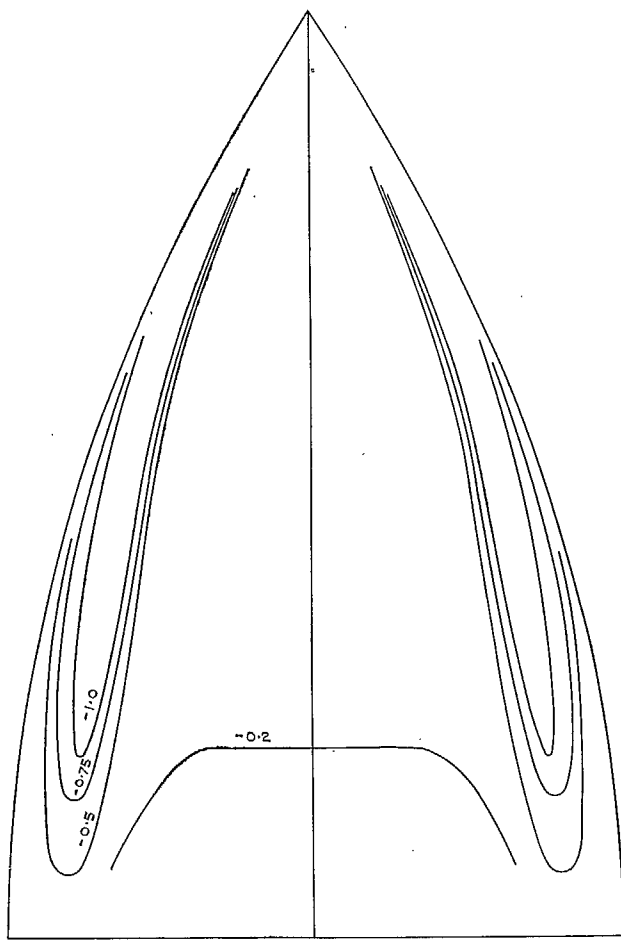


FIG. 60. Wing A. Upper-surface isobar pattern at $\alpha = 15.73$ deg. Values plotted: C_p .

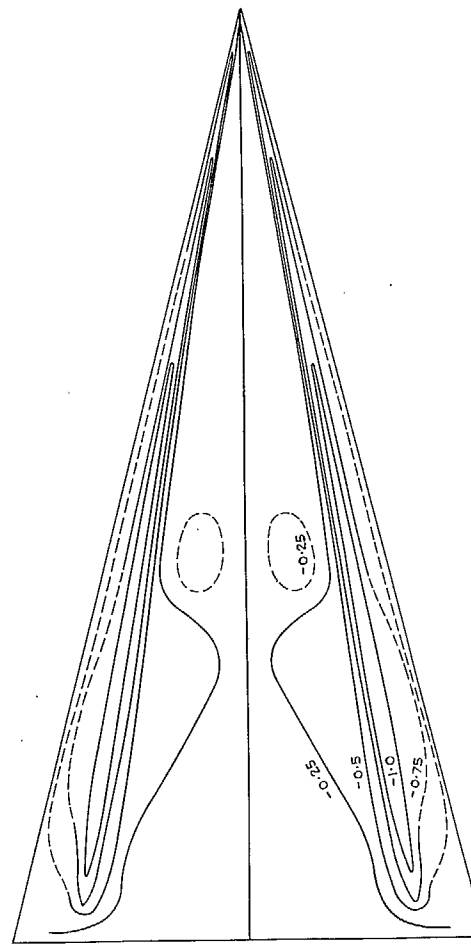


FIG. 61. Wing B. Upper-surface isobar pattern at $\alpha = 15.29$ deg. Values plotted: C_p .

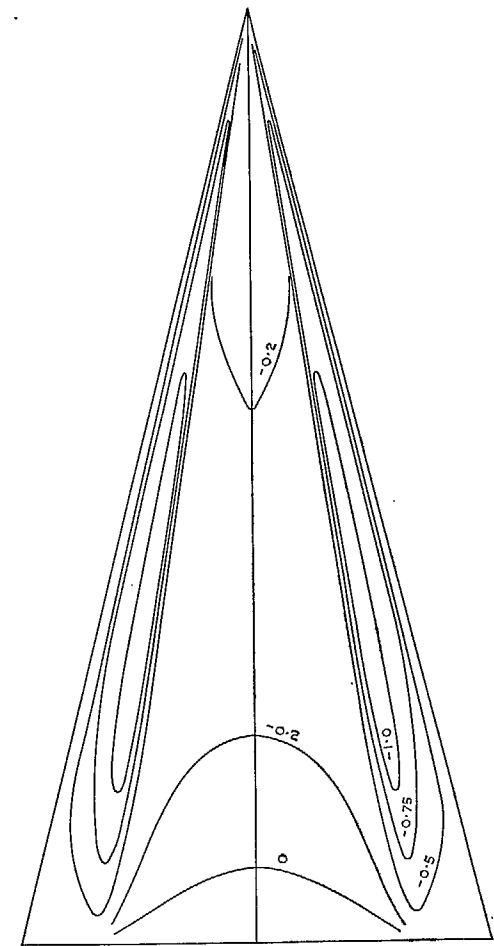


FIG. 62. Wing C. Upper-surface isobar pattern at $\alpha = 15.33$ deg. Values plotted: C_p .

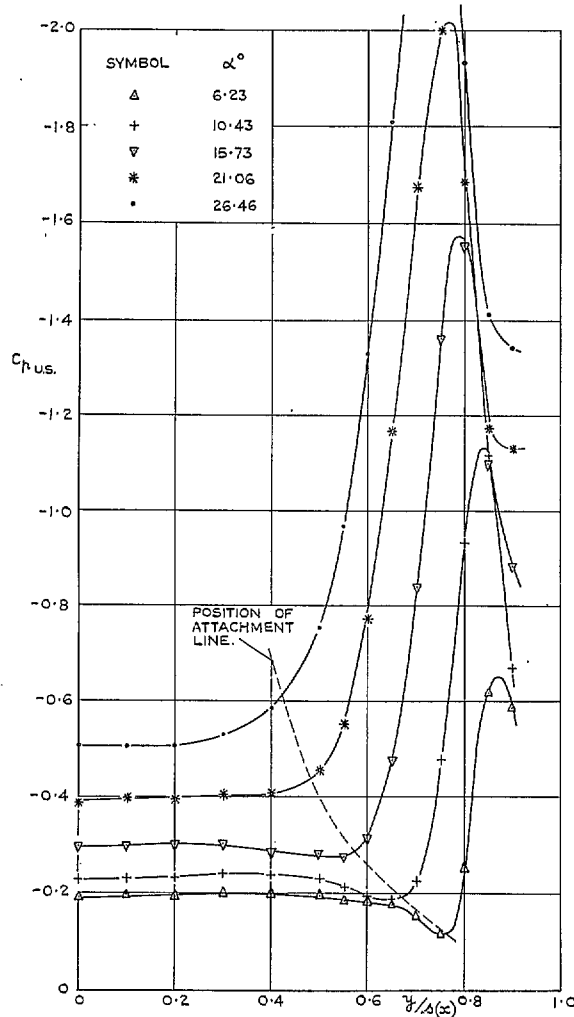


FIG. 63. Wing A. Typical spanwise variation of upper-surface pressure distribution with incidence. $x/c_0 = 0.6$.

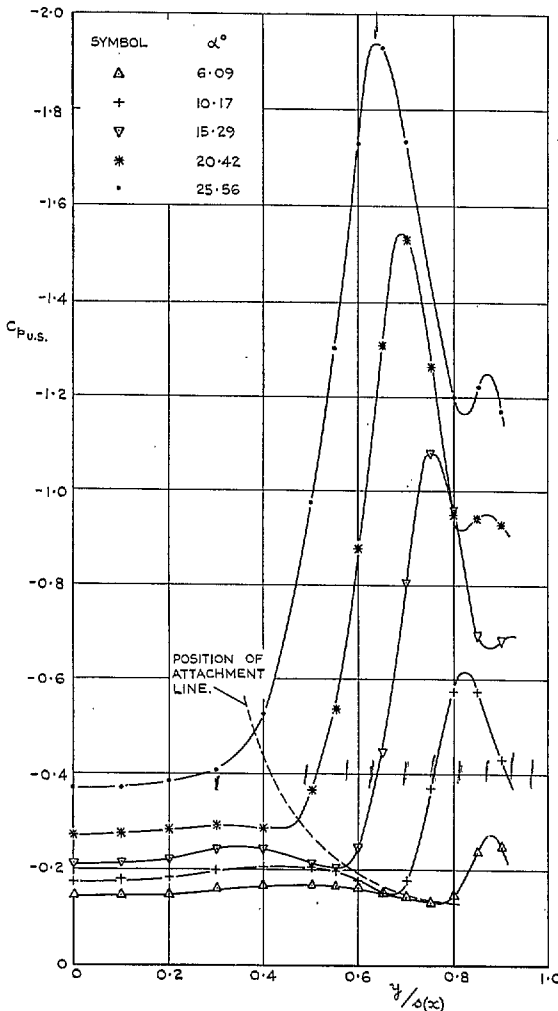


FIG. 64. Wing B. Typical spanwise variation of upper-surface pressure distribution with incidence. $x/c_0 = 0.5$.

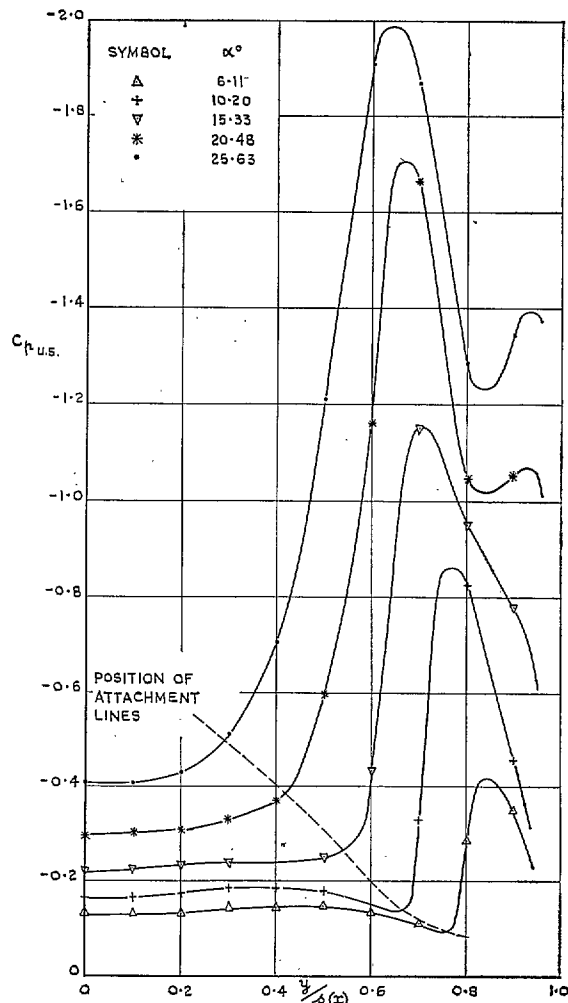


FIG. 65. Wing C. Typical spanwise variation of upper-surface pressure distribution with incidence. $x/c_0 = 0.5$.

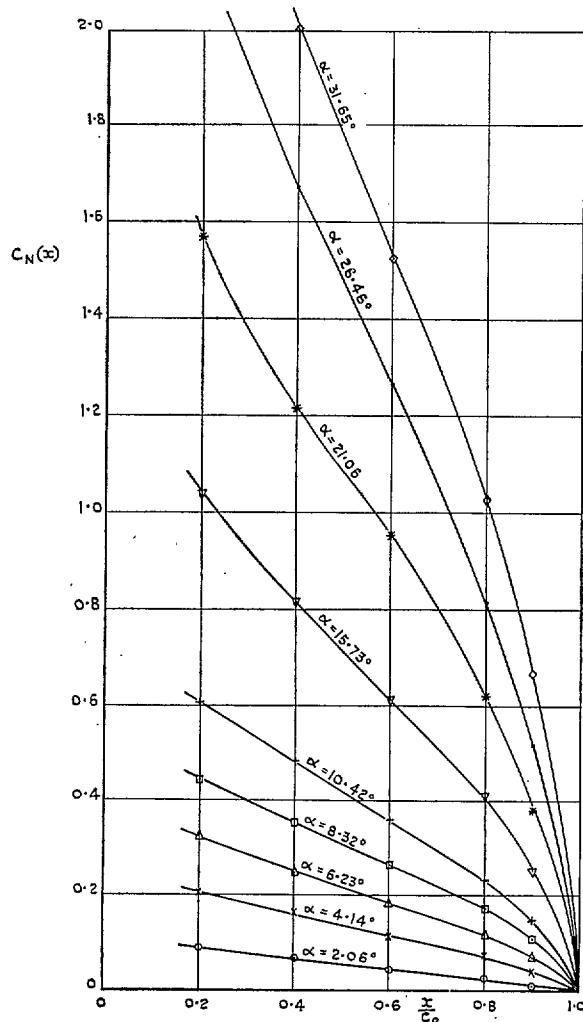


FIG. 66. Wing A. Longitudinal distribution of local cross-load coefficient.

$$C_N(x) = \int_0^1 \Delta C_p d \left[\frac{y}{s(x)} \right].$$

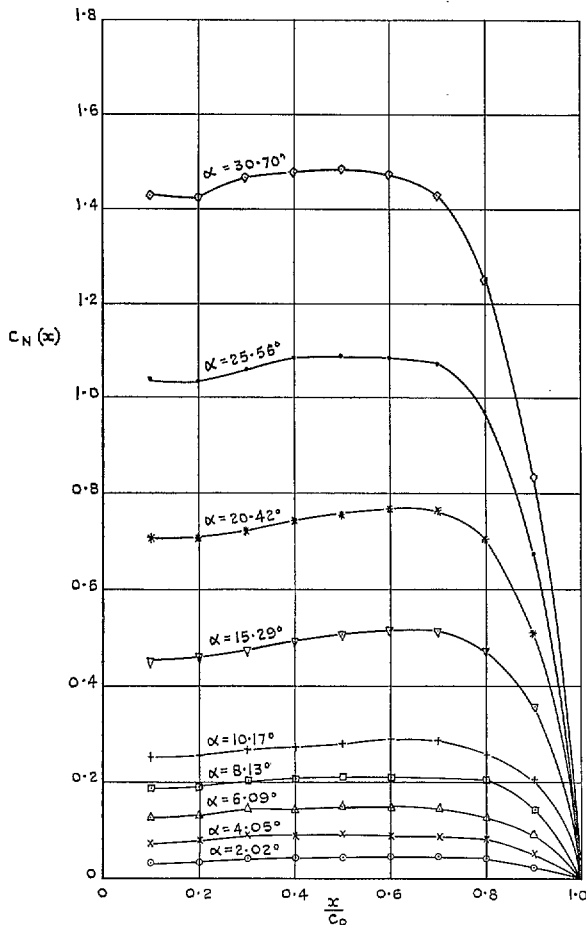


FIG. 67. Wing B. Longitudinal distribution of local cross-load coefficient.

$$C_N(x) = \int_0^1 \Delta C_p d \left[\frac{y}{s(x)} \right].$$

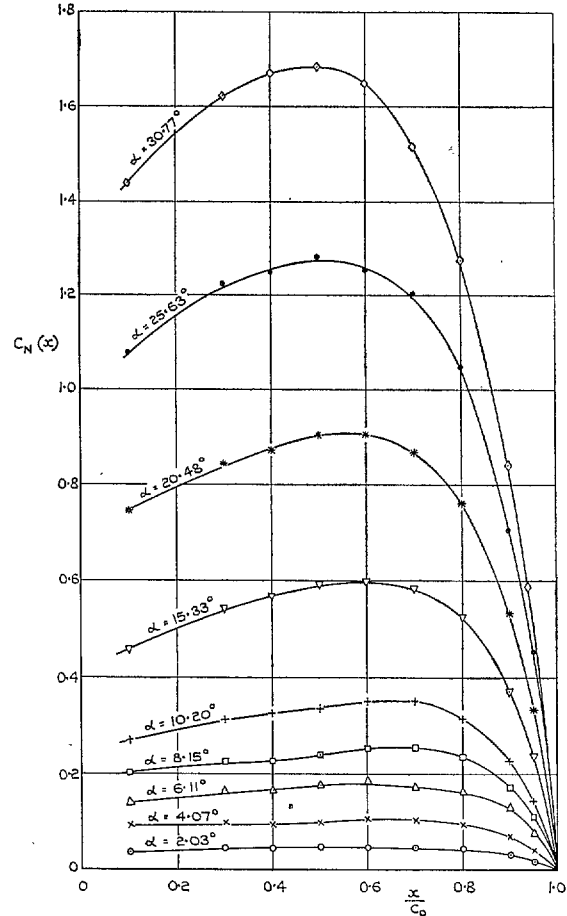
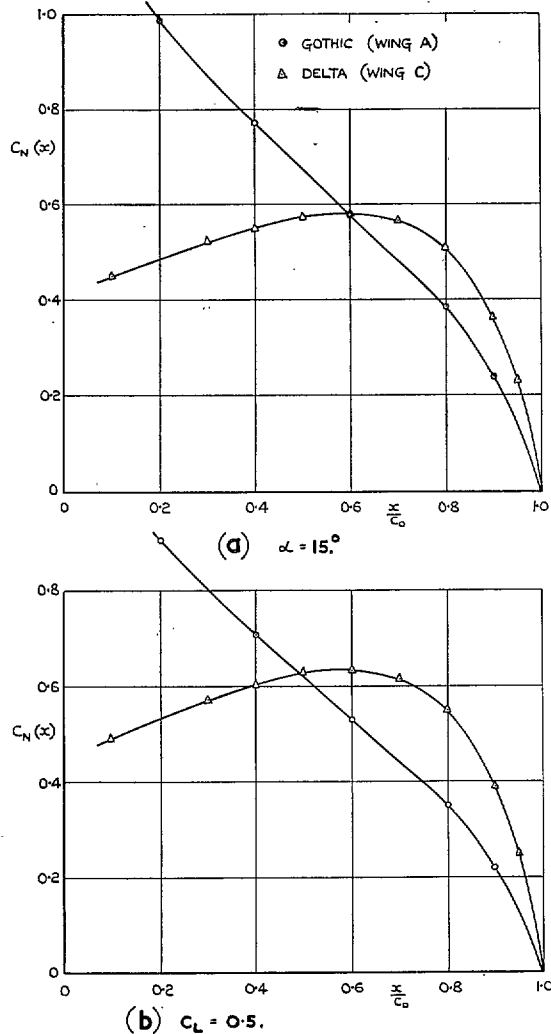


FIG. 68. Wing C. Longitudinal distribution of local cross-load coefficient.

$$C_N(x) = \int_0^1 \Delta C_p d \left[\frac{y}{s(x)} \right].$$



FIGS. 69a and 69b. Comparison of longitudinal distribution of local cross-load coefficient on gothic and delta wings.
 $A = 1.0$.

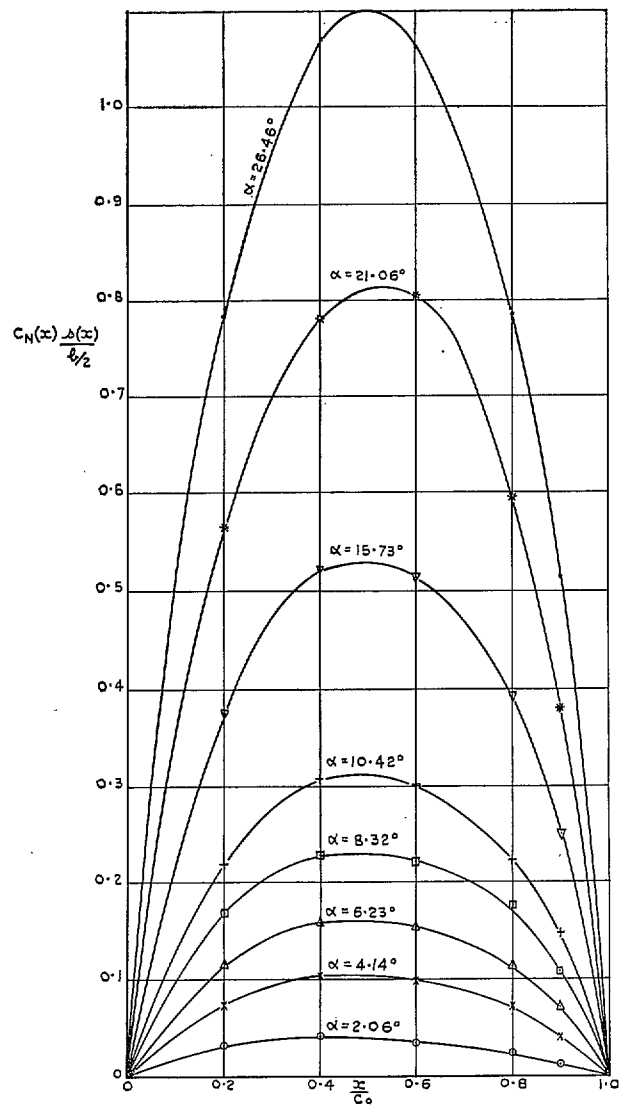


FIG. 70. Wing A. Longitudinal distribution of cross-load. Overall normal-force coefficient:

$$\bar{C}_N = \frac{3}{2} \int_0^1 C_N(x) \frac{s(x)}{b/2} d\left(\frac{x}{c_0}\right).$$

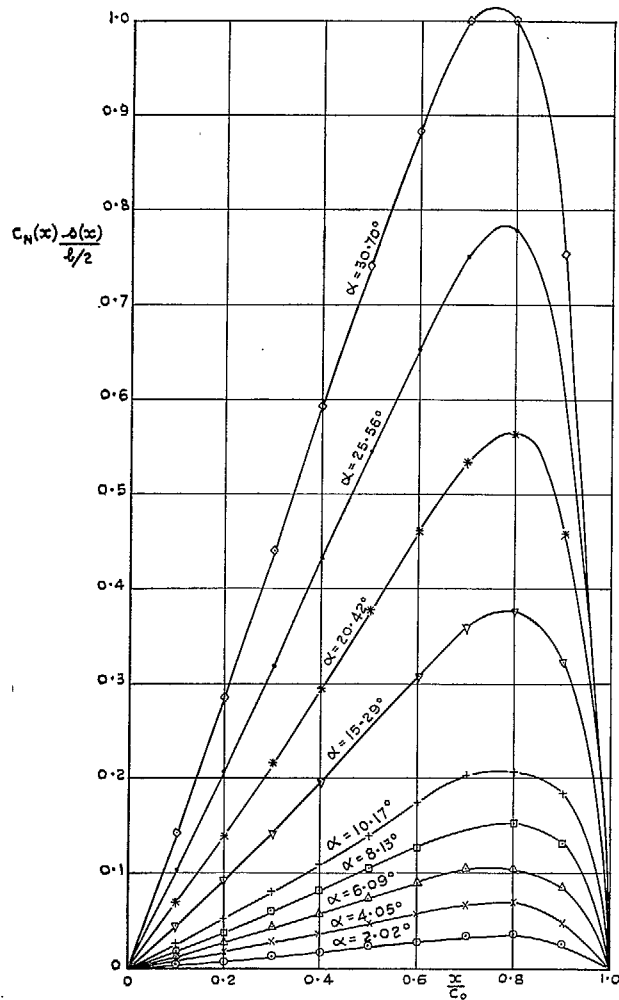


FIG. 71. Wing B. Longitudinal distribution of cross-load. Overall normal-force coefficient:

$$\bar{C}_N = 2 \int_0^1 C_N(x) \frac{s(x)}{b/2} d\left(\frac{x}{c_0}\right).$$

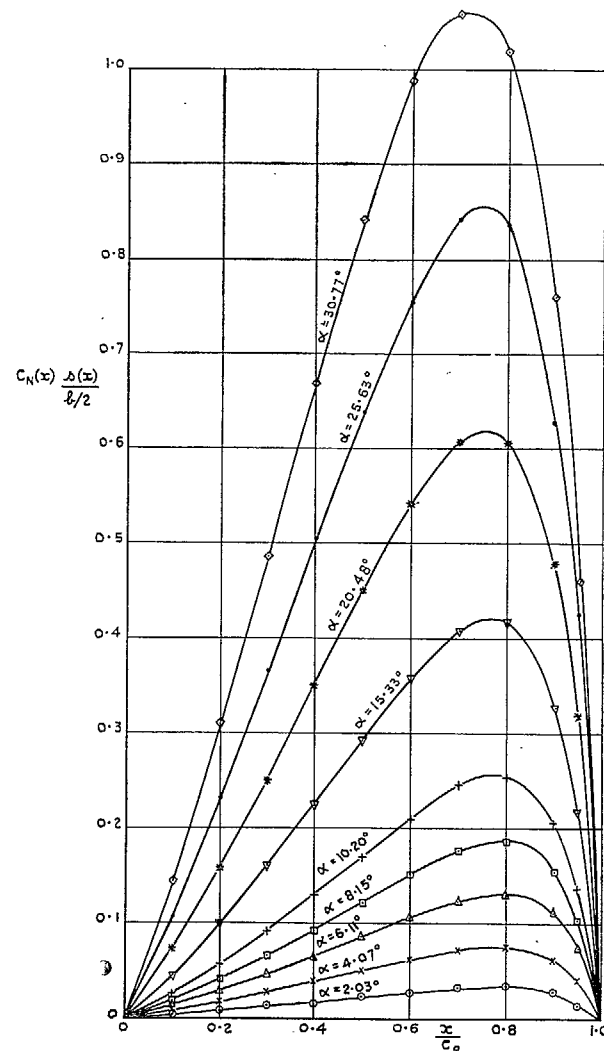


FIG. 72. Wing C. Longitudinal distribution of cross-load. Overall normal-force coefficient:

$$\bar{C}_N = 2 \int_0^1 C_N(x) \frac{s(x)}{b/2} d\left(\frac{x}{c_0}\right).$$

Publications of the Aeronautical Research Council

ANNUAL TECHNICAL REPORTS OF THE AERONAUTICAL RESEARCH COUNCIL (BOUNDED VOLUMES)

- 1941 Aero and Hydrodynamics, Aerofoils, Airscrews, Engines, Flutter, Stability and Control, Structures. 63s. (post 2s. 3d.)
- 1942 Vol. I. Aero and Hydrodynamics, Aerofoils, Airscrews, Engines. 75s. (post 2s. 3d.)
Vol. II. Noise, Parachutes, Stability and Control, Structures, Vibration, Wind Tunnels. 47s. 6d. (post 1s. 9d.)
- 1943 Vol. I. Aerodynamics, Aerofoils, Airscrews. 80s. (post 2s.)
Vol. II. Engines, Flutter, Materials, Parachutes, Performance, Stability and Control, Structures. 90s. (post 2s. 3d.)
- 1944 Vol. I. Aero and Hydrodynamics, Aerofoils, Aircraft, Airscrews, Controls. 84s. (post 2s. 6d.)
Vol. II. Flutter and Vibration, Materials, Miscellaneous, Navigation, Parachutes, Performance, Plates and Panels, Stability, Structures, Test Equipment, Wind Tunnels. 84s. (post 2s. 6d.)
- 1945 Vol. I. Aero and Hydrodynamics, Aerofoils. 130s. (post 3s.)
Vol. II. Aircraft, Airscrews, Controls. 130s. (post 3s.)
Vol. III. Flutter and Vibration, Instruments, Miscellaneous, Parachutes, Plates and Panels, Propulsion. 130s. (post 2s. 9d.)
Vol. IV. Stability, Structures, Wind Tunnels, Wind Tunnel Technique. 130s. (post 2s. 9d.)
- 1946 Vol. I. Accidents, Aerodynamics, Aerofoils and Hydrofoils. 168s. (post 3s. 3d.)
Vol. II. Airscrews, Cabin Cooling, Chemical Hazards, Controls, Flames, Flutter, Helicopters, Instruments and Instrumentation, Interference, Jets, Miscellaneous, Parachutes. 168s. (post 2s. 9d.)
Vol. III. Performance, Propulsion, Seaplanes, Stability, Structures, Wind Tunnels. 168s. (post 3s.)
- 1947 Vol. I. Aerodynamics, Aerofoils, Aircraft. 168s. (post 3s. 3d.)
Vol. II. Airscrews and Rotors, Controls, Flutter, Materials, Miscellaneous, Parachutes, Propulsion, Seaplanes, Stability, Structures, Take-off and Landing. 168s. (post 3s. 3d.)

Special Volumes

- Vol. I. Aero and Hydrodynamics, Aerofoils, Controls, Flutter, Kites, Parachutes, Performance, Propulsion, Stability. 126s. (post 2s. 6d.)
Vol. II. Aero and Hydrodynamics, Aerofoils, Airscrews, Controls, Flutter, Materials, Miscellaneous, Parachutes, Propulsion, Stability, Structures. 147s. (post 2s. 6d.)
Vol. III. Aero and Hydrodynamics, Aerofoils, Airscrews, Controls, Flutter, Kites, Miscellaneous, Parachutes, Propulsion, Seaplanes, Stability, Structures, Test Equipment. 189s. (post 3s. 3d.)

Reviews of the Aeronautical Research Council

1939-48 3s. (post 5d.) 1949-54 5s. (post 5d.)

Index to all Reports and Memoranda published in the Annual Technical Reports

1909-1947 R. & M. 2600 6s. (post 2d.)

Indexes to the Reports and Memoranda of the Aeronautical Research Council

- | | |
|------------------------|-------------------------------------|
| Between Nos. 2351-2449 | R. & M. No. 2450 2s. (post 2d.) |
| Between Nos. 2451-2549 | R. & M. No. 2550 2s. 6d. (post 2d.) |
| Between Nos. 2551-2649 | R. & M. No. 2650 2s. 6d. (post 2d.) |
| Between Nos. 2651-2749 | R. & M. No. 2750 2s. 6d. (post 2d.) |
| Between Nos. 2751-2849 | R. & M. No. 2850 2s. 6d. (post 2d.) |
| Between Nos. 2851-2949 | R. & M. No. 2950 3s. (post 2d.) |
| Between Nos. 2951-3049 | R. & M. No. 3050 3s. 6d. (post 2d.) |

HER MAJESTY'S STATIONERY OFFICE

from the addresses overleaf

© Crown copyright 1961

Printed and published by
HER MAJESTY'S STATIONERY OFFICE

To be purchased from
York House, Kingsway, London w.c.2
423 Oxford Street, London w.1
13A Castle Street, Edinburgh 2
109 St. Mary Street, Cardiff
39 King Street, Manchester 2
50 Fairfax Street, Bristol 1
2 Edmund Street, Birmingham 3
80 Chichester Street, Belfast 1
or through any bookseller

Printed in England